University of London
Imperial College of Science, Technology and Medicine
Department of Physics

Continuous Matrix Product States & Cavity QED

Aizar Enciso Dominguez

Submitted in part fulfilment of the requirements for the degree of

Doctor of Phylosophy in Controlled Quantum Dynamics of the University of London and

the Diploma of Imperial College

April 2018



I hereby declare that this thesis and the work reported herein was composed by and originated entirely from me. Information derived from the published and unpublished work of others has been acknowledged in the text and references are given in the list of sources.

Aizar Enciso Dominguez (2018)

The copyright of this thesis rests with the author and is made available under a Creative Commons Attribution Non-Commercial No Derivatives licence. Researchers are free to copy, distribute or transmit the thesis on the condition that they attribute it, that they do not use it for commercial purposes and that they do not alter, transform or build upon it. For any reuse or redistribution, researchers must make clear to others the licence terms of this work.

ABSTRACT

Existing studies [1] have proposed similarities between the continuous Matrix Product States (cMPS) which describes low energy states of quantum field theories, and the input-output formalism which describes the quantum state of electromagnetic field leaking out of an optical cavity. This research investigates the above relationship in greater detail, to understand and develop new tools to simulate exotic quantum field systems, focusing on bosonic gases in one dimension.

Using the formalism developed by [2, 1] we analysed the Lieb-Liniger model which describes a bosonic one-dimensional gas subject to a delta potential interaction. We produced a simpler algorithm to find the ground state energy of the Lieb-Liniger model. We demonstrated that its expectation value in terms of matrix products states can be rewritten as the expectation value of an effective closed Jaynes-Cummings Hamiltonian when we use a cavity-atom system as a simulator. The Hamiltonian of this simulator corresponds to a laser-driven atom in the Jaynes-Cummings model with a lossy cavity. This analytical approach makes two contributions to existing knowledge. First, it corrects an intrinsic error in the numerical simulation of [3] due to the normal order of the annihilation operators. Second, it gives us a better understanding of why the simulator used in [3], is so effective in reproducing the correlation properties of the Lieb-Liniger model. Furthermore, we also find that depending on the Hamiltonian used as a simulator, the form of the effective Hamiltonian that would describe the Lieb-Liniger model will reflect the dynamical properties of said simulator. Finally, we derived the transformation rules that relate the Hamiltonian of the simulator with the analytical form of the effective Hamiltonian, concluding with the analysis for the case of a mixture of gases. Thus, our findings could help in the selection of appropriate simulators for any given field theory.

ACKNOWLEDGEMENTS

I would like to thank my supervisors, Terry Rudolph and David Jennings, for stepping in after Professor Sean Barrett had to leave, and for their support, encouragement and faith in me when the going got tough. Thank you David for your encouraging words and insightful advice, both academic and personal, and for being concerned about my well-being.

I would also like to thank my family and friends, without whom this PhD would not have been possible nor I would have been able to survive. Thank you to my family, Vicente, Rosa Maria and Giazu, your support and love have helped me tremendously through my challenging journey. Thank you Izumi for your constant support, for sharing my best and my worst moments that always comforted me and whose company and ideas about how approach a problem were always spot on. Not forgetting the tasty food you often made to perk me up when things were not going smoothly for me. To Valeri Vaissier, my first close friend at Imperial who accepted me for what I am, to Erika for the moments she listened to my adventures, complaints and advices, to Agnieszka for the conversations about our PhD and life. Thank you being there in my moments of need. I am also grateful to Kristi, M.J., Audrey, Oz, Ioana, Ohm, Pauli, Yanni, Sherwin, Ayako, Aki, Claire, Roxana, Midori, Laura Fox and Marika Doshoris for being there as friends, partners, dancers and teachers in this life. To Makiko and Octavian for being such awesome people and for lending me a hand when I needed. Last but not least to the CQD group and the Dance society which have enabled me to meet diverse people who made my days at Imperial more fun and fulfilling. To Yameng for all the kinds of support, the physics conversations and the faith in me. You became a true brother and a family member. To Dr. Catherine Perry for her immense help and techniques to achieve a better PhD experience and the department of Physics in particular Loli Sanchez for all the support received during my studies at Imperial College. To Miranda Smith for all the help with administrative issues during my studies, for being such a great friend, and for the fun conversations alongside a cup of tea made me feel so welcome. To Lizzie Huckle who always supported me as an international student. Finally, thanks to CONACYT and Programa de Becas Complemento SEP for the support and funding.

CONTENTS

Introduction **2**

1 Background Theory **5**
1.1 Background on quantum fields 5
1.1.1 N-particle systems 6
1.1.2 Operators in first quantization 9
1.1.3 Operators in second quantization and field operators 10
1.2 Continuous Matrix Product States 14
1.2.1 Motivation 14
1.2.2 Core theory of cMPS states 15
1.3 Cavity QED, open system approach 19
1.3.1 Input-Output theory 19
1.3.2 Correlation functions in open systems 22
1.3.3 The interaction picture 24
1.3.4 Lieb-Liniger model 26

2 Toy model: Empty driven cavity **28**
2.1 Correlations of a cavity using Input-Output fields 28
2.2 Empty driven cavity 29
2.2.1 Expectation value of the annihilation operator $\langle \hat{a}(t) \rangle$ 30
2.2.2 Expectation value of the number operator $\langle \hat{n}(t) \rangle$ 32
2.2.3 Two point correlation functions 34
2.2.4 First order correlation function $g_1(\tau)$ 35
2.2.5 Second order correlation function $g_2(\tau)$ 37

3 Optimization of the energy density of the ground state for the Lieb-Liniger model using cMPS as variational states. **40**
3.1 Algorithm for minimization 41
3.2 Energy density and correlation functions 43
3.3 Alternative method 51
3.4 Luttinger parameters 56

4 Optimization of the energy density of the ground state of the Lieb-Liniger model using a cavity QED **60**
4.1 Atom inside the cavity 61
4.1.1 Two level atom 61
4.2 CMPS and cavity QED corrrespondence 73
4.3 Simulation with a cavity and a 2 level atom 75
4.3.1 Improved cQED/cMPS correspondence, analytical derivations . . 77
4.3.2 Improved simulation results: Energy density 80
4.3.3 Improved simulation results: Second order correlation function . 86

4.4 Discussion of results 88

5 Generalization for different Hamiltonians **91**
5.1 Jaynes-Cummings Hamiltonian in a two level atom 91
5.2 General case 94
5.2.1 Other cases with no interaction with the atom 96

Conclusions **99**

Bibliography **103**

A cMPS **104**

B Jaynes-Cummings Hamiltonian for a three level atom **108**

C Mixture of gases **112**

D Looking for extra variables in the cavity QED Hamiltonian **115**

E Computation of density matrix and probability amplitudes **118**

F Permission documents **120**

LIST OF FIGURES

1.1 Intuitive construction of a cMPS. An auxiliary system B, (the atom), interacts with a group of quantum mechanical harmonic oscillators one at a time, system A. 16
1.2 Input-Output description provides information of the incoming and outgoing fields in terms of operators $\hat{a}_{\text{in}}$ and $\hat{a}_{\text{out}}$ respectively in the Heisenberg picture. The operator $\hat{c}$ is a system operator involved in the interaction. 19

2.1 Temporal evolution of the real part of the expectation value of the annihilation operator a for arbitrary values $\kappa = 0.05, \omega - \omega_D = 0.1, E_0 = 0.5, \phi = 0$. For small values of t, we can appreciate the effect of the transient term as a variation in the amplitude but for longer times, approximately $t > 80$ the oscillator reach the steady state where the expectation value oscillates at the frequency of the laser ω_D at a constant amplitude. 32
2.2 Expectation value of the number of photons $\langle \hat{n}(t) \rangle$ in a leaking empty cavity. At $t = 0$ its value is zero as per the initial conditions. All graphs are increasing functions of t for its initial values since the laser is starting to produce photons. a) In blue, the off-resonant case, $\kappa = 0.05, \omega - \omega_D = 0.1, E_0 = 0.5$. b) In red, the resonant case $\kappa = 0.05, \omega - \omega_D = 0, E_0 = 0.3$.c) In green the limit case of κ close to zero that approximates to the case of a lossless cavity where the behaviour is quadratic in time $\kappa = 0.001, \omega - \omega_D = 0, E_0 = 0.04$. We reduced the intensity by an order of 10 since $\langle \hat{n}(t) \rangle$ grows faster in this case. 34
2.3 Two time second order correlation function $g_2(t, \tau)$ with t as a parameter. Notice that as the time increases, $t \longmapsto \infty$ the second correlation function $g_2(t, \tau)$ tends to the 1 $\forall$ τ, which is a signature of coherent light. The decay rate $\kappa = 0.05$, the detuning $\omega - \omega_D = 0.1$, and the amplitude of the electric field is $E_0 = 0.5$, for values of time $t = 5$ blue graph, $t = 8.5$ yellow graph , $t = 40$ green and $t = 400$ orange 39

3.1 Energy density $e(c)$ for one dimensional bosonic particles in the ground state as a function of the parameter c, the interaction strength, for values of D=2, 3, 4, 5, 6. Note as D increases, e(c) becomes bounded by $\pi^2/3$ which according to [4] is the limit value of the energy density as $c \to \infty$. Furthermore, in this limit we are in the Tonks-Girardeau regime of impenetrable bosons and according to [5] the ground state energy is the same as the ground state of the free Fermi gas. For $c = 0$ we recover the ideal gas where no interaction occurs and $e(c) = 0$. 45

3.2 Comparison of our results for the energy $e(c)$ density versus the interaction constant c with those of Cirac et al[1] and the Bethe ansatz. For $D = 2$ in red, $D = 4$ in green and $D = 6$ in yellow. Notice that for $D \geq 4$ there is little difference with the Bethe ansatz approach meaning that our optimizations are increasing accuracy with increasing dimension D. . . 46
3.3 Energy density, Kinetic energy ($T = \mathrm{Tr}\left(\rho_{ss}\left[Q,R\right]^{\dagger}\left[Q,R\right]\right)$) and Interaction potential energy ($V = c\mathrm{Tr}\left(\rho_{ss}(R^{\dagger})^{2}R^{2}\right)$) of the Lieb Liniger model as as function of the interaction strength c for $D = 4$ in black, red and blue respectively. According to [4] $T \to \frac{\pi^2}{3}$, $V \to 0$ when $c \to \infty$. This implies that for higher values of c, the contributions of the interaction energy will be negligible and only the kinetic energy will contribute to the total energy. For instance for $c = 60.2$ we have $T = 2.95$ and $V = 0.2067$ thus V contributes a 6.54% and $c = 625.95$ $T = 3.331$ $V = 0.0218$, V contributes a 0.65% This will have important effects when we use a cavity QED as a simulators 47
3.4 Two body density-density correlation function as a function of position x for the values of c=0.2,2,20,2000 (blue, red, light blue and green respectively) for matrices K, R of dimension $D = 4$. In the limit of $x \to \infty$ all correlation functions tend to 1. 49
3.5 Comparison of our plots with those of Cirac et al [1] for the second correlation function $g_2(x) = \langle n(x)n(0)\rangle$ versus x. From top to bottom $c = 0.2, 2, 20, 2000$. Despite we only used dimension $D = 4$, continuous lines, we are able to get an excellent agreement with their results, where they used a dimension $D = 14$, data points. 50
3.6 Comparison of $g_2(x)$ functions. Our method discused in 3.2 has proven to reproduce the $g_2(x)$ plots of [1] but it shows a discrepancy with [3]. This is explained when we note that they should have used the rescaled values: $\frac{Q}{d}$ and $\frac{R}{\sqrt{d}}$ we just discussed. 54
3.7 Reproducing $g_2(x)$ extracted from [3] using the alternate method described in section(3.3). 55
3.8 Luttinger parameters K and $v_{\mathrm{s}}/v_{\mathrm{F}}$ as a function of the interaction strength c of the Lieb-Liniger model. The isolated asterisks and circles represent our own calculation of Eq. (3.26) using cMPS to find the energy density $e(\rho, c)$ at different density of particles ρ for each selected value of the parameter c. The continuous and dashed lines represent the asymptotic approximations for small and large c. 58

4.1 Probabilities for the ground state and excited state for the driven two level atom system in the resonant case $\omega_l - \omega_0 = 0$. The zeros in ground state are in: $2\pi n/\Omega_{\mathrm{R}}$ for $n \in \mathbb{Z}$ 64
4.2 Probabilities for the ground state and excited state for the driven two level atom system in the off-resonant case $\delta_\omega = \omega_l - \omega_0 \neq 0$. The zeros in ground state are in: $2\pi n/\Omega$ for $n \in \mathbb{Z}$ where $\Omega_{\mathrm{R}} = 1$, $\delta_\omega = 2$, $\Omega = \sqrt{5}$. . 64
4.3 Probabilities for the ground state and excited state for the driven two level atom system that includes decay in the form of spontaneous emission in the resonance case. $\Omega_{\mathrm{R}} = 1$, $\omega_0 - \omega_l = 0$ and $\gamma = 0.5$. The total probability is conserved for all times even in the steady state. We still have an oscillatory behaviour but damped by γ. 65

4.4 Probabilities for the ground state and excited state for the driven two level atom system that includes decay in the form of spontaneous emission in the off resonance case. $\Omega_{\mathrm{R}} = 1$ $\omega_0 - \omega_l = 1$, $\gamma = 0.5$. The total probability is conserved at all times as shown for the points near the steady state. . 66
4.5 Cavity with 2 level atom, zeros in ground state are of the form $\frac{2\pi}{(g\sqrt{n+1})}k$ for $k \in \mathbb{Z}$ for our values: $g = 1$, $\omega_0 - \omega_l = 0$ and Initial state $|n = 0, e\rangle$ this means multiple integers of $2\pi/g$ similarly the zeros for the excited state are in the multiples of odd integers of π/g. 70
4.6 Cavity with 2 level atom, zeros in ground state are of the form: $\frac{2\pi}{\Omega_n}k = \frac{2\pi}{\sqrt{g^2(n+1)+(\omega_0-\omega_l)^2}}k$ for $k \in \mathbb{Z}$ for our values: $g = 1$, $\omega_0 - \omega_l = 2$ and initial state $|n = 0, e\rangle$. 70
4.7 Cavity with 2 level atom . Left: Initial state $|n = 0, g\rangle$ is uncoupled as no absorption can occur in absence of light quanta. Right: Initial state is $|n = 1, g\rangle$ and zeros in ground state are in the multiple integers of: $\frac{2\pi}{(g\sqrt{n+1})} = 2\pi$ for our values: $g = 1$, $\omega_0 = 13$, $\omega_l = 13$, $\gamma = 0$ and initial state $|n = 0, e\rangle$. 71
4.8 Driven 2 level atom in a cavity with $\Omega = 1$ g=1 $\omega_0 - \omega_l = 0$, $\omega_c - \omega_l = 2$, and initial state is $|n = 0, e\rangle$. 72
4.9 Driven 2 level atom in a cavity with $\Omega = 1$, g=1, $\omega_0 - \omega_l = 0$, $\omega_0 - \omega_c = 2$ and initial state $|n = 0, e\rangle$. Contribution of each mode. a) Probabilities for the mode n=0. b) Probabilities for the mode n=1. c) Probabilities for the mode n=2. 72
4.10 Minimum value for the energy density in the Lieb-Liniger Hamiltonian using a 2 level atom inside a cavity as simulator. In blue, extracted values from Barrett et al [3, 6] using a two level atom. In green our take on the simulation also using a 2 level atom showing the ground state energy density for values of $c = 0.07$, 3.95, 60.2, 120 and 180. On red same simulation but correcting for normal ordering of the annihilation operators. The small corrections for $c < 2$ will prove to be of importance at the moment of simulating second order correlation functions since will describe g_2 for smaller values of c much better than previous research. All plots use the same dimension for the truncated annihilation operator. $N = 4$ 81
4.11 Comparing energy densities, in blue, the values obtained by Barrett et.al [3, 6], in green and red our minimization using a 2 level atom for the uncorrected and corrected values of the energy. In black and pink simulations done with the mathematical cMPS for K and R matrices of dimensions $D = 2, 6$ respectively. 83
4.12 Comparing energy densities with and without corrections on the annihilation operators. Increasing the dimension of the annihilation operators while keeping the number of parameters constant, also proves to improve the simulations. The major change comes from using a dimension of $N = 6$ while no significant change seems to be produced is we calculate for $N = 8$. 84

4.13 a)-c) Values of the three parameters used in the optimization of the energy density of the L.L. model tend to decrease as the interaction strength increases. In this optimization we implemented the corrections for the annihilation operators of dimension $N = 4$. d)-f) Effect of the corrections made on the three variables used in the optimization of the energy density for a truncated annihilation operator of dimension $N = 4$. Notice that these corrections affect mainly the sector of weak gas interactions, that is to say, values of $c \ll 2$. Increasing the dimension of the truncated operators will improve even more the results but as we have shown, only up to dimension of the order of 6 there will be noticeable changes. . . . 85

4.14 Second order correlation functions obtained from the physical cMPS where the matrices K and R are proportional to the Hamiltonian of a driven cavity-QED system and the intracavity annihilation operator a respectively. All the plots describe the values $c = 0.07, 3.95, 60.2, 625.95$. a) Plot extracted from [3] where the dimension of the annihilation operator is $N = 4$ b) Our simulation for $g_2(t)$ with the truncation error for $N = 4$. c) $g_2(t)$ for $N = 4$ using the energy density that fixes the truncation error Eq. (4.54). d) $g_2(t)$ with no truncation error and dimension of the annihilation operator $N = 6$ 87

4.15 The g_2 functions a) bosonic gas simulated using the cMPS and b) simulation of the bosonic gas using a cavity QED system. 88

B.1 Three level atom system with states $|g_1\rangle$ and $|e\rangle$ coupled by a laser of frequency ω_l, the states $|g_2\rangle$ and $|e\rangle$ by a cavity of frequency ω_c and the states $|g_1\rangle$ and $|g_2\rangle$ coupled by a laser of frequency ω_2 . The detunings are given by Δ_1 and Δ_2 108

D.1 Density-density correlation functions (a) cMPS with the structure of the two level atom and cavity system defining R as the tensor product of a truncated annihilation operator $\hat{a}$ of dimension 4 and the identity of a 2 level atom. $K = K^\dagger$ and $R = \gamma\hat{a} \otimes \mathbb{1}$. Number of total variables is $D^2 + 1 = 65$ (b) Results predicted by Cirac from [1]. 117

INTRODUCTION

The ability to simulate physical systems is essential to understanding the basic rules governing natural phenomena, particularly once we go beyond analysing very simple scenarios and try to understand the complex and continuous interaction of millions of particles. Moreover as technology advances, the sizes of the systems we can control, manipulate, and quantum effects become increasingly important. Unfortunately quantum many-body systems are notoriously difficult to simulate on a classical computer [7]. Absent a fully digital, fault-tolerant quantum computer, an alternative approach is to use a quantum system whose properties are well understood and controllable to simulate the physics of a completely different quantum system. Such quantum simulations (possibly better termed emulation [8]) are beginning to come online already. One way in which this could work is to find a direct mapping between the Hamiltonians of the two systems involved [9] . Such simulators should be expected to be limited in the class of problems they can tackle. A different, potentially more widely applicable, approach is to try to use the quantum simulator to perform a variational calculation over some class of quantum states. Methods to calculate the properties of quantum physical systems based on the renormalization group [10] and the density matrix renormalization group (DMRG) [11] have proven to be successful in certain simplified scenarios, and recently have inspired new classical algorithms based upon matrix product states (MPS) [12] to calculate properties of a wide variety of strongly correlated quantum systems. It is natural, therefore, to investigate whether quantum simulators could perform such calculations, potentially going beyond simply "mapping between Hamiltonians" would imply.

A proposal for simulating the Lieb-Liniger model [4] along these latter lines by Barrett et al [3], and extended in [6], has recently been experimentally implemented using a Jaynes-Cummings type interaction within a superconducting cavity-QED system [13].

The results of these papers are intriguing because a very small number of variational parameters yields a quantum simulation capturing qualitatively many of the intricate physical features one might expect only from a much larger calculation/simulation. In this thesis we will delve deeper into these quantum simulations investigated in these papers. We will show several ways in which it can be significantly improved, and discover a surprising connection wherein the main quantity of interest can be re-written as the expectation value of a completely different, somewhat fictitious, Jaynes-Cummings interacting system, unrelated to the actual Jaynes-Cummings interaction describing the physics of the simulator.

In the chapter 1, we give the background needed field theory needed to understand the bosonic systems of many particles and we will proceed to define the continuous matrix product states (cMPS). It is shown that they are the continuous limit of the already known MPS used in spins systems. We will also introduce the Input-Output formalism and the correlation functions in open systems. They will allow us to make the connections between cavity quantum electrodynamics (cavity QED) and the cMPS. Finally we define the Lieb-Liniger model. The chapter 2 describes a toy model of an empty driven cavity that allowed us to have the needed intuition to understand the physical variables at play. In chapter 3 we propose a simpler algorithm used to find the energy density of the ground state for the Lieb-Liniger model using the cMPS as variational states allowing us to calculate the second correlation function. We compare those results with [1]. We also compare our method with [3] and provide a few advantages in our approach. Chapter 4 discusses how to find the energy density of the Lieb-Liniger model but using a driven two level atom inside lossy cavity as a simulator. Our main result will demonstrate that the expectation value of the ground state energy density of the Lieb-Liniger model in terms of matrix products states can be written as the expectation value of an effective closed Hamiltonian of a Jaynes-Cummings model when we use a cavity-atom system as a simulator, the Hamiltonian of this simulator corresponds to a laser driven atom in the Jaynes-Cummings model with a lossy cavity. This analytical approach corrects an intrinsic error in the numerical simulation process previously done by the works of [3] due to the normal order of the annihilation operators. Finally we attempt to answer, why this two level atom simulator works so well and what could

be the physical reasons to that. We also discuss the case of a simulator being a three level atom in a lambda configuration inside a cavity. Finally we left in the appendix A, some mathematical relations of the cMPS and in appendix B we derived the rules for generalising the Hamiltonian of the simulator to more general Hamiltonians,there we establish the connections between the Hamiltonian of the simulator and the effective Hamiltonian that describes the Lieb-Liniger model. We hope that those mathematical relations would give a clue for what type of Hamiltonians we should use to simulate more complicated filed theories. The appendix C gives an overview of how the mixed gases would look in these analytical approach that we derived.

CHAPTER 1

BACKGROUND THEORY

1.1 Background on quantum fields

In some cases in a physical system, the number of particles contained in it can vary during the reactions taking place, for example by absorption and emission in a photonic gas, collision processes in high energetic particles, or interactions that modify the excited quanta of phonons. Furthermore, the number of atoms or molecules constituting a macroscopic system may not be known with precision, consequently it is useful to use grand canonical statistical ensembles where the number of particles is allowed to fluctuate. Furthermore, it is convenient to have a description of states with undetermined number of particles and of interactions that does not conserve the number of particles. In the next section, we will be following [14] to review a few concepts on first and second quantization to conclude with the expressions for field operators used through out the rest of the thesis. We recall that we can describe a wave function in the one particle Hilbert space $\psi(r) \in \mathcal{H}$ in terms of Dirac notation as $\langle r|\psi\rangle$ and in particular for set of eigenfunctions $\phi_\nu(r)$ as:

$$\phi_\nu(r) := \langle r|\nu\rangle, \tag{1.1}$$

where the label ν describes a complete set of quantum numbers that describe the state $|\nu\rangle$ and $\langle r|$ is the vector representing the configuration space in which the state is projected. Furthermore, the wave functions must obey the normalization and completeness. The first one guarantees that a particle in a quantum state $\phi_\nu(r)$ has the probability equal to 1 of being somewhere in the configuration space. That is to say $\int dr\phi^*(r)\phi(r) = 1$

which in turn, using Eq. 1.1 leads to

$$\langle\nu|\left(\int dr|r\rangle\langle r|\right)|\nu\rangle = 1. \tag{1.2}$$

On the other hand, using Dirac notation on a normalized state $|\nu\rangle$ and the identity operator $\mathbb{1}$ to represent the norm of the state, we can write the norm as $\langle\nu|\mathbb{1}|\nu\rangle = 1$ which allow us to derive the useful relation:

$$\int dr|r\rangle\langle r| = \mathbb{1}. \tag{1.3}$$

In a similar way, the concept of completeness says that a set of states $\phi_n(r)$ form a complete basis if $\sum_\nu \langle\phi|\nu\rangle\langle\nu|\phi\rangle = 1$ which means that all the possible states ν that the particle can take, are considered and the summation of the probability of being in any of those states is equal to one. This leads us to the expression

$$\langle r|\left(\sum dr|\nu\rangle\langle\nu|\right)|r\rangle = 1, \tag{1.4}$$

and using again the identity operator $\langle\phi|\mathbb{1}|\phi\rangle = 1$ we arrive at:

$$\sum_\nu |\nu\rangle\langle\nu| = \mathbb{1}. \tag{1.5}$$

Finally, using Eqs. (1.1, 1.3, 1.5), the wave function $\psi(r)$ written in terms of a basis of states $\phi_\nu(r)$ can be written in terms of the configuration space

$$\psi(r) = \sum_\nu \phi_\nu(r) \int dr' \phi^*_\nu(r')\psi(r'), \tag{1.6}$$

or in the Dirac notation as:

$$\langle r|\psi\rangle = \sum_\nu \langle r|\nu\rangle\langle\nu|\psi\rangle. \tag{1.7}$$

1.1.1 N-particle systems

When dealing with N-particle systems, the complex wave function $\phi(r)$ defined in the three dimensional space for a single particle, is naturally extended to the N particle

state complex wave function $\phi(r_1, r_2, \ldots, r_N)$ but now defined in a $3N$ dimensional configuration space. The concept of probability is still related to the modulus squared as

$$|\phi(r_1, r_2, \ldots, r_N)|^2 \prod_{j=1}^{N} dr_j, \tag{1.8}$$

which is understood as the probability of finding$N$ particles in the $3N$ dimensional volume $\prod_{j=1}^{N} dr_j$ surrounding the point $(r_1, r_2, \ldots, r_N)$. The construction of N-particle states that span the space $\mathcal{H}^{\otimes N}$ from the one particle states can be better explained without using any particular representation. Consider the set $|\phi_i\rangle$, $i = 1, ..., N$ of the single particle states in $\mathcal{H}$, one associates the state of N independent particles, denoted by $|\phi_1\rangle \otimes ... \otimes |\phi_N\rangle = |\phi_1 \otimes ... \otimes \phi_N\rangle$. So the i-particle will be in the state ϕ_i for all $i = 1, ..., N$. In that case, we define the total wave function as the product of the individual wave functions $\phi_i(x)$ as [15]:

$$\langle r_1, ..., r_N | \phi_1 \otimes ... \otimes \phi_N \rangle = \phi_1(r_1)...\phi_N(r_N). \tag{1.9}$$

The vector space generated by all of the linear combination of vectors $|\phi_1 \otimes ... \otimes \phi_N\rangle$ and completed by the scalar product defined as

$$\langle \phi_1 \otimes ... \otimes \phi_N | \psi_1 \otimes ... \otimes \psi_N \rangle = \langle \phi_1 | \psi_1 \rangle \langle \phi_2 | \psi_2 \rangle ... \langle \phi_N | \psi_N \rangle, \tag{1.10}$$

forms a Hilbert space denoted by the tensor product $\mathcal{H} \otimes ... \otimes \mathcal{H} = \mathcal{H}^{\otimes N}$ which is by definition, the tensor product of N copies of the single particle space $\mathcal{H}$. That is to say, if the set of vectors $|\phi_\nu\rangle$, $\nu = 1, 2, ...$ form a basis of $\mathcal{H}$, then one can obtain a basis of $\mathcal{H}^{\otimes N}$ by considering all of the vector products $|\phi_{\nu_1} \otimes ... \otimes \phi_{\nu_N}\rangle, \nu_1, \nu_2, ... = 1, 2, ...$ Thus, any N-particle wave function $\phi(r_1, r_2, \ldots, r_N)$, even those which are not factorized, can be expanded in the basis formed from the product of one particle states $|\phi_\nu\rangle$, resulting in the expansion:

$$\phi(r_1, r_2, \ldots, r_N) = \sum_{\nu_1, \nu_2, ..., \nu_N} A_{\nu_1, \nu_2, ..., \nu_N} \phi_{\nu_1}(r_1) \phi_{\nu_2}(r_2) \cdots \phi_{\nu_N}(r_N), \tag{1.11}$$

where $A_{\nu_1, \nu_2, ..., \nu_N}$ are just complex coefficients. Another important ingredient is the concept of indistinguishably. We recall that if we deal with identical particles, in clas-

sical mechanics it is possible to distinguish them just by assigning a label to each one of the particles. In that way, we can follow its individual trajectory in phase space. This is not the case in quantum mechanics as any form of labelling will disturb the system. Moreover we have regimes in which particles with identical quantum numbers are fundamentally indistinguishable (such as for electrons or photons), which implies that under any interchange of coordinates the state that describe the N-particle system, will behave in two of the following ways:

$$\phi(r_1, r_2, ..., r_i, ..., r_j .., r_N) = -\phi(r_1, r_2, ..., r_j, .., r_i, ..., r_N), \tag{1.12}$$

$$\phi(r_1, r_2, ..., r_i, ..., r_j .., r_N) = +\phi(r_1, r_2, ..., r_j, .., r_i, ..., r_N), \tag{1.13}$$

where Eq. (1.12) describes fermionic particles like protons and electrons and Eq. (1.13) refers to the bosonic particles like the photons or atoms of $He-4$. Since we are interested in the bosonic particle case, we need to incorporate this symmetry to each element of the basis, through the operator S defined as:

$$S\prod_{j=1}^{N}\phi_{\nu_j}(r_j) = \sum_{p\in S_N}\left[\prod_{j=1}^{N}\phi_{\nu_j}(r_{p_j})\right] \tag{1.14}$$

with S_N the group of $N!$ permutations p for the set of N coordinates.As an example consider a system of two particles that can be in three possible states such that $\nu_i \in 1, 2, 3$, Thus for a particular element of the basis of the N-particle system $\phi_{\nu_1}(r_1)\phi_{\nu_2}(r_2)\phi_{\nu_3}(r_3)$, if we select $\nu_1 = 1; \nu_2 = 2; \nu_3 = 3$ we have,

$$\begin{aligned}\hat{S}\phi_1(r_1)\phi_2(r_2)\phi_3(r_3) =& \phi_1(r_1)\phi_2(r_2)\phi_3(r_3) + \phi_1(r_1)\phi_2(r_3)\phi_3(r_2) \\ &+\phi_1(r_2)\phi_2(r_1)\phi_3(r_3) + \phi_1(r_2)\phi_2(r_3)\phi_3(r_2) \\ &+\phi_1(r_3)\phi_2(r_1)\phi_3(r_2) + \phi_1(r_3)\phi_2(r_2)\phi_3(r_1).\end{aligned} \tag{1.15}$$

It is obvious that for a large number of particles, the process of symmetrization becomes cumbersome as $N! - 1$ terms need to be added for each element of the N particle basis.

1.1.2 Operators in first quantization

We can construct the N-particles operators from individual operators originally defined for one particle. This is possible since they keep their form whenever they operate on N-particle states. For our case of interest we consider the one particle operator $T_j = T(r_j, \nabla_{r_j})$ defined to act on a particle with position observable r_j. If we project it on the singe particle basis, it takes the form:

$$T_j = \sum_{\nu_a,\nu_b} T_{\nu_a,\nu_b} |\phi_{\nu_b}(r_j)\rangle\langle\phi_{\nu_a}(r_j)|, \tag{1.16}$$

with T_{ν_a,ν_b} expressed as:

$$T_{\nu_a,\nu_b} = \langle\phi_{\nu_b}(r_j)|T_j|\phi_{\nu_a}(r_j)\rangle = \int dr_j \phi^*_{\nu_b}(r_j) T_j \phi_{\nu_a}(r_j), \tag{1.17}$$

where we used Eq. (1.3) to obtain the right hand side. The corresponding symmetric extensive observable for the N-particle systems corresponds to:

$$T_{\text{tot}} = \sum_{j=1}^{N} T_j. \tag{1.18}$$

For the case of a two body operator acting on a two particle space $\mathcal{H} \otimes \mathcal{H}$, like the interaction potential which depends on the distance between two particles as $V(r_j - r_k)$ we define V_{jk} acting on $\mathcal{H}^{\otimes N}$ as the operator which acts on the jth and kth factors of $\mathcal{H}^{\otimes N}$ and trivially on the others. In the particle representation, and using the basis $|\phi_{\nu_a}(r_j)\rangle|\phi_{\nu_b}(r_k)\rangle$

$$V_{jk} = \sum_{\nu_a\nu_b\nu_c\nu_d} V_{\nu_c\nu_d,\nu_a\nu_b} |\phi_{\nu_c}(r_j)\rangle|\phi_{\nu_d}(r_k)\rangle\langle\phi_{\nu_a}(r_j)|\langle\phi_{\nu_b}(r_k)|, \tag{1.19}$$

where $V_{\nu_c\nu_d,\nu_a\nu_b}$ is expressed as:

$$V_{\nu_c\nu_d,\nu_a\nu_b} = \int dr_j dr_k \phi^*_{\nu_c}(r_j)\phi^*_{\nu_d}(r_k) V(r_j - r_k)\phi_{\nu_a}(r_j)\phi_{\nu_b}(r_k), \tag{1.20}$$

and the corresponding observable for the N-particle system

$$V_{\text{tot}} = \sum_{j>k}^{N} V_{jk} = \frac{1}{2}\sum_{j\neq k}^{N} V_{jk}, \tag{1.21}$$

where the sum is made over the $N(N-1)/2$ pairs of particles. Notice that since V_{tot} is acting on two identical particles, then it must be invariant under the exchange of pairs of particles, thus $V_{i,j} = V_{j,i}$ so the second expression is obtained.

1.1.3 Operators in second quantization and field operators

When we first introduced the N-particle systems, we explained that a if proper basis is able to describe the bosons, it needs to be symmetric under particle interchange. This was achieved with the symmetrization operator S defined in Eq. (1.14). This creates a potential problem since it adds $N!-1$ extra terms. The way around this is to introduce the second quantization formalism, in other words, we reformulate the problem in terms of occupation numbers of single particle states, which will allow us to count the number of particles that are in each state $|\nu\rangle$. Therefore the basis states for an N-particle system in terms of the occupation number representation is defined as follows:

$$|n_{\nu_1}, n_{\nu_2}, n_{\nu_3}, \ldots\rangle \in \mathcal{F}, \qquad \sum_j n_j = N, \tag{1.22}$$

where each n_{ν_j} represents the number of particles occupying the state ν_j. We define the Fock space $\mathcal{F}$ as the space spanned by all the vectors contained in the direct sum of spaces $\mathcal{F}_N$ as $\mathcal{F} = \mathcal{F}_0 \oplus \mathcal{F}_1 \oplus \mathcal{F}_2 \oplus \cdots$ where each $\mathcal{F}_N = \text{span}\left\{|n_{\nu_1},, n_{\nu_2}, \ldots\rangle | \sum n_{\nu_j} = N\right\}$, that is to say, for each value of N, $\mathcal{F}_N$ is spanned by states with finite particle number N. Thus any state $|\Phi\rangle \in \mathcal{F}$ might have an unbounded number of particles but $\langle\Phi|\hat{N}|\Phi\rangle < \infty$. Furthermore, each occupation number n_{ν_j} is naturally related to the occupation number operators $\hat{n}_{\nu_j}$ as

$$\hat{n}_{\nu_j}|n_{\nu_j}\rangle = n_{\nu_j}|n_{\nu_j}\rangle \text{ with } n_{\nu_j} = \{0, 1, 2...\}, \tag{1.23}$$

where $|n_{\nu_j}\rangle$ and n_{ν_j} are its eigenvectors and eigenvalues respectively. In the same way as for the quantum harmonic oscillator, the creation and annihilation operators are defined

as:

$$[b_{\nu_j}, b^\dagger_{\nu_k}] = \delta_{\nu_j,\nu_k} \qquad b_\nu|n_\nu\rangle = \sqrt{n_\nu}|n_\nu - 1\rangle \qquad b^\dagger_\nu|n_\nu\rangle = \sqrt{n_\nu + 1}|n_\nu + 1\rangle, \tag{1.24}$$

which imply, $\hat{n}_\nu = b^\dagger_\nu b_\nu$. These relations allow us to identify:

$$S|\phi_{\nu_1}(r_1)\phi_{\nu_2}(r_2)\cdots\phi_{\nu_N}(r_N)\rangle = b^\dagger_{\nu_1} b^\dagger_{\nu_2}\cdots b^\dagger_{\nu_N}|0\rangle, \tag{1.25}$$

where in both cases we are describing a completely symmetric N-particle state. Thus representing a state is much simpler and natural in the particle occupation state basis with the further advantage that this representation takes intrinsically into account the symmetrization. Eq. (1.25) will allow us to show that all operators can be expressed in terms of the fundamental creation $b^\dagger_\nu$ and annihilation operators b_ν. For instance let us see how the one particle operator $T_{\rm tot}$ acts on an element of the particle occupation state basis

$$T_{\rm tot} b^\dagger_{\nu_1} b^\dagger_{\nu_2}\cdots b^\dagger_{\nu_{n_j}}\cdots b^\dagger_{\nu_N}|0\rangle = \sum_{\nu_a\nu_b} T_{\nu_a\nu_b} \sum_{j=1}^{N} \delta_{\nu_a,\nu_{n_j}} b^\dagger_{\nu_{n_1}} ... b^\dagger_{\nu_b} ... b^\dagger_{\nu_{n_N}}|0\rangle, \tag{1.26}$$

where we used Eq. (1.25) and the fact that $[S, T_{\rm tot}] = 0$. Notice how the operator b_{ν_b} took the place of $b_{\nu_{n_j}}$. In order to make both kets equal and find an identity between the operators we need to reinsert $b^\dagger_{\nu_{n_j}}$ on the right hand side. Without loss of generality let us suppose that in the left hand side, there are $p > 0$ particles in the same state $\nu = \nu_{n_j}$. That means a contribution of the form, $(b^\dagger_\nu)^p|0\rangle$ but on the right hand side the corresponding contribution became $(b^\dagger_{\nu_b})(b^\dagger_\nu)^{p-1}|0\rangle$. However, using the relations on Eq. (1.24) we get the identity:

$$(b^\dagger_\nu)^{p-1}|0\rangle = \frac{b_\nu}{p}(b^\dagger_\nu)^p|0\rangle, \tag{1.27}$$

then we have $(b^\dagger_{\nu_b})(b_{\nu^\dagger_{n_j}})^{p-1}|0\rangle = \frac{1}{p}(b^\dagger_{\nu_b})b_{\nu n_j}(b_{\nu^\dagger_{n_j}})^p|0\rangle$ so substituting in Eq. (1.26) and summing over all the particles we find that the term $\sum_{j=1}^N \delta_{\nu_a,\nu_j}$ will produce p terms different from zero for the case that $\nu_a = \nu$ thus cancelling the p in the denominator of Eq.(1.27). This will lead to:

$$T_{\rm tot}\left[b^\dagger_{\nu_1} b^\dagger_{\nu_2}\cdots b^\dagger_{\nu_N}|0\rangle\right] = \sum_{\nu_a\nu_b} T_{\nu_a\nu_b} b^\dagger_{\nu_b} b_{\nu_a}\left[b^\dagger_{\nu_1} b^\dagger_{\nu_2}\cdots b^\dagger_{\nu_N}|0\rangle\right]. \tag{1.28}$$

Since this is valid for any element of the particle occupation state basis, it implies:

$$T_{\text{tot}} = \sum_{\nu_a,\nu_b} T_{\nu_a,\nu_b} b^\dagger_{\nu_a} b_{\nu_b}. \tag{1.29}$$

A similar process can be done for two body operators such giving the expression:

$$V_{\text{tot}} = \frac{1}{2} \sum_{\nu_i\nu_j\nu_k\nu_l} V_{\nu_i\nu_j,\nu_k\nu_l} b^\dagger_{\nu_i} b^\dagger_{\nu_j} b_{\nu_l} b_{\nu_k}. \tag{1.30}$$

Thus we arrive to the interesting result that operators in second quantization can be written in terms of creation and annihilation operators multiplied by the matrix elements of the same operator calculated in the first quantization approach. Let us recall that for different operators, there are basis that are more suitable than others to study the different properties of the observables. So changes of basis are needed. Let us consider two different ordered single particle basis states $\{|\phi_{\nu_1}\rangle, |\phi_{\nu_2}\rangle, \cdots\}$ and $\{|\psi_{\mu_1}\rangle, |\psi_{\mu_2}\rangle, \cdots\}$. From the completeness condition Eq. (1.5) we have the basic transformation law for single-particle states:

$$|\phi_\nu\rangle = \sum_\mu |\psi_\mu\rangle\langle\psi_\mu|\phi_\nu\rangle = \sum_\mu \langle\phi_\nu|\psi_\mu\rangle^* |\psi_\mu\rangle. \tag{1.31}$$

We can define annihilation operators $a^\dagger_\nu$ and $\tilde{a}^\dagger_\mu$ for both basis sets which satisfy $|\phi_\nu\rangle = a^\dagger_\nu|0\rangle$ and $|\psi_\mu\rangle = \tilde{a}^\dagger_\mu|0\rangle$ respectively and comparing with Eq. (1.31) we get to the transformation between annihilation operators:

$$\tilde{a}^\dagger_\nu = \sum_\mu \langle\phi_\nu|\psi_\mu\rangle^* a^\dagger_\mu, \tag{1.32}$$

which can be generalized for the N particle systems. It is worth to point out that this transformation preserves the commutation relations established in Eq. (1.24) and the total number of particles $N_{\text{total}} = \sum_\nu a^\dagger_\nu a_\nu$. Eq. (1.32) will allow us to focus on a particular second quantization representation, the real space representation, that leads to the definition of quantum field operators used throughout the rest of the work. From Eq. (1.32), if we consider the continuous position basis set such that $|\phi_\nu\rangle = |x\rangle$, with x the continuous index describing the position in real space, and denoting $\tilde{a}^\dagger_\mu$ as $\Psi^\dagger(x)$ we

obtain the relation:

$$\Psi^\dagger(x) = a^\dagger(|x\rangle) = \sum_n \phi_n^*(x) a_n^\dagger, \qquad \Psi(x) = a(|x\rangle) = \sum_n \phi_n(x) a_n. \tag{1.33}$$

Thus the quantization operators $\Psi^\dagger(x)$ and$\Psi(x)$ can be understood as a summation of all the ways a particle can be created at the position x weighted by the first quantization wave functions $\phi_n(x)$. It can be shown that this operators follow the usual commutation relations for bosonic particles $\left[\Psi(x_1), \Psi(x_2)^\dagger\right] = \delta(x_1 - x_2)]$. With the definition of the field operators, we can express any other operator in the real space representation. For instance for the operator T_{tot} in Eq. (1.29) if we express T_{ν_a,ν_b} in the configuration space as depicted in the right hand side of Eq. (1.17) we get to:

$$\begin{aligned} T_{\text{tot}} &= \sum_{i,j} \left[\int dx \phi_{\nu_i}^*(x) T(x, \nabla_x) \phi_{\nu_j}^*(x) \right] b_{\nu_i}^\dagger b_{\nu_j} \\ &= \int dx \left(\sum_{\nu_i} \phi_{\nu_i}^* a_{\nu_i}^\dagger \right) T(x, \nabla_x) \left(\sum_{\nu_i} \phi_{\nu_i} a_{\nu_i} \right) = \int dx \Psi^\dagger(x) T(x, \nabla_x) \Psi(x), \end{aligned} \tag{1.34}$$

so for the particular case of the kinetic energy operator $T(x, \nabla_x) = -\nabla^2$

$$T_{\text{tot}} = \int dx \frac{d\hat{\Psi}^\dagger(x)}{dx} \frac{d\hat{\Psi}(x)}{dx}. \tag{1.35}$$

In a similar way for the two point operator for the delta potential $V(x - y) = \delta(x - y)$ and writing $V_{\nu_c\nu_d,\nu_a\nu_b}$ in the configuration space:

$$\begin{aligned} V_{\text{tot}} &= \frac{1}{2} \sum_{\nu_c\nu_d\nu_a\nu_b} \int dr_j dr_k \phi_{\nu_c}^*(r_j) \phi_{\nu_d}^*(r_k) V(r_j - r_k) \phi_{\nu_a}(r_j) \phi_{\nu_b}(r_k) b_{\nu_c}^\dagger b_{\nu_d}^\dagger b_{\nu_b} b_{\nu_a} \\ &= \frac{1}{2} \int dx dy \Psi^\dagger(x) \Psi^\dagger(y) \delta(x - y) \Psi(x) \Psi(y) = \frac{1}{2} \int \Psi^\dagger(x) \Psi^\dagger(x) \Psi(x) \Psi(x), \end{aligned} \tag{1.36}$$

where we just renamed the variables as $r_j = x$ and $r_k = y$.

1.2 Continuous Matrix Product States

1.2.1 Motivation

The study of strongly correlated quantum spin systems and many body quantum systems has led to the development of different simulation techniques like Wilson's numerical renormalization group (NRG) [10], or White's density matrix renormalization group (DMRG) [11]. Those have proven to be useful describing spin systems in terms of matrix product states (MPS)[16]. This formalism has shown to be very valuable as it portrays the correlations and entanglement that appear in ground states of one dimensional quantum systems of interacting spins.[17] Furthermore, the numerical techniques developed can be understood as *variational methods* where the ground state of quantum spin systems can be parametrized in terms of these MPS. Due to these characteristics, the MPS can be generalized to study non relativistic quantum field theories in one spatial dimension. Thus, quantum fields, with infinite degrees of freedom, in principle, can be described by defining their *continuous matrix product states* (cMPS) [2, 1, 18]. It is proven in [2, 1] that cMPS can be understood as the continuous limit of MPS. In addition, among their properties, the parametrization allows to use cMPS as variational states for finding the ground state of quantum field theories. According to [1], we define a cMPS by considering a one dimensional ring of bosons (fermions) on a ring of length L, mathematically that is achieved by imposing periodic boundary conditions to the system. The respective position dependent field operators, $\hat{\psi}(x)$ obey the commutation (anticommutation) relations $\left[\hat{\psi}(x), \psi^{\dagger}(y)\right]_{\pm} = \delta(x-y)$ where $x, y \in [0, L]$. Then the cMPS is given by

$$|\chi\rangle = \mathrm{Tr}_{\mathrm{aux}}\left[\mathcal{P}\mathrm{e}^{\int_0^{\mathrm{L}} \mathrm{dx}\left[\mathrm{Q(x)}\otimes\mathbb{1}+\mathrm{R(x)}\otimes\hat{\psi}^{\dagger}\mathrm{(x)}\right]}\right]|\Omega\rangle, \tag{1.37}$$

here $Q(x)$, $R(x)$ are finite dimensional $D \times D$ matrices that in general will depend on position coordinates. These matrices are defined in an auxiliary system, the meaning of which will become apparent in subsequent paragraphs. $|\Omega\rangle$ is the vacuum state such that $\hat{\psi}(x)|\Omega\rangle = 0$. $\mathcal{P}e^{\mathcal{O}}$ stands for a path ordered exponential of the operator $\mathcal{O}$ and $\mathrm{Tr}_{\mathrm{aux}}$ is the partial trace over the auxiliary system.

1.2.2 Core theory of cMPS states

Using the theory of continuous measurements, in which a quantum system is subjected to a sequence of weak measurements of a POVM (positive operator valued measurement), we explain a core method to produce cMPS [2]. The discrete case is described to obtain an insight about cMPS and at the end of the discussion, we will outline the continuous limit of MPS as cMPS. Consider a family of DxD complex matrices $R(x)$ with $x \in [0, L]$, and as depicted in Fig. (1.1) we can imagine an atom with their levels truncated as an auxiliary system B, which interacts instantaneously just at the times $\epsilon, 2\epsilon, \ldots n\epsilon$ through the matrices $R(x)$ with a collection of n quantum harmonic oscillators, which we will call the system A. At other times, B evolves according to some free Hamiltonian K(t). Then, following [19], the total Hamiltonian is:

$$H(t) = K(t) \otimes \mathbb{1} + H_I(t), \tag{1.38}$$

with the interaction given by:

$$H_I(t) = \sqrt{\epsilon} \sum_{r=1}^{n} \delta(t - r\epsilon) \left(iR(r\epsilon) \otimes a^\dagger_{r\epsilon} - iR^\dagger(r\epsilon) \otimes a_{r\epsilon} \right), \tag{1.39}$$

where the operator $a^\dagger_{r\epsilon}$ and $a_{r\epsilon}$ are the creation and annihilation operators describing the oscillators at discrete sites separated by a distance ϵ. The explicit dependence of time reflects the fact that the system is not closed.The parameter $\sqrt{\epsilon}$ is chosen to avoid trivial dynamics for example the system and the auxiliary system not interacting [19]. As we take the limit $n \to \infty$, the number of oscillators increase to infinity, and $\epsilon \to 0$ where the total length $L = n\epsilon$ is left constant. At this point, the evolution operator is just given by:

$$U(L) = \mathcal{P} e^{-i \int_0^L H(s) ds}, \tag{1.40}$$

where $\mathcal{P}$ denotes the path ordered exponential. Now, if we use the definition of a discretized field operator as: $\psi(r\epsilon) = a_{r\epsilon}/\sqrt{\epsilon}$, the evolution operator of the total system A and B is:

$$|\chi\rangle = \mathrm{Tr}_{\mathrm{aux}} \left[\mathcal{P} \mathrm{e}^{\int_0^{\mathrm{L}} \mathrm{dx} \left[\mathrm{K(x)} \otimes \mathbb{1} + \mathrm{iR(x)} \otimes \hat{\psi}^\dagger(\mathrm{x}) - \mathrm{iR}^\dagger(\mathrm{x}) \otimes \hat{\psi}(\mathrm{x}) \right]} \right] |\Omega\rangle, \tag{1.41}$$

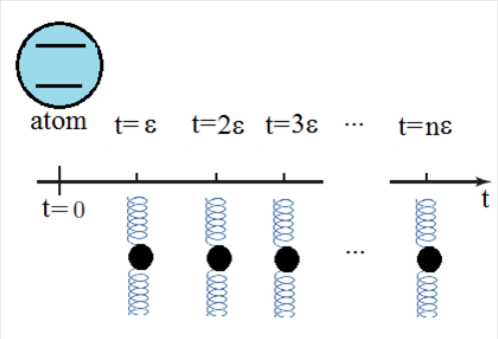


Figure 1.1: Intuitive construction of a cMPS. An auxiliary system B, (the atom), interacts with a group of quantum mechanical harmonic oscillators one at a time, system A.

where $\mathrm{Tr}_{\mathrm{aux}}$ denotes de trace over the auxiliary system B. In the continuous limit, the discrete creation operator becomes the continuous one dimensional field operator $\psi(x)$. If instead of taking directly the limit, we re-express (1.40) by using the definition (A.3), we will end up with products of terms of the form: $V(b,a) = \tau e^{-\int_a^b K(s)ds}$ and $W(r\epsilon) = e^{\sqrt{\epsilon}\left(R(r\epsilon)\otimes a^\dagger_{r\epsilon} - R^\dagger(r\epsilon)\otimes a_{r\epsilon}\right)}$. Rewriting the terms $W(r\epsilon)$ as:

$$e^{\sqrt{\epsilon}\left(R(r\epsilon)\otimes a^\dagger_{r\epsilon} - R^\dagger(r\epsilon)\otimes a_{r\epsilon}\right)}\mathbb{1}_{\mathrm{B}}\otimes|0\rangle_{\mathrm{A}} = e^{-\frac{\epsilon}{2}R^\dagger(r\epsilon)R(r\epsilon)}e^{\sqrt{\epsilon}R(r\epsilon)\otimes a^\dagger_{r\epsilon}}\mathbb{1}_{\mathrm{B}}\otimes|0\rangle_{\mathrm{A}}, \tag{1.42}$$

where the Baker-Hausdorff formula was used up to first order in ϵ. Reinserting this expression into the evolution operator, we have:

$$U(L) = \mathcal{P}e^{\int_0^L dx\left[Q(x)\otimes\mathbb{1}+R(x)\otimes\hat{\psi}^\dagger(x)\right]}, \tag{1.43}$$

where:

$$Q = -\frac{1}{2}R^\dagger R - iK. \tag{1.44}$$

Finally, by taking the trace over the auxiliary system, we recover the original definition (1.37). This argument suggest that the cMPS can actually be constructed under a sequential preparation prescription in the same way as the MPS thus appearing in a natural way as proved in [20]. We should highlight that the form of Eq. (1.44) arises because the state $|\chi\rangle$ is invariant under the gauge transformation $Q \to XQX^{-1}$, $R \to XRX^{-1}$ for any invertible matrix X [1, 21]. Thus in order to fix the gauge, the

relation $Q + Q^\dagger + R^\dagger R = 0$ is imposed which allows Q to be written as in Eq. (1.44) where $K = K^\dagger$ and $R^\dagger R$ is a diagonal matrix. Note that in this discussion there is an implicit correspondence between the time and the position, which will be used later. If we follow A.1 we can have an alternative description of the cMPS states, through the expression:

$$|\chi\rangle = \sum_{n=0}^{\infty} \int_{0<x_1<\ldots<x_n<L} dx_1 \ldots dx_n \phi_n \hat{\psi}^\dagger(x_1) \ldots \hat{\psi}^\dagger(x_n)|\Omega\rangle, \tag{1.45}$$

where

$$\phi_n = \mathrm{Tr}_{\mathrm{aux}}\left[\mathrm{u_Q(x_1, 0)Ru_Q(x_2, x_1)R...Ru_Q(L, x_n)}\right], \tag{1.46}$$

and $u_Q(y, x) = \mathcal{P}\exp[\int_x^y Q(x)dx]$. We can think of (1.45) as the expansion of the state $|\chi\rangle$ in the basis $A = \{|\Omega\rangle, |y_1\rangle, |y_1, y_2\rangle \cdots\}$ where $|y_i, \ldots y_k\rangle = \psi^\dagger(y_i) \cdots \psi^\dagger(y_j)|\Omega\rangle$ is the state of the bosonic system with k particles at the positions $y_i, \ldots, y_k$. Here, ϕ_n represent the amplitude given to each member of the basis. In addition, for the operators inside ϕ_n, we know that R is responsible of the interaction of the system (the field) with the auxiliary system (the atom), furthermore it is related to the creation of a particle. The term $u_Q(y, x)$ can be reinterpreted as an evolution operator with an effective Hamiltonian given by Eq. (1.44) where $R^\dagger R$ takes into account the loss of bosons due to the leaking throughout the cavity. Then ϕ_n has information about the probable positions where the bosons where created. By interacting the system A and the auxiliary system B according to the operator U(L), starting the auxiliary system (the atom) in a state ρ_{B}, the system (the field) in a quantum state $\omega_{\mathrm{A}} = |\Omega\rangle\langle\Omega|$ and taking the partial trace of the auxiliary system it is possible to obtain information about the quantum state of the system as:

$$\sigma_{\mathrm{A}} = \mathrm{Tr_B}\left[\mathrm{U(L)}(\omega_{\mathrm{A}} \otimes \rho_{\mathrm{B}})\mathrm{U}^\dagger(\mathrm{L})\right], \tag{1.47}$$

or instead if we take the partial trace of the system, we have the information of the auxiliary system which we must remind, for our particular case is the cavity plus the atom. Then we have in the discrete case:

$$\rho(r\epsilon) = \mathrm{Tr_A}\left[\mathrm{U(r\epsilon)}\left(\omega_{\mathrm{A}} \otimes \rho(0)_{\mathrm{B}}\right)\mathrm{U}^\dagger\left(\mathrm{r\epsilon}\right)\right]. \tag{1.48}$$

If we expand up to second order and attempt to calculate the derivative respect to the position, we can see that the density matrix describing the state of the auxiliary system, obeys a master equation in the Lindblad form.

$$\frac{d}{dx}\rho(x) = \mathcal{L}\rho(x), \tag{1.49}$$

where the Liouvillian $\mathcal{L}$ is defined via

$$\mathcal{L}\rho(x) := -i\,[K, \rho(x)] + R\rho(x)R^\dagger - \frac{1}{2}R^\dagger R\rho(x) - \frac{1}{2}\rho(x)R^\dagger R. \tag{1.50}$$

This equation will allow us to have only one solution for the steady state, $\lim_{x\to\infty} \dot{\rho}_{ss}(x) = 0$, we therefore have

$$\mathcal{L}\rho_{ss}(x) = 0. \tag{1.51}$$

With the previous discussion and the expansion outlined in Appendix (A.1) and proposed in [1] for the expectation values in the steady state, we have the following relations:

$$\langle\hat{\psi}^\dagger(x)\hat{\psi}(x)\rangle = \mathrm{Tr}[\mathrm{R}^\dagger\mathrm{R}\rho_{\mathrm{ss}}], \tag{1.52}$$

$$\langle\hat{\psi}^\dagger(0)\hat{\psi}^\dagger(x)\hat{\psi}(x)\hat{\psi}(0)\rangle = \mathrm{Tr}\left[\mathrm{R}e^{\tilde{\mathrm{T}}\mathrm{x}}(\mathrm{R}\rho_{\mathrm{ss}}\mathrm{R}^\dagger)\mathrm{R}^\dagger\right], \tag{1.53}$$

$$\langle\hat{\psi}^\dagger(x)\left[-\frac{d^2}{dx^2}\right]\hat{\psi}(x)\rangle = \mathrm{Tr}\left[([\mathrm{Q},\mathrm{R}])^\dagger\,[\mathrm{Q},\mathrm{R}]\,\rho_{\mathrm{ss}}\right], \tag{1.54}$$

$$\langle\hat{\psi}^\dagger(x)\hat{\psi}(0)\rangle = \mathrm{Tr}[\mathrm{R}^\dagger e^{\tilde{\mathrm{T}}\mathrm{x}}(\mathrm{R}\rho_{\mathrm{ss}})], \tag{1.55}$$

$$\langle\hat{\psi}^\dagger(x)\hat{\psi}^\dagger(x)\hat{\psi}(x)\hat{\psi}(x)\rangle = \mathrm{Tr}\left[\mathrm{R}(\mathrm{R}\rho_{\mathrm{ss}}\mathrm{R}^\dagger)\mathrm{R}^\dagger\right], \tag{1.56}$$

with $\tilde{T}$ the superoperator satisfying the master equation Eq. (1.49) and Tr the trace over the auxiliary system. These expressions will be of importance when we establish the correspondence between the field that describes a bosonic model and the optical field leaking out of the cavity described in quantum optics.

1.3 Cavity QED, open system approach

1.3.1 Input-Output theory

Our system under consideration will be a cavity with one of the mirrors semi-transparent. Inside the cavity will be placed an atom. We will be looking at the leaking field that goes through one of the mirrors, with the goal being, to control the cavity in such a way that the effect of the intracavity dynamics reflected in the quantum statistics of the output field has the behaviour that we want [22]. In order to analyse our particular system,

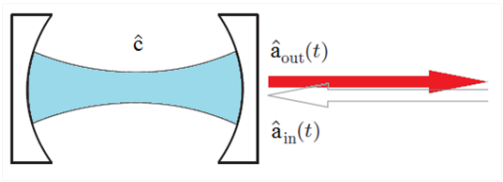


Figure 1.2: Input-Output description provides information of the incoming and outgoing fields in terms of operators $\hat{a}_{\text{in}}$ and $\hat{a}_{\text{out}}$ respectively in the Heisenberg picture. The operator $\hat{c}$ is a system operator involved in the interaction.

the Input-Output approach turns out to be very convenient. Unlike using a master equation, this approach makes distinction between the the input field, (i.e. the light sent to the cavity throughout the mirror), and the output field, (the light leaking out of the cavity) as depicted in Fig. (1.2). This treatment is done via Heisenberg picture operators. To that end, and following [23, 24, 25], we consider a system interacting with a bosonic bath which yields the Hamiltonian:

$$\mathcal{H} = \mathcal{H}_{\text{sys}} + \mathcal{H}_B + \mathcal{H}_{\text{int}}, \tag{1.57}$$

$$\mathcal{H}_B = \hbar \int_{-\infty}^{\infty} d\omega \omega \hat{b}^\dagger(\omega)\hat{b}(\omega), \tag{1.58}$$

$$\mathcal{H}_{\text{int}} = i\hbar \int_{-\infty}^{\infty} d\omega \tilde{\kappa}(\omega) \left[\hat{b}^\dagger(\omega)\hat{c} - \hat{c}^\dagger \hat{b}(\omega)\right], \tag{1.59}$$

where $\mathcal{H}_{\text{sys}}$ is the Hamiltonian of the system, which we leave at the moment unspecified. For our particular problem, it should contain information of the intracavity field mode and any interactions with matter that may be present inside. In addition, $\hat{b}(\omega)$ are the boson annihilation operators for the bath, that obey:

$$\left[\hat{b}(\omega), \hat{b}^\dagger(\omega)\right] = \delta(\omega - \omega'), \tag{1.60}$$

$\tilde{\kappa}(\omega)$ is the coupling constant and $\hat{c}$ represents one of the system operators that is involved in the interaction in $\mathcal{H}_{\text{int}}$. We should point out that although this Hamiltonian comes from many simplifications, provides an accurate model for a range of experimentally accessible regimes. Furthermore, it can be shown that the resultant dynamics is Markovian [23]. The idealization lies in the use of the rotating wave approximation (RWA) and the fact that the limits of integration are from $(-\infty, \infty)$, instead of $(0, \infty)$. The approximation eliminates the rapidly oscillating terms of the complete Hamiltonian, which would be of the form $\mathcal{H}_{\text{int}} \propto \left[\hat{b}^\dagger(\omega) + \hat{b}(\omega)\right]\left[\hat{c} - \hat{c}^\dagger\right]$. Terms like $\hat{c}^\dagger\hat{b}^\dagger(\omega)$ and $\hat{c}\hat{b}(\omega)$ are always fast oscillating so contribute weakly to the interaction. On the other hand, the oscillation in the remaining terms is almost constant. This allows to shift the lower limit to $-\infty$ as those extra frequencies will contribute very little to the integral. From the Heisenberg equation of motion we have that any general operator evolve according to:

$$\dot{\mathcal{O}} = -\frac{i}{\hbar}\left[\mathcal{O}, \mathcal{H}\right]. \tag{1.61}$$

The equations of motion for $\hat{b}(\omega)$ and any arbitrary system operator $\hat{a}$ are derived using the Hamiltonian given in Eq. (1.57) as:

$$\begin{aligned}
\dot{\hat{b}}(\omega) &= -\frac{i}{\hbar}\left[\mathcal{O}, \mathcal{H}_B\right] - \frac{i}{\hbar}\left[\mathcal{O}, \mathcal{H}_{\text{int}}\right] \\
&= -i\omega\hat{b}(\omega) + \tilde{\kappa}(\omega)\hat{c}, &(1.62)\\
\dot{\hat{a}} &= -\frac{i}{\hbar}\left[\mathcal{O}, \mathcal{H}_{\text{sys}}\right] - \frac{i}{\hbar}\left[\mathcal{O}, \mathcal{H}_{\text{int}}\right] \\
&= -\frac{i}{\hbar}\left[\hat{a}, \mathcal{H}_{\text{sys}}\right] + \int d\omega\tilde{\kappa}(\omega)\left\{\hat{b}^\dagger(\omega)\left[\hat{a}, \hat{c}\right] - \left[\hat{a}, \hat{c}^\dagger\right]\hat{b}(\omega)\right\}, &(1.63)
\end{aligned}$$

where it is assumed that $\hat{a}$ and $\hat{b}(\omega)$ commute as they act on different Hilbert spaces. Solving Eq. (1.63) and defining $\hat{b}_0(\omega) = \hat{b}(\omega)|_{t=t_0}$[1] we end up with:

$$\hat{b}(\omega) = e^{-i\omega(t-t_0)}\hat{b}_0(\omega) + \kappa(\omega)\int_{t_0}^{t} e^{-i\omega(t-t')}\hat{c}(t')dt', \tag{1.64}$$

[1]Note: This operators also obey: $\left[\hat{b}_0(\omega), \hat{b}_0^\dagger(\omega')\right] = \delta(\omega - \omega')$.

where the initial condition is such that, $t_0 < t$. If we substitute in Eq. (1.63), we obtain:

$$\begin{aligned}\dot{\hat{a}} =& -\frac{i}{\hbar}\left[\hat{a}, \mathcal{H}_{\text{sys}}\right] \\ &+ \int d\omega \tilde{\kappa}(\omega) \left\{ e^{i\omega(t-t_0)} \hat{b}_0^\dagger(\omega) \left[\hat{a}, \hat{c}\right] - \left[\hat{a}, \hat{c}^\dagger\right] e^{-i\omega(t-t_0)} \hat{b}_0(\omega) \right\} \\ &+ \int d\omega \left[\tilde{\kappa}(\omega)\right]^2 \int_{t_0}^{t} dt' \left\{ e^{i\omega(t-t')} \hat{c}^\dagger(t') \left[\hat{a}, \hat{c}\right] - \left[\hat{a}, \hat{c}^\dagger\right] e^{-iw(t-t')} \hat{c}(t') \right\},\end{aligned} \tag{1.65}$$

where the time argument was dropped in the terms inside the commutator for sake of simplicity. The next step is to make the Markov approximation by assuming that the coupling constant κ independent of the frequency. This is a good approximation within the frequency range of interest like the resonant frequency in a cavity.

$$\tilde{\kappa}(\omega) = \sqrt{\kappa/2\pi}. \tag{1.66}$$

Now, the in-field is defined as:

$$\hat{b}_{\text{in}}(t) = \frac{1}{\sqrt{2\pi}} \int d\omega e^{-i\omega(t-t_0)} \hat{b}_0(\omega), \tag{1.67}$$

which also satisfies their own commutation relations, $\left[\hat{b}_{\text{in}}(t), \hat{b}_{\text{in}}^\dagger(t')\right] = \delta(t-t')$. Using Eq. (1.67) with the properties:

$$\int_{-\infty}^{\infty} d\omega e^{-i\omega(t-t')} = 2\pi\delta(t-t'), \tag{1.68}$$

$$\int_{t_0}^{t} \hat{c}(t')\delta(t-t')dt' = \frac{1}{2}\hat{c}(t), \tag{1.69}$$

the quantum Langevin equation is obtained as:

$$\dot{\hat{a}} = -\frac{i}{\hbar}\left[\hat{a}, \mathcal{H}_{\text{sys}}\right] - \left[\hat{a}, \hat{c}^\dagger\right] \left[\frac{\gamma}{2}\hat{c} + \sqrt{\gamma}\hat{b}_{\text{in}}\right] + \left[\frac{\gamma}{2}\hat{c}^\dagger + \sqrt{\gamma}\hat{b}_{\text{in}}^\dagger\right] \left[\hat{a}, \hat{c}\right]. \tag{1.70}$$

For the simpler case of the system being a cavity see [25], the term $\frac{\gamma}{2}\hat{c}$ is interpreted as damping while $\hat{b}_{\text{in}}$ is understood as quantum noise. If we note that the terms $\frac{\kappa}{2}\hat{c} + \sqrt{\kappa}\hat{b}_{\text{in}}$ and $\frac{\kappa}{2}\hat{c}^\dagger + \sqrt{\kappa}\hat{b}_{\text{in}}^\dagger$ commute with all system operators, then integrating $\hat{b}(\omega)$:

$$\frac{1}{\sqrt{2\pi}} \int d\omega \hat{b}(\omega) = \hat{b}_{\text{in}} + \frac{\sqrt{\kappa}}{2}\hat{c}(t). \tag{1.71}$$

Now by a similar process, if we take the time such that $t_1 > t$, that is to say, the *final conditions* in analogy to (1.64), it is obtained:

$$\hat{b}(\omega) = e^{-i\omega(t-t_1)}\hat{b}_1(\omega) + \tilde{\kappa}(\omega)\int_t^{t_1} e^{-i\omega(t-t')}\hat{c}(t')dt', \tag{1.72}$$

where similarly it can be defined the output field as:

$$\hat{b}_{\text{out}}(t) = \frac{1}{\sqrt{2\pi}}\int d\omega e^{-i\omega(t-t')}\hat{b}_1(\omega), \tag{1.73}$$

And in the same way as with (1.70), we can arrive to a Langevin equation in terms of the output field as:

$$\dot{\hat{a}} = -\frac{i}{\hbar}\left[\hat{a}, \mathcal{H}_{\text{sys}}\right] - \left[\hat{a}, \hat{c}^\dagger\right]\left[\frac{\kappa}{2}\hat{c} + \sqrt{\kappa}\hat{b}_{\text{out}}\right] + \left[\frac{\kappa}{2}\hat{c}^\dagger + \sqrt{\kappa}\hat{b}^\dagger_{\text{out}}\right]\left[\hat{a}, \hat{c}\right]. \tag{1.74}$$

and after integrating $\hat{b}(\omega)$ a similar expression as (1.71) is derived:

$$\frac{1}{\sqrt{2\pi}}\int d\omega\hat{b}(\omega) = \hat{b}_{\text{out}} + \frac{\sqrt{\kappa}}{2}\hat{c}(t). \tag{1.75}$$

Then, subtracting (1.71) and (1.75) we arrive to the input output relation:

$$\hat{b}_{\text{out}} - \hat{b}_{\text{in}} = \sqrt{\kappa}\hat{c}(t). \tag{1.76}$$

Then all the information of the leaking field is quite intuitive in terms of the input field sent towards the cavity plus the behaviour of the system operator that interacts with the fields. We expect that this operator would be of the form of a lowering operator in order to describe the photons leaking out of the cavity.

1.3.2 Correlation functions in open systems

In an abstract way, a general system obeys a master equation that can be written as:

$$\dot{\rho}(t) = L(t)\rho(t), \tag{1.77}$$

where L is a linear superoperator, (that is, transform operators to operators) and may depend explicitly of the time. The formal solution to that equation can be written as:

$$\rho(t) = \mathcal{P} \exp\left\{ \int_{t_0}^{t} dt' L(t') \right\} \rho(t_0) = V(t, t_0)\rho(t_0), \tag{1.78}$$

where $\mathcal{P}$ stands for time ordered exponential and $V(t, t_0)$ is the evolution operator which satisfies the same equation (1.77) as $\rho(t)$. On the other hand, it is usual that we need to calculate the correlation functions from system operators in order to measure certain quantities as:

$$\langle A(t+\tau)B(t)\rangle = \mathrm{Tr}_{\mathrm{sys}}\left\{ \mathrm{Tr}_B \left\{ A(t+\tau)B(t)\rho_s \otimes \rho_B \right\} \right\}, \tag{1.79}$$

where the operators are in the Heisenberg picture. One way to calculate this is by writing explicitly the evolution operator as:

$$\langle A(t+\tau)B(t)\rangle = \mathrm{Tr}_{\mathrm{sys}}\left\{ \mathrm{Tr}_B \left\{ e^{iH(t+\tau)} A e^{-iH(t+\tau)} e^{iH(t)} B e^{-iH(t)} \rho_s \otimes \rho_B \right\} \right\}. \tag{1.80}$$

Now, by using the properties of commutation of the trace, and assuming that A and B are operators of the system, then we can rewrite the last expression to obtain:

$$\langle A(t+\tau)B(t)\rangle = \mathrm{Tr}_{\mathrm{sys}}\left\{ A\mathrm{Tr}_B \left\{ e^{-iH(\tau)} B \rho_{\mathrm{tot}}(t) e^{iH(\tau)} \right\} \right\}. \tag{1.81}$$

The trace of the term in brackets is the evolution of the total density matrix. The equation of motion for this expression is:

$$X(\tau, t) = e^{-iH(\tau)} B \rho_{\mathrm{tot}} e^{iH(\tau)}, \tag{1.82}$$

and in terms of τ is:

$$i\hbar \frac{\partial}{\partial \tau} X(\tau, t) = [H, X(\tau, t)], \tag{1.83}$$

then it can be deduced that $\mathrm{Tr}\{X(\tau,t)\}$ obeys the master equation as a function of τ, where

$$\begin{aligned}\mathrm{Tr}_B\{X(\tau,t)\} =& V(t+\tau,t)\mathrm{Tr}_B\{X(0,t)\}\\ =& V(t+\tau,t)\{B\rho(t)\}.\end{aligned} \tag{1.84}$$

Then the correlation function in terms of just operators and density matrix of the system is:

$$\langle A(t+\tau)B(t)\rangle = \mathrm{Tr}_{\mathrm{sys}}\{AV(t+\tau,t)\{B\rho(t)\}\}. \tag{1.85}$$

In a similar way the following relations can be obtained:

$$\langle A(t_0)B(t_1)C(t_1)D(t_0)\rangle = \mathrm{Tr}_{\mathrm{sys}}\{BCV(t_1,t_0)D\rho(t_0)A\}, \tag{1.86}$$

$$\langle A(t)B(t+\tau)\rangle = \mathrm{Tr}_{\mathrm{sys}}\{BV(t+\tau,t)\rho(t)A\}, \tag{1.87}$$

$$\langle B(t+\tau)A(t)\rangle = \mathrm{Tr}_{\mathrm{sys}}\{BV(t+\tau,t)A\rho(t)\}. \tag{1.88}$$

This expressions will be useful when we try to calculate the correlation functions for the leaking field of the cavity.

1.3.3 The interaction picture

In quantum theory, when considering electromagnetic fields it is necessary to consider the interaction between light and matter. Therefore a Hilbert space that describes the quantized electromagnetic field and the charged particles needs to be constructed. In addition, in the experiments we are interested in, the interaction energy between the charged particles and the radiation field is smaller than the energy of individual photons thus, it is useful to rewrite the Hamiltonian as

$$H^{(S)} = H_0^{(S)} + H_{\mathrm{int}}^{(S)}, \tag{1.89}$$

where $H^{(S)}$ is the Schrodinger picture Hamiltonian of the total system. $H_0^{(S)}$, the unperturbed Hamiltonian, represents the non- interacting terms as it describes the particles and fields without interaction and the terms describing the radiation-matter interaction are contained in the interaction Hamiltonian $H_{\mathrm{int}}^{(S)}$. In the cases where the Schrodinger

equation with the full Hamiltonian $H^{(S)}$ can not be solved exactly, because the interacting term is too complicated, if the interaction is weak, it is possible to find an approximate solution by perturbative methods and when this is not possible, if we add the the resonant wave approximation [26] we still can find useful approximations. For this purpose, it is useful to separate the fast (hight energy) evolution due to $H_0^{(S)}$ from the slow (low energy) evolution due to $H_{\text{int}}^{(S)}$. To this end, the interaction picture state vector is defined by the unitary transformation

$$|\psi^{(I)}\rangle = U_0^\dagger(t)|\psi^{(S)}\rangle, \tag{1.90}$$

where

$$U_0(t) = \exp\left[-\frac{i(t-t_0)}{\hbar}H_0^{(S)}\right], \tag{1.91}$$

which is a unitary operator that evolves according to

$$i\hbar\frac{\partial}{\partial t}U_0(t) = H_0^{(S)}U_0(t), \qquad U_0(t_0) = \mathbb{1}. \tag{1.92}$$

This picture possesses states and operators which all vary with time. In the interaction picture, the state $|\psi^{(I)}\rangle$ will evolve at a slower rate then the state vector does not change appreciably over an optical period as it can be proved by taking the partial derivative in time of the interaction picture

$$i\hbar\frac{\partial}{\partial t}|\psi^{(I)}\rangle = H_{\text{int}}^{(I)}(t)|\psi^{(I)}\rangle. \tag{1.93}$$

The operators are transformed according to:

$$X^{(I)}(t) = U_0^\dagger(t)X^{(S)}U_0(t), \tag{1.94}$$

in order to preserve the norm

$$\langle\Psi_{(I)}|X^{(I)}(t)|\Phi_{(I)}\rangle = \langle\Psi_{(S)}|X^{(S)}(t)|\Phi_{(S)}\rangle. \tag{1.95}$$

Moreover, they evolve in time according to

$$i\hbar\frac{\partial}{\partial t}X^{(I)}(t) = \left[X^{(I)}, H_0\right], \tag{1.96}$$

with the obvious exception of the free Hamiltonian

$$H_0^{(I)}(t) = U_0^{\dagger}(t)H_0^{(S)}U_0(t) = H_0^{(S)}. \tag{1.97}$$

1.3.4 Lieb-Liniger model

We introduce the model of study known as the Lieb-Liniger. This, describes a non relativistic gas of bosonic particles constrained in a one dimensional container. These particles are interacting under a delta function potential. In the original paper published in 1963 [4], they showed that this model can be solved exactly using the Bethe Ansat approach. Originally it was just a toy model that allowed to study if the Bogoliubov perturbation theory was in agreement with his model. Which turned out to be valid only for small values of the coupling constant. The reason to introduce such model was to find a two body potential that was local, time and velocity independent were one could derive without any approximations, the energy levels and wave functions of the system [27]. It is a realistic model although in the experiments, the potentials used to trap the particles generally break the translational invariance. It is a perfect model complex enough but exactly solvable, continuous and integrable using techniques like the Bethe Ansatz approach. [4], since then, there has been more developments on this model [28]. Following [4] and [28], the system in the first quantized form, obeys a Hamiltonian of the form:

$$H = -\sum_{i=1}^{N}\frac{\partial^2}{\partial x_i^2} + 2c\sum_{i<j}^{N}\delta(x_i - x_j), \tag{1.98}$$

which represents N particles in one dimension interacting through a delta function potential, where each of the variables x_i are defined in the region $[0, L]$ and the wave function that satisfies $H\psi = E\psi$ has imposed periodic boundary conditions. We are interested in the repulsive case, $c \geq 0$, which represents the interaction strength of the potential. If we transform the Hamiltonian into the second quantization form, and using

Eq. (1.35)

$$\mathcal{H} = \int_{-\infty}^{+\infty} dx \left[\frac{d\hat{\psi}^\dagger(x)}{dx} \frac{d\hat{\psi}(x)}{dx} + c\hat{\psi}^\dagger(x)\hat{\psi}^\dagger(x)\hat{\psi}(x)\hat{\psi}(x) \right], \tag{1.99}$$

where the quantum Bose fields $\hat{\psi}(x)$ satisfy the commutation relations

$$[\hat{\psi}(x), \hat{\psi}^\dagger(x)] = \delta(x-y), \qquad [\hat{\psi}(x), \hat{\psi}(x)] = [\hat{\psi}^\dagger(x), \hat{\psi}^\dagger(x)] = 0. \tag{1.100}$$

Also following [4], it is possible to define the particle number operator $\hat{N}$ and the momentum operator $\hat{P}$

$$\hat{N} = \int_0^L \hat{\psi}^\dagger \hat{\psi} dx, \qquad \hat{P} = -\frac{i}{2} \int_0^L \left[\frac{\partial \hat{\psi}^\dagger}{\partial x} \right] \hat{\psi} dx, \tag{1.101}$$

which commute with the Hamiltonain $\mathcal{H}$ Eq. (1.99) i.e. $[\mathcal{H}, \hat{P}] = [\mathcal{H}, \hat{N}] = 0$. Thus these operators represent conserved quantities. In the limit of infinite interaction strength, $c \to \infty$ the model reduces the one of impenetrable bosons discussed by Girardeau [5]. This is an important characteristic that our simulation will recover. At this limit, all the bosons confined to the one dimensional line cannot pass each other and will not be able to exchange places, the motion of the bosons will become strongly correlated given the infinite value of c and in [5] it is demonstrated that the case of impenetrable bosons is equivalent fermions with no interactions. since the Fermi wave functions will vanish as soon as two bosons come together. Nowadays it is possible to create such a system and developed techniques to measure its properties like the energy density [29] For example by measuring the correlation function g_2, it is possible to determine the local pair correlation function over a wide range of coupling strengths.[30] In the case of [29] done by Toshiya Kinoshita, Trevor Wenger, and David Weiss, they created a system of freely moving 1D Bose gases of cold rubidium-87 atoms are confined in an ensemble of long cigar-shaped tubes made by a combination of two light traps. The atomic interaction strength can be varied by changing the trap depths.

CHAPTER 2

TOY MODEL: EMPTY DRIVEN CAVITY

As a reminder of the intentions of this work, our ultimate goal will be to use a cavity QED system as a quantum simulator and show that we can reproduce the physical properties of 1-dimensional gases. Furthermore, we hope to understand why that is the case. That knowledge will help us to propose more interesting simulators. However although the complex interactions between a simple cavity, and an atom are widely understood in the Jaynes-Cummings model, the introduction of a driving laser coupled to the atom and a field leaking from an open cavity not only will enrich the properties of the simulator but also it will make more difficult to create an intuitive picture. The simplest solution to this obstacle is to simplify our problem by first analysing the output field of an empty driven cavity system and build up our intuition from there.

2.1 Correlations of a cavity using Input-Output fields

If we want to describe a simple driven cavity with a leaking field, in other words an open system, we will require to deal separately with the leaking field that we are interested in measuring and the intra-cavity field, the field that occurs inside the cavity, which affects the leaking field. From section (1.3.1) , it was discussed that this kind of open systems are best treated using the input-output theory as in principle this treatment will allow us to determine the effect of the intra-cavity fields on the statistics of the leaking field . Thus if we define the intra-cavity field operator $\hat{a}$, the leaking rate as κ and the input and output operators describing the incoming and outgoing fields as $\hat{a}_{\text{in}}(t)$ and $\hat{a}_0(t)$ then from Eq. (1.76) the following relation holds: $\hat{a}_0(t) = \hat{a}_{\text{in}}(t) + \sqrt{\kappa}\hat{a}(t)$. This expression describes the leaking field in terms of the input field and the

intracavity operator. Furthermore, by using causality arguments and the commutation relations of the input fields $\left[\hat{a}_{\text{in}}(t), \hat{a}^{\dagger}_{\text{in}}(t')\right] = \delta(t-t')$ described in section (1.3.1), we can establish a connection between the correlation functions of the output operators with those describing the intracavity field according to [23, 24] as:

$$\langle \hat{a}_0^{\dagger}(t)\hat{a}_0(t')\rangle = \kappa\langle \hat{a}^{\dagger}(t)\hat{a}(t')\rangle, \tag{2.1}$$

$$\langle \hat{a}_0(t)\hat{a}_0(t')\rangle = \kappa\langle \hat{a}(t_{\text{max}})\hat{a}(t_{\text{min}})\rangle, \tag{2.2}$$

$$\langle \hat{a}_0^{\dagger}(t)\hat{a}_0^{\dagger}(t')\rangle = \kappa\langle \hat{a}^{\dagger}(t_{\text{min}})\hat{a}^{\dagger}(t_{\text{max}})\rangle, \tag{2.3}$$

$$\langle \hat{a}_0(t)\hat{a}_0^{\dagger}(t')\rangle = \kappa\langle \hat{a}^{\dagger}(t')\hat{a}(t)\rangle + \delta(t'-t), \tag{2.4}$$

provided that there is no input field i.e. $\hat{a}_{\text{in}}(t)|0\rangle = 0$ where $t_{\text{min}} < t_{\text{max}}$. Eqs. (2.1, 2.2, 2.3) show us that we can focus exclusively on correlation functions of the intra-cavity operator since the only difference with the correlation functions of the output field operator is a constant of proportionality κ. The Dirac delta in the case of the fourth expression comes from the fact that we need to reorder the operators in normal order. Thus there is a direct relationship between both correlation functions furthermore, the photon statistics of the output field will be the same as the intra-cavity field.

2.2 Empty driven cavity

We will start our analysis with an empty cavity driven by a single mode laser. The walls of the cavity are considered to be mirrors but one of them is totally reflective and the other semitransparent. The leaking rate will be described by the constant κ. Our task at hand will be to find the corresponding Hamiltonian to characterize this system and from it to find the master equation that will describe its dynamics. Let us consider for this particular case, that the cavity is driven by a classical laser at a frequency ω_D, amplitude E_0 and arbitrary phase ϕ, also the natural frequency of the cavity is ω. The Hamiltonian $\mathcal{H}$ describing the system in the *Schrödinger* picture is given by

$$\mathcal{H} = \omega\hat{a}^{\dagger}\hat{a} + E_0\cos(\omega_D t + \phi)(\hat{a} + \hat{a}^{\dagger}), \tag{2.5}$$

where $\hat{a}$ is the intra-cavity annihilation operator. The first term describes the free field energy while the second term describes the energy interaction of the driving field with the cavity. We now use that Hamiltonian to characterize the state of this system, given by the density matrix $\rho(t)$. The dynamics that it obeys, is given by the master equation in the Lindblad form as:

$$\dot{\rho}(t) = -i\left[\mathcal{H}, \rho\right] + 2\kappa\hat{a}\rho\hat{a}^{\dagger} - \kappa\hat{a}^{\dagger}\hat{a}\rho - \kappa\rho\hat{a}^{\dagger}\hat{a}, \tag{2.6}$$

where the last three terms describe the losses of the cavity at the rate κ. Given the strength of the optical fields, we can use the standard rotating wave approximation approach to get rid of the fast rotating terms, and rewrite $\mathcal{H}$ as:

$$\mathcal{H} = \omega\hat{a}^{\dagger}\hat{a} + \frac{E_0}{2}\left\{\hat{a}e^{i\omega_D t + i\phi} + \hat{a}^{\dagger}e^{-i\omega_D t - i\phi}\right\}. \tag{2.7}$$

The solution of Eq. (2.6) for the density matrix $\rho(t)$, will allow us to calculate the temporal evolution of observables . However, as we will show in the next section, we only need to know the differential equation Eq. (2.6) to calculate the evolution of expectation values and other correlation functions of interest such as g_1 and g_2. This will be used in the next chapters to characterize our cavity QED simulator so it will be a good idea to get familiar with them for this simple model.

2.2.1 Expectation value of the annihilation operator $\langle\hat{a}(t)\rangle$

As we mentioned in the previous section, in order to obtain the evolution of the expectation value for different operators, we only need to know the differential equation that obeys $\rho(t)$ and the Hamiltonian of the system we are interested in. To illustrate the idea, we will calculate the expectation value of the annihilation operator $\hat{a}(t)$ as well as the creation operator $\hat{a}^{\dagger}(t)$. One way to calculate them is using the fact that $\langle\dot{\hat{a}}(t)\rangle = \mathrm{Tr}[\hat{a}\dot{\rho}(t)]$, where Tr represents the trace. That means that to calculate the temporal variation of the expectation value of the annihilation operator, we just need to calculate the trace of the the temporal variation of the density matrix times the annihilation operator at at time zero. In our particular example, if we substitute Eq. (2.6) on the right hand side and define $A(t)$ as the expectation value of the annihilation operator

$A(t) = \langle \hat{a}(t) \rangle$, we obtain:

$$\dot{A}(t) + (\kappa + i\omega)A(t) = -i\frac{E_0}{2}e^{-i\omega_D t - i\phi}, \tag{2.8}$$

where (2.7) was the Hamiltonian used to calculate the commutator in (2.6). This new differential equation, is similar to the one of a driven damped oscillator given by the function $A(t)$ subject to the oscillatory driving force $-i\frac{E_0}{2}e^{-i\omega_D t - i\phi}$ given by the laser and a friction term $\kappa A(t)$ due to the leaking of photons from the cavity. If we assume that the cavity is initially empty, then the corresponding initial condition $\langle \hat{a}(0) \rangle = 0$ gives a solution of the form:

$$\langle \hat{a}(t) \rangle = \frac{E_0 e^{-\kappa t - i\omega t - i\phi}}{2\left(-i\kappa - \omega_D + \omega\right)} + \frac{E_0 e^{-i\omega_D t - i\phi}}{2\left(i\kappa + \omega_D - \omega\right)}, \tag{2.9}$$

where the first expression is a transient term that oscillates at the natural frequency of the cavity ω and tends exponentially to zero for larger times. The second expression represents the steady state solution which survives for larger times and and represents a sinusoidal oscillation at the frequency of the laser ω_D. This behaviour is showcased in Fig. (2.1) where the real part of $\langle \hat{a}(t) \rangle$ is shown. Note how the transient term is the responsible of the variation of the amplitude at the beginning of the oscillation as it tends to a constant value approximately for times $t > 80$. Furthermore, similarly to its classical counterpart, the amplitude now depends on the inverse of the decay rate κ and the inverse of the off-resonant term $\omega - \omega_D$ this result makes sense since larger values of κ means a large flux of photons leaking of the cavity and the bigger the off-resonant term the less likely that an excitation is produced inside the cavity. Both of these cases will result in a decrease in the amplitude. This features will be inherited when we include the atom into the system. As a final remark, note that in the non RWA case, we just need to add the hermitian conjugate expressions of Eq. (2.9). The next step will be to calculate expectation values that involve more than one operator such as the expectation value of the number of photons. This will provide us with information of the dependence of the number of photons inside the cavity respect to the diverse parameters of the system. More over it will allow us to generalize our method to find differential equations of expectation values of products of operators and ultimately calculate the

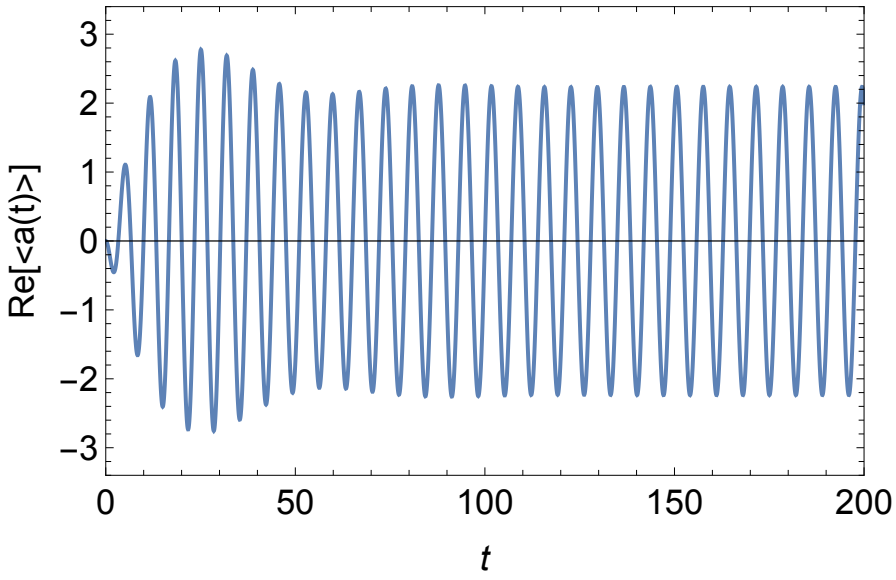


Figure 2.1: Temporal evolution of the real part of the expectation value of the annihilation operator a for arbitrary values $\kappa = 0.05, \omega - \omega_D = 0.1, E_0 = 0.5, \phi = 0$. For small values of t, we can appreciate the effect of the transient term as a variation in the amplitude but for longer times, approximately $t > 80$ the oscillator reach the steady state where the expectation value oscillates at the frequency of the laser ω_D at a constant amplitude.

correlation functions g_1 and g_2 used to describe the performance of our simulator.

2.2.2 Expectation value of the number operator $\langle \hat{n}(t) \rangle$

Let us recall that the number density operator, is defined as $\hat{n}(t) = \hat{a}^\dagger(t)\hat{a}(t)$. Thus, in a similar way to the previous section, the expectation value of the number density operator $\langle \hat{n}(t) \rangle = \langle \hat{a}^\dagger(t)\hat{a}(t) \rangle$ can be rewritten as $\langle \hat{n}(t) \rangle = \mathrm{Tr}[\hat{a}^\dagger \hat{a} \rho(t)]$. If we define $n(t) = \langle \hat{n}(t) \rangle$ and using again Eq. (2.6) inside the trace, we can obtain the differential equation for $n(t)$ as:

$$\dot{n}(t) + 2\kappa n(t) = i\frac{E_0}{2} e^{-i\omega_D t - i\phi} * A(t) + h.c. \tag{2.10}$$

$$= \frac{iE_0^2 \left(1 - e^{-\kappa t + it(\omega_D - \omega)}\right)}{4\left(i\kappa + \omega_D - \omega\right)} + h.c. \tag{2.11}$$

Note how Eq. (2.10) depends on our previous solution, the expectation value of the annihilation operator $A(t)$, Eq. (2.9). The homogeneous differential equation will be only an exponentially decaying function at the decaying rate 2κ. However, the full equation, corresponds to the differential equation of an exponentially decaying function

driven by a constant force and an oscillatory decaying force. Solving for the initial condition of no photons in the cavity at time $t = 0$, corresponds to define $n(0) = 0$ then the expectation value $n(t) = \langle \hat{n}(t) \rangle$ takes the form:

$$\langle \hat{n}(t) \rangle = \frac{E_0^2 \left(-e^{t(-\kappa - i\omega_D + i\omega)} - e^{t(-\kappa + i\omega_D - i\omega)} + e^{-2\kappa t} + 1 \right)}{4 \left(\kappa^2 + (\omega_D - \omega)^2 \right)} \tag{2.12}$$

$$= \frac{E_0^2 e^{-t\kappa} \left(\cosh(\kappa t) - \cos\left(t \left(\omega_D - \omega \right) \right) \right)}{2 \left(\kappa^2 + (\omega_D - \omega)^2 \right)}, \tag{2.13}$$

which is independent of any phase ϕ of the laser. The second term of Eq. (2.13) corresponds to oscillations depending on the off-resonant term $(\omega_D - \omega)$. This dependence is a reflection of the interaction of the laser and the cavity. Note that the more the difference between the frequency of the laser and the frequency of the cavity, the faster the oscillations for the mean number of photons. The oscillation is modulated by an exponentially decaying function so for larger times it will tend to zero. On the other hand the first term $e^{-t\kappa} \cosh(\kappa t)$ will tend to the constant value 1/2. Fig. (2.2) (blue line) shows that is the case for the off-resonant case where starting with no photos at time zero, the laser start to increase that number and after a damped oscillation it tends to a constant value. The resonant case Fig. (2.2) (red line) lack of any oscillation and just limits to grow to a constant value after its initial condition of zero photons according to the relation $\frac{E_0^2}{4\kappa}(1 - \exp(\kappa t))^2$ obtained from Eq. (2.13) after the condition $\omega = \omega_D$. The constant value obtained in both cases comes from the limit for larger times for Eq. (2.13), where we arrive to a simple expression for the steady state:

$$\langle \hat{n}(t) \rangle_s = \frac{E_0^2}{4(\kappa^2 + (\omega_D - \omega)^2)}, \tag{2.14}$$

which simply indicates that the expectation value of the density of photons will tend to a constant value in terms of the decay rate κ and the off-resonant term $\omega_D - \omega$. This means that the number of photons will naturally increase if the leaking rate diminishes, thus leaving most of the photons inside the cavity. In addition, the closer to resonance the more photons will be produced inside the cavity. Finally, from Eq. (2.13) it is interesting to note that as $\kappa \to 0$, $n(t) \to \frac{E_0^2 t^2 \operatorname{sinc}^2((\omega - \omega_D)t)}{4}$ which goes as a quadratic function of t for the resonant case $\omega = \omega_D$, shown in Fig. (2.2) (green line). This only reflects that the number of photons grows infinitely as time increases since all of them

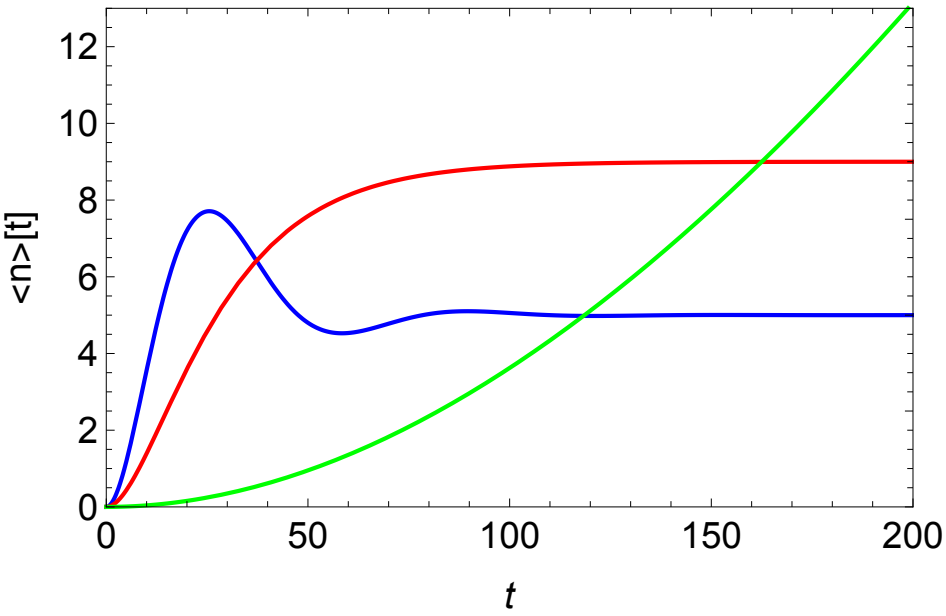


Figure 2.2: Expectation value of the number of photons $\langle \hat{n}(t) \rangle$ in a leaking empty cavity. At $t = 0$ its value is zero as per the initial conditions. All graphs are increasing functions of t for its initial values since the laser is starting to produce photons. a) In blue, the off-resonant case, $\kappa = 0.05, \omega - \omega_D = 0.1, E_0 = 0.5$. b) In red, the resonant case $\kappa = 0.05, \omega - \omega_D = 0, E_0 = 0.3$.c) In green the limit case of κ close to zero that approximates to the case of a lossless cavity where the behaviour is quadratic in time $\kappa = 0.001, \omega - \omega_D = 0, E_0 = 0.04$. We reduced the intensity by an order of 10 since $\langle \hat{n}(t) \rangle$ grows faster in this case.

will remain in the cavity.

As a final remark, If we decide to calculate $\langle \hat{a}(t)\hat{a}^\dagger(t) \rangle$, we will discover that it obeys the same differential equation (2.10) apart from an additive constant and the initial condition $\langle \hat{a}(0)\hat{a}^\dagger(0) \rangle = 1$ since at $t = 0$ the commutation relation holds. Thus we find that

$$\langle \hat{a}(t)\hat{a}^\dagger(t) \rangle = 1 + \langle n(t) \rangle. \tag{2.15}$$

This tells us that the expectation value of the commutation relations over time is equal to:

$$\langle [\hat{a}(t), \hat{a}^\dagger(t)] \rangle = 1. \tag{2.16}$$

2.2.3 Two point correlation functions

In the following section, we will just generalize our method of obtaining differential equations of expectations values now for an arbitrary product of creation and annihilation operators of order $n + m$ such as: $\langle \hat{a}^{\dagger n}(t)\hat{a}^m(t) \rangle$. This will be useful later on to,

calculate the differential equations of correlation functions which depend on 2 different values of time. In order to achieve that generalization, let us remember again that $\langle \hat{a}^{\dagger n}(t)\hat{a}^m(t)\rangle = \mathrm{Tr}\left[\hat{a}^{\dagger n}\hat{a}^m\dot{\rho}\right]$, where $\dot{\rho}$ is given by Eq. (2.6) with the Hamiltonian given by (2.7). After substitution of those equations and applying mathematical induction over n and m, we derived the following expression:

$$\begin{aligned}\mathrm{Tr}\left[\hat{a}^{\dagger n}\hat{a}^m\dot{\rho}\right] =& -\left(i\omega(m-n)+\kappa(m+n)\right)\mathrm{Tr}\left[\hat{a}^{\dagger n}\hat{a}^m\rho\right] \\ &+i\alpha n\mathrm{Tr}\left[\hat{a}^{\dagger n-1}\hat{a}^m\rho\right] - i\alpha^* m\mathrm{Tr}\left[\hat{a}^{\dagger n}\hat{a}^{m-1}\rho\right],\end{aligned} \tag{2.17}$$

where $\alpha = \frac{E_0}{2}e^{i\omega_D t+i\phi}$. This is a recurrence relationship where the differential equation of the expectation value will depend on expectation values of lower order. Finally, notice that the operators are in normal order. Thus for other cases, it is necessary first to reorder the operators by using the usual commutation relation $[\hat{a},\hat{a}^\dagger]=1$.

Quantum Regression Theorem

Moving on to calculating the two point correlation functions, that is expectation values of operators that depend on different times, we make use of the quantum regression theorem. According to [25, 31], if there exist a complete set of system operators $\hat{A}_\mu$, with $\mu = 1, 2, ...$, such that

$$\langle\dot{\hat{A}}_\mu\rangle = \sum_\lambda M_{\mu\lambda}\langle\hat{A}_\lambda\rangle, \tag{2.18}$$

then for arbitrary operators $\hat{O}_1$, $\hat{O}_2$ and time $\tau \geq 0$ it is true that

$$\frac{d}{d\tau}\langle\hat{O}_1(t)\hat{A}_\mu(t+\tau)\hat{O}_2(t)\rangle = \sum_\lambda M_{\mu\lambda}\langle\hat{O}_1(t)\hat{A}_\lambda(t+\tau)\hat{O}_2(t)\rangle. \tag{2.19}$$

This means that the temporal variation in τ for the term in the left of Eq. (2.19) is equal to the same linear combination of constant values $M_{\mu\nu}$ from Eq. (2.18) with the substitution of $\langle\hat{A}_\lambda\rangle \to \langle\hat{O}_1(t)\hat{A}_\lambda(t+\tau)\hat{O}_2(t)\rangle$.

2.2.4 First order correlation function $g_1(\tau)$

Classically the first-order correlation function is related to the interferometry experiments on the electromagnetic fields to measure the degree of coherence of two signals.

In our particular case, the degree of coherence of a signal measured at two points in time. The nature of the field correlation function and hence of the interference fringes depends on the light incident on the interferometer. If the statistical properties of the light source are stationary, namely the influences that dictate the fluctuations do not change with time then we can define the quantum equivalent of the two-point first correlation function as [32]

$$g_1(t,\tau) = \frac{\langle \hat{a}^\dagger(t)\hat{a}(t+\tau)\rangle}{\langle \hat{a}^\dagger(t)\hat{a}(t)\rangle}. \tag{2.20}$$

For our particular toy model, we will be able to deduce the analytical value of $\langle \hat{a}^\dagger(t)\hat{a}(t+\tau)\rangle$ defined Eq. (2.20) using the quantum regression theorem. First we note that Eq. (2.8) can be rewritten in the form of Eq. (2.18) as:

$$\langle \dot{\hat{a}}(t)\rangle = -(\kappa + i\omega)\langle \hat{a}(t)\rangle - i\frac{E_0}{2}e^{-i\omega_D t - i\phi}\langle \mathbb{1}(t)\rangle, \tag{2.21}$$

for $\hat{A}_\lambda = \{\hat{a}(t), \mathbb{1}(t)\}$, where the average of the identity operator $\mathbb{1}$ is 1 for all t. Note that the coefficients $M_{\mu\nu} = \{-(\kappa+i\omega), -i\frac{E_0}{2}e^{-i\omega_D t - i\phi}\}$ can depend on t. Now following Eq. (2.19) for $\hat{O}_1(t) = \hat{a}^\dagger(t)$ and $\hat{O}_2(t) = \mathbb{1}(t)$ we obtain the differential equation for $\hat{A}_\mu = \langle \hat{a}^\dagger(t)\hat{a}(t+\tau)\rangle$

$$\frac{d\langle \hat{a}^\dagger(t)\hat{a}(t+\tau)\rangle}{d\tau} = -(\kappa + i\omega)\langle \hat{a}^\dagger(t)\hat{a}(t+\tau)\rangle - i\frac{E_0}{2}e^{-i\omega_D t - i\phi}\langle \hat{a}^\dagger(t)\rangle, \tag{2.22}$$

where $\mathbb{1}(t+\tau) = \mathbb{1}$ so it doesn't affect $\langle \hat{a}^\dagger(t)\rangle$. Note that we need to know a lower order expectation value, the creation operator $\langle \hat{a}^\dagger(t)\rangle$, which reflect a recursive relation that will come across as we use the quantum regression theorem Eq. (2.19). The solution is of the form:

$$\begin{aligned}\langle \hat{a}^\dagger(t)\hat{a}(t+\tau)\rangle = &\frac{E_0^2\left(-e^{-i(\tau\omega_D + t(-i\kappa+\omega_D-\omega))} - e^{-i(-t\omega_D+(\omega-i\kappa)(t+\tau))}\right)}{4\left((\omega_D-\omega)^2+\kappa^2\right)} \\ &+ \frac{E_0^2\left(e^{-i\tau\omega_D} + e^{-\kappa(2t+\tau)-i\tau\omega}\right)}{4\left((\omega_D-\omega)^2+\kappa^2\right)},\end{aligned} \tag{2.23}$$

with this expression and $\langle \hat{a}^\dagger(t)\hat{a}(t)\rangle$ Eq. (2.13) we finally have $g_1(t,\tau)$ which depends inversely on the detuning $\omega_D - \omega$ and the decay rate κ and proportional to the intensity

E_0^2. In a more illustrative case, if we take the limit where $t \to \infty$

$$\lim_{t\to\infty} \langle \hat{a}^\dagger(t)\hat{a}(t+\tau)\rangle = \frac{E_0^2 e^{-i\omega_D \tau}}{4\left((\omega_D - \omega)^2 + \kappa^2\right)}, \tag{2.24}$$

note that the terms that multiply the exponential are the same as the steady state of $\langle \hat{n(t)}\rangle = \langle \hat{a}^\dagger(t)\hat{a}(t)\rangle$ shown in Eq. (2.14) and if we define $g_1(\tau) = g_1(t \to \infty, \tau)$ we get to the simple expression in the steady state:

$$g_1(\tau) = e^{-i\omega_D \tau}, \tag{2.25}$$

which is the corresponding expression that describes coherent light [32].

2.2.5 Second order correlation function $g_2(\tau)$

The second correlation function is classically understood as an interference of intensities occurring in phenomena such as Hanbury Brown and Twiss effect. In quantum mechanics we follow [32] to define the quantum version of second correlation function $g_2(t, \tau)$ as:

$$g_2(t,\tau) = \frac{\langle \hat{a}^\dagger(t)\hat{a}^\dagger(t+\tau)\hat{a}(t+\tau)\hat{a}(t)\rangle}{\langle \hat{a}^\dagger(t)\hat{a}(t)\rangle^2}. \tag{2.26}$$

This second correlation function in the steady-state will characterize our simulator, so understanding its properties and dependency with the variables of the system will be useful to develop our intuition. To find an analytical form we first define

$$G_2(t,\tau) = \langle \hat{a}^\dagger(t)\hat{a}^\dagger(t+\tau)\hat{a}(t+\tau)\hat{a}(t)\rangle, \tag{2.27}$$

and noticing that the two central terms represent the density of particles operator $\hat{n}(t+\tau) = \hat{a}^\dagger(t+\tau)\hat{a}(t+\tau)$, we make use of the quantum regression theorem Eq. (2.19) to find the differential equation of the two point correlation function $G_2(t, \tau)$. First note that differential equation for the number density operator $\langle \hat{n}(t)\rangle$ Eq. (2.10) can be rewritten as the sum of expectation values of linear operators given in Eq. (2.18) as:

$$\langle \dot{\hat{n}}(t)\rangle = -2\kappa\langle \hat{n}(t)\rangle - i\frac{E_0}{2}e^{-i\omega_D t - i\phi}\langle \hat{a}(t)\rangle + i\frac{E_0}{2}e^{i\omega_D t + i\phi}\langle \hat{a}^\dagger(t)\rangle, \tag{2.28}$$

where $\hat{A}_\lambda = \{\hat{n}(t), \hat{a}(t), \hat{a}^\dagger(t)\}$ is the corresponding complete set of operators describing $\langle \dot{\hat{n}}(t) \rangle$ and $M_{\mu\nu} = \{-2\kappa, -i\frac{E_0}{2}e^{-i\omega_D t - i\phi}, i\frac{E_0}{2}e^{i\omega_D t + i\phi}\}$ the respective time dependent coefficients. Thus, following the quantum regression theorem Eq. (2.19) for the operators $\hat{O}_1 = \hat{a}^\dagger(t)$ and $\hat{O}_2 = \hat{a}(t)$ the differential equation for $G_2(t,\tau)$ in the variable τ takes the form:

$$\frac{dG_2(t,\tau)}{d\tau} + 2\kappa G_2(t,\tau) = i\frac{E_0}{2}e^{i\omega_D(t+\tau)}\langle \hat{a}^\dagger(t)\hat{a}(t+\tau)\hat{a}(t)\rangle + h.c. \tag{2.29}$$

with $G_2(t,0) = \langle \hat{a}^\dagger(t)\hat{a}^\dagger(t)\hat{a}(t)\hat{a}(t)\rangle$ as initial condition. Note that Eq. (2.29) is a recursive differential equation that require us to know the time evolution of a two point correlation function that involves the product of a reduced number of annihilation operators, in this case a product of 3 operators, $\langle \hat{a}^\dagger(t)\hat{a}(t+\tau)\hat{a}(t)\rangle$. This can be calculated in a similar way using the quantum regression theorem Eq. (2.19), whilst the function that represents the initial condition $G_2(t,0) = \langle \hat{a}^\dagger(t)\hat{a}^\dagger(t)\hat{a}(t)\hat{a}(t)\rangle$ is an equal time product of operators $\hat{a}^\dagger$, $\hat{a}$ that can be calculated using the recursive relation Eq. (2.17). After solving a series of repetitive recursive differential equations, the final result becomes:

$$G_2(t,\tau) = \frac{E_0^4 e^{-\kappa(2t+\tau)}(\cos(t(\omega_D-\omega))-\cosh(\kappa t))(\cos((\omega_D-\omega)(t+\tau))-\cosh(\kappa(t+\tau)))}{4((\omega_D-\omega)^2+\kappa^2)^2}, \tag{2.30}$$

thus $g_2(t,\tau)$ takes the form:

$$g_2(t,\tau) = \frac{G_2(t,\tau)}{\langle \hat{n}(t)\rangle^2}. \tag{2.31}$$

We can get some insight into this complicated expression if we plot $g_2(t,\tau)$ versus τ, taking t as a parameter that needs to be taken to infinity in the steady-state Fig. (2.3). For small values of the parameter $t = 5$ we appreciate oscillations at a frequency given by the detuning $\omega_D - \omega$, and exponential decay to a constant value, also note the inverse dependency of the detuning $\omega_D - \omega$ and the decay rate κ which also occurred in $g_1(t,\tau)$. As the time t increases the amplitude of the oscillations decreases, $t = 8.5$, and for larger values of $t \gg 1$ our correlation $g_2(t,\tau)$ seems to reduce to a constant of unity value. This can be demonstrated analytically since in the steady-state, namely in the limit for

$t \longmapsto \infty$, $G_2(t,\tau)$ becomes a familiar expression:

$$G_{2s}(\tau) = \frac{E_0^4}{16\left(\left(\omega_D - \omega\right)^2 + \kappa^2\right)^2} = \langle \hat{n}(t) \rangle_s^2, \tag{2.32}$$

which is the square of $\langle \hat{n}(t) \rangle$ in the steady state Eq. (2.14). Thus the two point correlation function $g_2(t,\tau)$ in the steady state becomes the unity which is the signature of the coherent light.

$$g_{2s}(\tau) = g_2(\infty,\tau) = 1. \tag{2.33}$$

This result only confirms the idea that we need to introduce a non-linearity in our

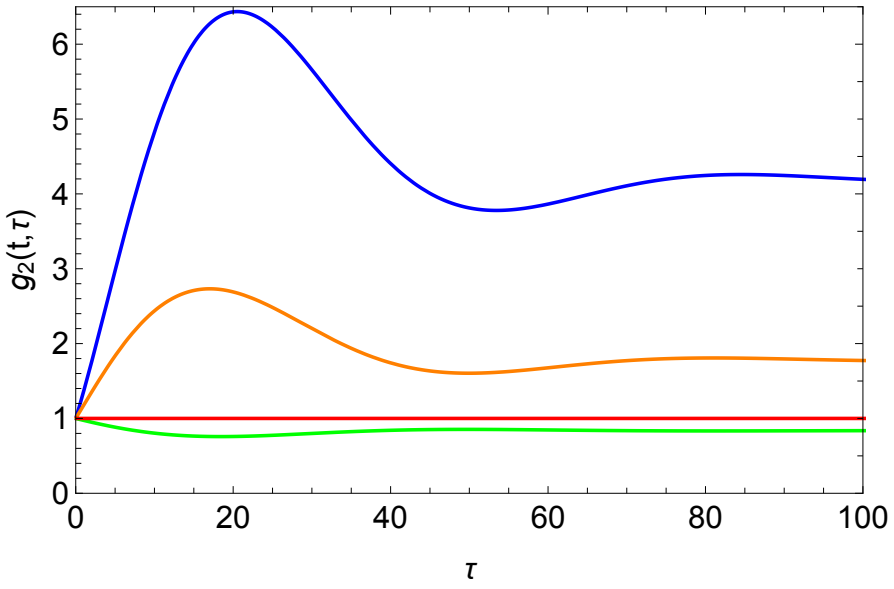


Figure 2.3: Two time second order correlation function $g_2(t,\tau)$ with t as a parameter. Notice that as the time increases, $t \longmapsto \infty$ the second correlation function $g_2(t,\tau)$ tends to the 1 $\forall$ τ, which is a signature of coherent light. The decay rate $\kappa = 0.05$, the detuning $\omega - \omega_D = 0.1$, and the amplitude of the electric field is $E_0 = 0.5$, for values of time $t = 5$ blue graph, $t = 8.5$ yellow graph , $t = 40$ green and $t = 400$ orange .

cavity if we want to use it as a simulator of bosonic gases. This non-linearity as we will study in the next sections will come in the form of a driven two-level atom inside the cavity. As a final remark, this simple model shows us that oscillations and in particular, the second order correlation function oscillations will appear whenever we have detuning and that the amplitude will decrease inversely to the power of $(\omega_D - w)$ and κ. It is natural to think that these general features will keep appearing somehow as we add the non-linearity into the cavity.

CHAPTER 3

OPTIMIZATION OF THE ENERGY DENSITY OF THE GROUND STATE FOR THE LIEB-LINIGER MODEL USING CMPS AS VARIATIONAL STATES.

In the following chapter, we shift our attention to the continuous Matrix Product States (cMPS) defined in section (1.2). Our goal is to explain the method that uses the cMPS to find the ground state energy of complex continuous systems much in the same way as their discrete counterpart (MPS) were used to describe the ground state of one-dimensional spin systems [16]. The cMPS were first proposed in [1] and used as variational states, trial states dependent of many adjustable parameters, to find the ground state energy of a one-dimensional bosonic gas system known as the Lieb-Liniger model defined in section (1.3.4). Once the parameters that described the ground state were found, they were used to calculate the density-density correlation function of the model. Comparison of their results with other numerical models such as Monte Carlo simulations and the Bethe ansatz proved their description to be successful and paved the way for exploring more complex systems like [33] for a Lieb-Liniger model with exponentially decaying interactions, or [34] for tomography of quantum transport experiments, also the works of [35] reformulating one-dimensional cMPS as path integrals opened the possibility to study higher dimensional cMPS such as [36] where they extended the concept of cMPS to interacting fields. In the next section, we will explain the steps behind the method that will allow us to find the critical values of the cMPS which minimize the expectation value of the energy density of a Hamiltonian for a particular field theory.

Naturally, this minimum value will correspond to the expectation value of the ground state energy of the particular field theory studied in our case the Lieb-Liniger model. The critical values obtained will correspond to the matrix elements of the matrices K and R of the cMPS defined in section (1.2). We will proceed to compare our results with those of [1] and show that by relaxing some of the constraints, we can still reproduce the same plots for the energy density. Moreover, we will be able to use smaller dimensions ($D = 4$) and still reproduce accurately the second correlation functions of [1] where $D = 14$. Besides, we will show that our minimization method is more general and avoids rescaling the parameters involved in the minimization as done in [3] which may lead to some errors at the moment of calculating other correlation functions. Finally, we will explore the use of these optimal parameters to calculate other quantities of interest like the Luttinger parameters. In the next chapters, we will give a physical meaning to the cMPS formalism. This will be done by recalling that cMPS can be understood as the states resulting from the interaction of the field studied and an auxiliary system. Thus we will describe diverse configurations of cavity QED systems that will serve as physical candidates for the "auxiliary system" needed in the cMPS. Furthermore, by studying the properties of these physical systems we will be in better shape to comprehend the inner workings of this formalism that include the cMPS as its main ingredient.

3.1 Algorithm for minimization

We now proceed to explain how to apply the cMPS formalism to the Hamiltonian density of the Lieb-Liniger model Eq. (1.99). First of all, remember that the expectation value of the energy density for that particular Hamiltonian and any arbitrary state $|\phi\rangle \in \mathcal{H}$, where $\mathcal{H}$ is the Hilbert space of the bosonic system, is expressed as:

$$e(c) = \langle\phi| \left[\frac{d\hat{\psi}^\dagger(x)}{dx} \frac{d\hat{\psi}(x)}{dx} + c\hat{\psi}^\dagger(x)\hat{\psi}^\dagger(x)\hat{\psi}(x)\hat{\psi}(x) \right] |\phi\rangle, \tag{3.1}$$

with the field operators $\hat{\psi}(x)$ acting on the state $|\phi\rangle$ and c is a measure of the strength of the contact interaction. Note that Eq. (3.1) can be rewritten as the sum of the expectation value of the kinetic energy and the interaction energy for the state $|\phi\rangle$. In particular we can select $|\phi\rangle = |\chi\rangle$, the cMPS defined in Eq. (1.37) whose parameters

are the values of the matrices K and R such as:

$$e(c) = \langle\chi| \left[\frac{d\hat{\psi}^\dagger(x)}{dx} \frac{d\hat{\psi}(x)}{dx} \right] |\chi\rangle + c\langle\chi| \left[\hat{\psi}^\dagger(x)\hat{\psi}^\dagger(x)\hat{\psi}(x)\hat{\psi}(x) \right] |\chi\rangle, \tag{3.2}$$

we want to point out that all the possible values that can take K and R in $|\chi\rangle$ describe a subset S_{cMPS} of all the possible states in $\mathcal{H}$ such as $S_{cMPS} \subset \mathcal{H}$. What we want in the end is to use the state $|\chi\rangle$ as a variational state, and rewrite the expectation value of the energy of the Lieb-Liniger Hamiltonian in terms of parameters we can adjust. Furthermore, from section (1.2.2) those are exactly the properties that the cMPS have at the moment of calculating expectation values, where those parameters will be the matrices K and R that parametrize $|\chi\rangle$. Thus from the relations between expectation values of the fields and cMPS, Eq. (1.54) and Eq. (1.56), we can rewrite the expectation value of the kinetic energy and the interaction energy respectively as:

$$e(c) = \mathrm{Tr}\left(\rho_{ss} \left[Q, R\right]^\dagger \left[Q, R\right] \right) + c\mathrm{Tr}\left(\rho_{ss} (R^\dagger)^2 R^2 \right), \tag{3.3}$$

where Tr is the trace over the auxiliary system, $Q = -iK - \frac{1}{2}R^\dagger R$, for K,R matrices of arbitrary dimension D , $[*,*]$ is the usual commutation relation and ρ_{ss} is the density matrix in the steady state of the auxiliary system previously discussed in section (1.2.2).

Let us pause for a moment to understand what we have achieved. Originally, we had the expectation value of a system described by infinite-dimensional operators $\hat{\psi}(x)$, $\hat{\psi}^\dagger(x)$ however, this was transformed into expectation values of a second system, that we have coined as auxiliary system, which is described by finite-dimensional operators in the form of the matrices K and R. That was thanks to the definition of the cMPS which, according to section (1.2.2) can be generated as a result of two interacting systems, in this case, the Lieb-Liniger system and an auxiliary system. That ultimately means that we have managed to map the expectation values from the bosonic Lieb-Liniger system into the expectation values of the auxiliary system.[1] Also, note that given that this auxiliary system is of finite dimension, then we are only describing a subset of the infinite-dimensional states that live in $\mathcal{H}$, the Hilbert space of the bosonic system.

Returning to Eq. (3.3), note that to obtain ρ_{ss}, we need to look at the variation in

[1] Note from Eq. (3.3) that the traces are of the form $\mathrm{Tr}\left(\rho_{\mathrm{ss}}\mathcal{O}\right) = \langle\mathcal{O}\rangle$ where $\mathcal{O}$ is a general finite-dimensional operator.

position of the density matrix in the steady state, which should obey:

$$\lim_{x\to\infty} \dot{\rho}_{ss}(x) = 0, \tag{3.4}$$

and given that the evolution of the density matrix $\rho(x)$ is determined by the master equation in the Lindblad form Eq. (1.49), thus $\rho_{ss}(x)$ should follow the equation:

$$-i\left[K, \rho_{ss}\right] + R\rho_{ss}R^{\dagger} - \frac{1}{2}R^{\dagger}R\rho_{ss} - \frac{1}{2}\rho_{ss}R^{\dagger}R = 0, \tag{3.5}$$

thus every time we adjust the parameters in Eq. (3.3) we need to ensure Eq. (3.5) still holds. Finally, we believe it is important to stress that Eq. (3.3) is describing the expectation value of the energy density of a system given by the bosonic gas in terms of the expectation value of a quantity, at the moment an unknown operator, that lives in the same space where the auxiliary system is defined. Thus the energy of the system is exclusively described by quantities belonging to the auxiliary system. This will be very important to understand our results in the next chapter.

3.2 Energy density and correlation functions

In order to find the expectation value of the energy density $e(c)$ in Eq. (3.3), we first need to obtain the density matrix $\rho_{ss}(K, R)$ in terms of K and R from Eq. (3.5). Thus, the expectation value of the energy density for any cMPS $|\chi\rangle$ of the form of Eq. (1.37), depends solely on the finite-dimensional matrices K, R and the interaction parameter c, as $e(c, K, R)$. We still need to specify the optimal values of K and R to obtain the ground state energy. To find those values, we make use of the variational method. Succinctly, it states that the expectation value of a Hamiltonian has a lower bound equal to the energy E_0 of the ground state. As an example, and for the sake of simplicity consider a discrete system in the non-degenerate case, with a complete set of eigenfunctions ψ_n of the corresponding Hamiltonian H, whose eigenvalues are λ_n, or in ket notation, $H|\psi_n\rangle = \lambda_n|\psi_n\rangle$. Thus, an arbitrary state $|\phi\rangle$ admits an expansion of the form:

$$|\phi\rangle = \sum_n \left(\langle\psi_n|\phi\rangle\right)|\phi_n\rangle, \tag{3.6}$$

this implies that the expectation value of the energy for the state ϕ satisfies:

$$\langle\phi|H|\phi\rangle = \sum_n \lambda_n \left|\langle\psi_n|\phi\rangle\right|^2 \geq \sum_n E_0 \left|\langle\psi_n|\phi\rangle\right|^2 = E_0, \tag{3.7}$$

where we used $\lambda_n \geq E_0$ and the completeness property of the set $\{|\psi_n\rangle\}$. In consequence, finding e(K, R, c) defined in Eq. (3.3) becomes a variational minimization problem with respect to the $2D^2$ real entries of K and R.[2] However, if we were to decrease the energy density, we need to avoid decreasing the density of particles in the system as this would lead to a trivial result (zero energy due to zero particles in the system). To save this situation, we need to minimize under the constraint of a constant density of particles, in other words, the expectation value of the number of bosonic particles for the cMPS should follow $\langle\hat{N}\rangle = \langle\chi|\psi^\dagger(x)\psi(x)|\chi\rangle = 1$ in accordance with [1]. Using the cMPS relation given by Eq. (1.52) in the first equality we can rewrite the expectation value in terms of quantities of the auxiliary system as follows:

$$\langle\hat{N}\rangle = \mathrm{Tr}\left[\rho_{ss}R^\dagger R\right] = 1, \tag{3.8}$$

an important remark is that since we are parametrizing the ground state with $2D^2$ variables, it is to be expected that as we increase D, the dimension of the matrices K and R, the results obtained should increase its accuracy. The minimization was performed using MATLAB Global Optimization Toolbox, this solver is designed to search through more than one basin of attraction, the set of initial vectors that lead to the same local minimum. Then it analyses and rejects those vectors that are unlikely to provide a better local minimum than the one already found, thus increasing the probability of finding an actual global minimum. The process consisted of providing a random start vector X_0 of dimension $2D^2$ that represented the entries of K and R. Then the code ran a local optimization algorithm (fmincon interior-point algorithm) using that vector as a starting point for the energy density function, Eq. (3.3) under the constraints of a fixed density of particles given in Eq. (3.8). After that, it used the scatter search algorithm [37] to generate a set of trial points selecting those that are most likely to get a minimum. Finally, it used a local optimization for the selected points given

[2]Here we stress that R is a real matrix and K is a hermitian matrix at all times of the minimization procedure and $K, R \in DxD$

the tolerance and number of chosen iterations. The output was the optimal values for the entries of the matrices K and R. Those optimal entries, substituted in Eq. (3.3) will give the minimum expectation value of the energy. As a test of our method,

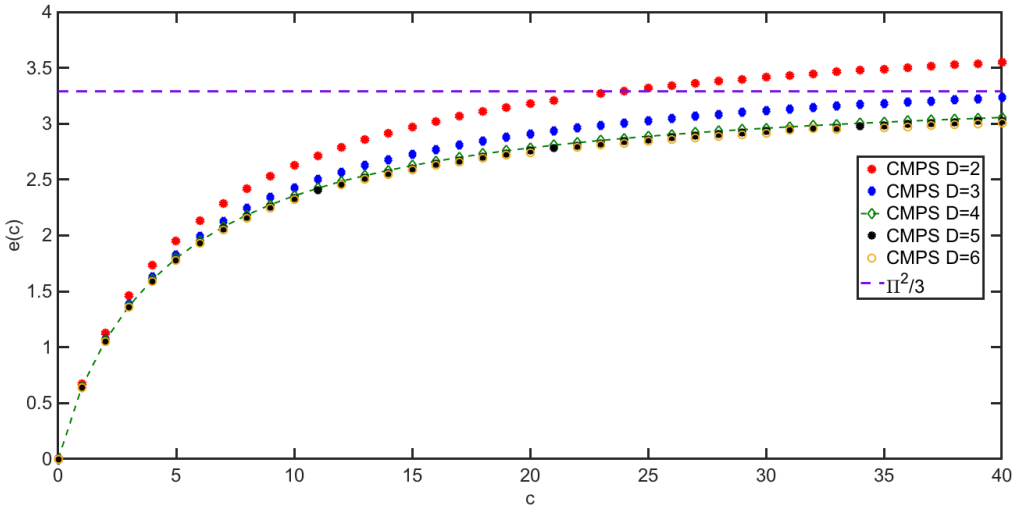


Figure 3.1: Energy density $e(c)$ for one dimensional bosonic particles in the ground state as a function of the parameter c, the interaction strength, for values of D=2, 3, 4, 5, 6. Note as D increases, e(c) becomes bounded by $\pi^2/3$ which according to [4] is the limit value of the energy density as $c \to \infty$. Furthermore, in this limit we are in the Tonks-Girardeau regime of impenetrable bosons and according to [5] the ground state energy is the same as the ground state of the free Fermi gas. For $c = 0$ we recover the ideal gas where no interaction occurs and $e(c) = 0$.

Fig. (3.1) shows the optimization done for the energy density $e(c)$ as a function of the interaction parameter c. We used the optimal values found for the matrices K and R for each dimension $D = 2, 4, 6, 8$ and substituted them in the expression for the energy density Eq. (3.3). Note that for $D \geq 4$, the graphs become indistinguishable and as a consequence for relative small dimensions we can obtain accurate results saving us computational time. A more quantitative comparison will show the accuracy of our results respect to [1] proving that our method is capable of replicating those results. In Table (3.1) we compare a few selected values that we obtained with the ones in Cirac et.al [1]. Our calculated values match those of [1] up to orders of 10^{-4} in most cases. While D increases, $e(c = 2)$ is decreasing, improving the accuracy to the value reported in the Bethe ansatz of $e(c = 2) = 1.0504$ except $D = 12$ were the value suddenly increases. This discrepancy is possibly due to the precision of the minimization algorithm used. Although it would be possible to increase the number of iterations and the precision to improve our results, it would be at the cost of increasing time in the optimization

D	Values reported by [1]	Our values
2	1.1241	1.12407
4	1.0618	1.06182
6	1.0531	1.05311
8	1.0515	1.05183
10	1.0512	1.05117
12	1.0508	1.05122

Table 3.1: Values for the energy density for the interaction parameter $c = 2$. The Bethe ansatz reported in [1] gives 1.0504, while the Monte Carlo used by them, was reported as $e = 1.0518$. In both cases, we report an increase in accuracy with increasing dimensions except in our values for $D = 12$ due to lack of computational power.

process. Finally, we show in Fig. (3.2)[3] a plot comparison between our results for the

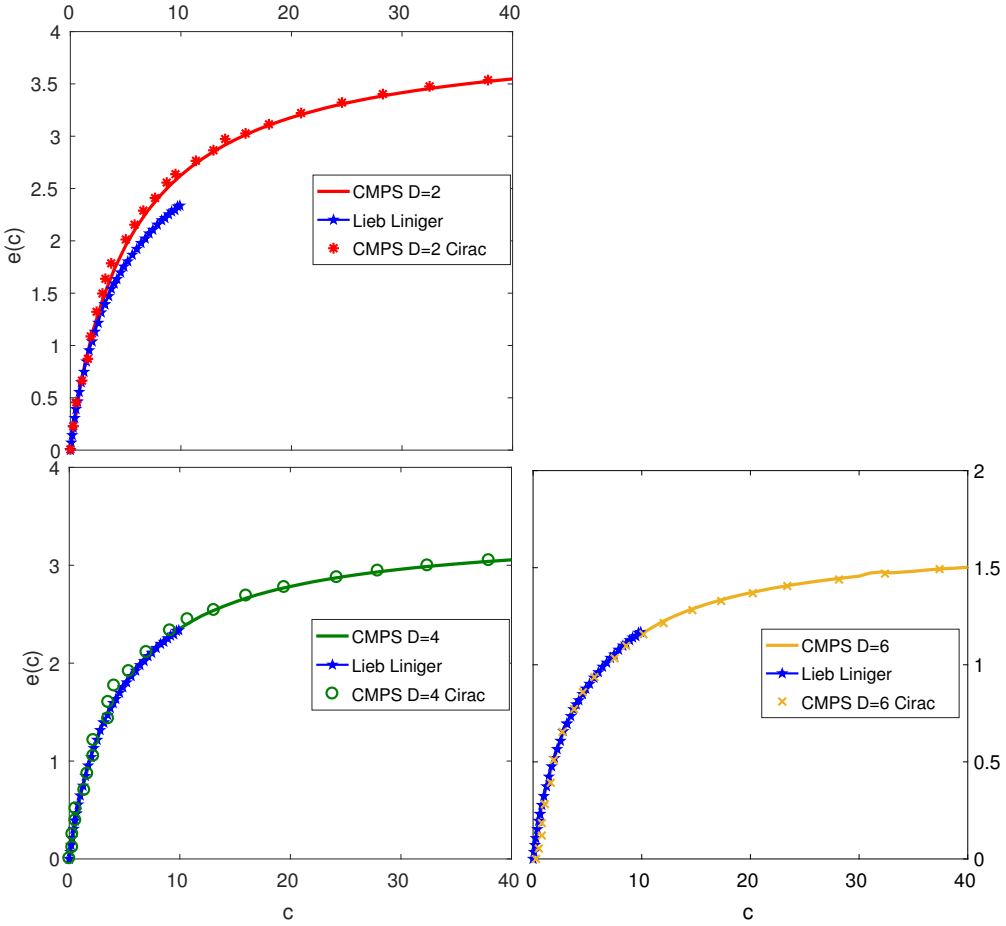


Figure 3.2: Comparison of our results for the energy $e(c)$ density versus the interaction constant c with those of Cirac et al[1] and the Bethe ansatz. For $D = 2$ in red, $D = 4$ in green and $D = 6$ in yellow. Notice that for $D \geq 4$ there is little difference with the Bethe ansatz approach meaning that our optimizations are increasing accuracy with increasing dimension D.

energy density $e(c)$ with those obtained by [1] for $D = 2, 4, 6$. We obtained these data points directly from their paper using a program to extract them. We included the Bethe ansatz approximation reported in [1] as a reference using the same program to obtain the data points. We observe that in all three values of D, the extracted data points from Cirac et al. are consistent with our plots. The small discrepancies in Fig. (3.2) between our results (continuous lines) and those of Cirac et al [1] (isolated points) are due to the accuracy of the computer program and the manual calibration performed to extract the data points from the original paper. Up to this point, we have only justified the accuracy

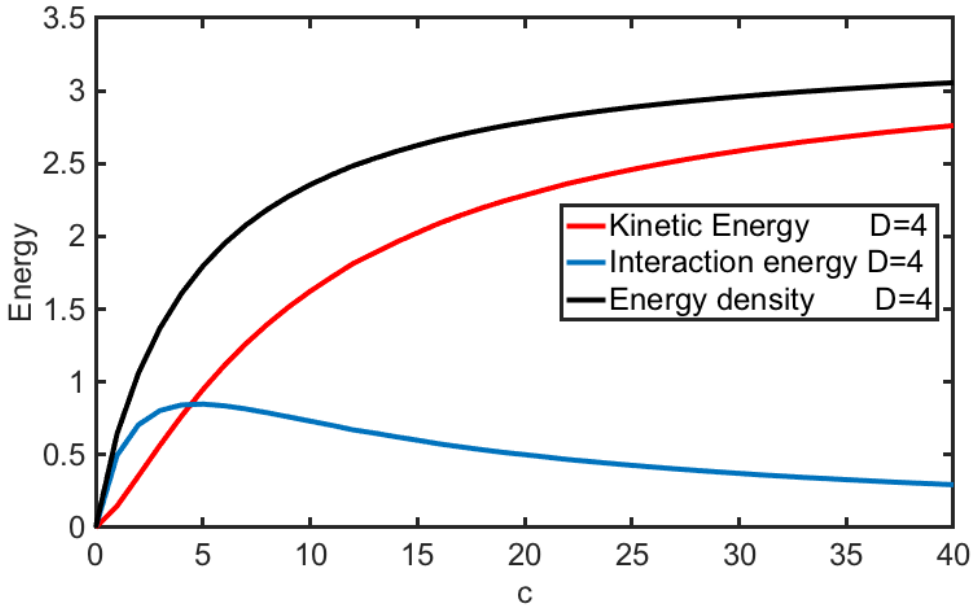


Figure 3.3: Energy density, Kinetic energy ($T = \mathrm{Tr}\left(\rho_{ss}\left[Q, R\right]^{\dagger}\left[Q, R\right]\right)$) and Interaction potential energy ($V = c\mathrm{Tr}\left(\rho_{ss}(R^{\dagger})^2 R^2\right)$) of the Lieb Liniger model as as function of the interaction strength c for $D = 4$ in black, red and blue respectively. According to [4] $T \to \frac{\pi^2}{3}$, $V \to 0$ when $c \to \infty$. This implies that for higher values of c, the contributions of the interaction energy will be negligible and only the kinetic energy will contribute to the total energy. For instance for $c = 60.2$ we have $T = 2.95$ and $V = 0.2067$ thus V contributes a 6.54% and $c = 625.95$ $T = 3.331$ $V = 0.0218$, V contributes a 0.65% This will have important effects when we use a cavity QED as a simulators

of our results by comparing them with [1]. However, we can extract more information from our results if we analyse the contributions towards the total energy density $e(c)$ of the terms corresponding to the kinetic energy T and the potential interaction energy V. Figure (3.3) shows that for $c \ll 1$, the main contribution to the energy comes from the

[3] "Reprinted figure with permission from F Verstraete and J. I. Cirac, Continuous Matrix Product States for Quantum Fields, Volume 104, Issue 19, pages 1-4, 2010 Copyright (2010) by the American Physical Society."

interaction potential $e(c) \sim V$ while for $c \to \infty$ the kinetic energy becomes the main contributor to the energy density $e(c) \sim T$. Furthermore, T tends to the constant value of $\frac{\pi^2}{3}$ according to [4]. This results will be more interesting when in the next chapter we relate $e(c)$ to cavity QED terms and in particular $V = cg_2(0)$ thus predicting that $g_2(0)$, the second correlation function of the cavity QED system will tend to zero when $c \to \infty$ and that the remaining cavity QED term associated with T will be the only term responsible for describing the particle interactions of the gas in the limit of $c \to \infty$.

Moving on, the optimal parameteres K and R are useful not only to calculate the energy density $e(c)$, they will also allow us to evaluate different expectation values of products of field operators $\hat{\psi}(x)$ and $\hat{\psi}^\dagger(x)$. For instance in [1] is defined the density-density correlation function as the expectation value of $\langle\hat{\psi}^\dagger(0)\hat{\psi}^\dagger(x)\hat{\psi}(x)\hat{\psi}(0)\rangle$ and since we know now the optimal parameters for the cMPS $|\chi\rangle$ that corresponds to the ground state, we can use the relation given in Eq. (1.54) to rewrite this expectation value as the trace of products of finite dimensional matrices in the auxiliary space as:

$$\langle\hat{\psi}^\dagger(0)\hat{\psi}^\dagger(x)\hat{\psi}(x)\hat{\psi}(0)\rangle = \mathrm{Tr}\left[Re^{\mathcal{L}x}(R\rho_{ss}R^\dagger)R^\dagger\right], \tag{3.9}$$

with $\mathcal{L}$, the Liouvillian superoperator defined in Eq. (1.50). In order to find the density matrix in the steady state ρ_{ss}, we used a code in Matlab that vectorizes a density matrix ρ through a linear transformation of the form:

$$\rho = \sum_{i,j} \rho_{ij}|i\rangle\langle j| \longmapsto |\rho\rangle = \sum_{i,j} \rho_{ij}|i\rangle \otimes |j\rangle, \tag{3.10}$$

with ρ_{ij} the matrix elements of ρ and $\otimes$ the outer vector product. In the same way it can transform the matrices that act on the left hand side and the right hand side of ρ as:

$$\begin{aligned} A\rho &= \sum_{i,j} \rho_{ij}(A|i\rangle)\langle j| \longmapsto \sum_{ij} \rho_{ij}A|i\rangle \otimes |j\rangle = (A \otimes \mathbb{1})|\rho\rangle, \\ \rho A &= \sum_{i,j} \rho_{ij}|i\rangle(\langle j|A) \longmapsto \sum_{ij} \rho_{ij}|i\rangle \otimes (A^\top|j\rangle) = (\mathbb{1} \otimes A^\top)|\rho\rangle, \end{aligned} \tag{3.11}$$

with $A^\top$ denoting the transpose of A and $A \otimes \mathbb{1}$ is the generalization of the outer product to matrices. Notice how this operation simplify all the left and right products

of matrices mapping them into left hand side products of the vector $|\rho\rangle$. These allows us to transform the equation for the steady state in the Lindblad form Eq. (3.5) into:

$$\mathcal{L}\rho_{ss} = (Q \otimes \mathbb{1} + \mathbb{1} \otimes \bar{Q} + R \otimes \bar{R})|\rho_{ss}\rangle = 0, \tag{3.12}$$

with $Q = -iK - \frac{1}{2}R^\dagger R$, and the bar on top of the operators represents complex conjugation. This transformation re-expresses $\mathcal{L}$ as a superoperator in a matrix form acting on the vector $|\rho_{ss}\rangle$. Thus finding the density matrix in the steady-state is reduced to finding the vector $|\rho_{ss}\rangle$ that lives in the kernel of the matrix defined in Eq. (3.12). Finally, note that the exponential term defined in Eq. (3.9) is just the exponential operator of the matrix defined in Eq. (3.12). With those elements, we can plot the density-density correlation function Eq. (3.9) which, in the future will be denoted as second correlation function g_2. The plots obtained are shown in Fig. (3.4), notice that as $c \to 0$, the

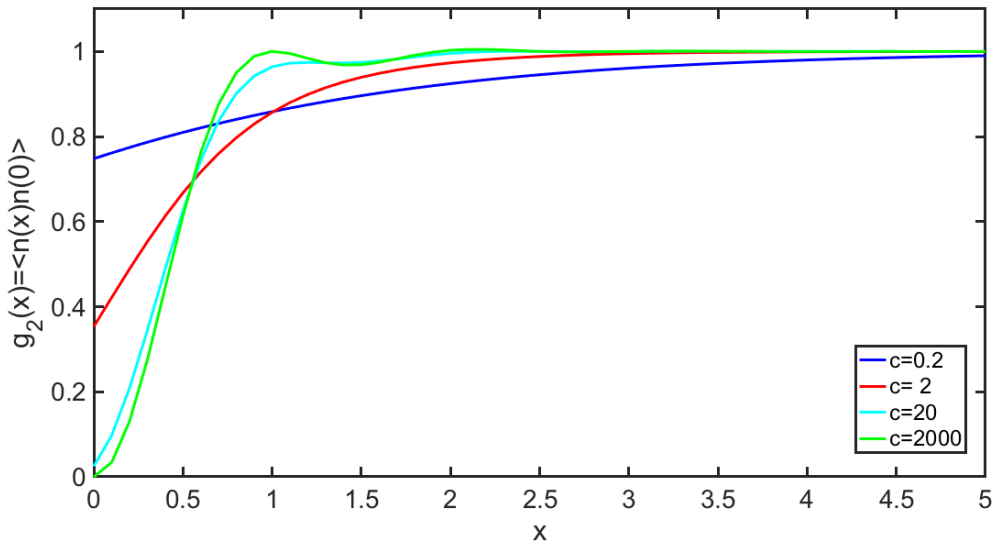


Figure 3.4: Two body density-density correlation function as a function of position x for the values of c=0.2,2,20,2000 (blue, red, light blue and green respectively) for matrices K, R of dimension $D = 4$. In the limit of $x \to \infty$ all correlation functions tend to 1.

second correlation function $g_2(0) \to 1$. This is consistent with the ideal gas limit since for non interacting particles the probability of finding two of them in the same point will tend to 1 [38]. Conversely, for $c \to \infty$, the probability of of finding two particles in the same position decreases $g_2(0) \to 0$, consistent with the strong interacting regime. However note that for weaker interactions there is still a finite probability that two par-

ticles are in the same position. Finally, for high values of $c \gtrsim 60$, we have oscillations as expected from the Tonks Girardeau gas [39], the limit of strongly correlated gases. In our case that correspond to the region $x \in [1, 2]$ for $c = 2000$. In Fig.(3.5)[4] we compared

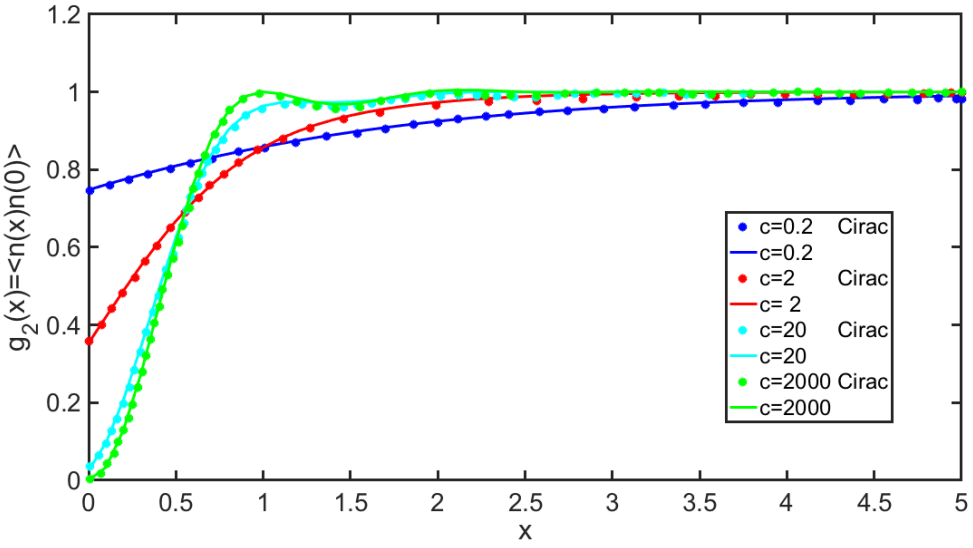


Figure 3.5: Comparison of our plots with those of Cirac et al [1] for the second correlation function $g_2(x) = \langle n(x)n(0)\rangle$ versus x. From top to bottom $c = 0.2, 2, 20, 2000$. Despite we only used dimension $D = 4$, continuous lines, we are able to get an excellent agreement with their results, where they used a dimension $D = 14$, data points.

our results for the second correlation function $g_2(x)$ with those of [1]. In their work, they calculated the second correlation functions for $D = 14$ but we are getting the same results for $D = 4$. One possibility for this is that we relaxed the condition that $R^\dagger R$ is a diagonal matrix given in [1] for R being just a real matrix. The other possibility is that in the same way as for the plots of the energy density $e(c)$ becoming indistinguishable for values of $D \geq 4$, Fig. (3.1) then $g_2(x)$ will behave the same way and the correlation functions for higher dimensions D will become indistinguishable.

Let us now focus our discussion on the limit for $c \gg 1$, the strongly correlated Tonks-Girardeau (TG) regime describing a gas of impenetrable bosons. It will be interesting to understand this regime and the physics describing the particles so we can compare those mechanisms at play with our results in the next chapter which, use the physics of photon interactions to describe the impenetrable bosons. In the TG regime, the bosons are not only still confined to a one-dimension but also, their energy is not enough to tunnel

[4] "Reprinted figure with permission from F Verstraete and J. I. Cirac, Continuous Matrix Product States for Quantum Fields, Volume 104, Issue 19, pages 1-4, 2010 Copyright (2010) by the American Physical Society."

through the strong repulsive potential thus they will not be able to pass each other, exchange places nor be in the same position in space. We can think of this behaviour as an effective Fermi exclusion principle [38]. A formal demonstration of this fermionic behaviour comes from Girardeau [5] establishing a direct mapping of the wave function of hard-core impenetrable interacting bosons and the wave function of spinless fermions where their probability distributions and energy spectra turn out to be identical. In our particular case where the core is reduced to a point, defined as a delta interaction, the fermionic wave function for point interactions is equivalent to a non-interacting one since the fermion wave functions vanish when two particles get together. In that case, the energy eigenfunctions will correspond to the ones of a free Fermi gas and, according to the theorem developed in [5], so does the boson energy eigenfunctions. In particular, for a density of particles $n = 1$, the free Fermi energy corresponds to the value $\pi^2/3$ which corresponds to the bound limit shown in Fig. (3.1). Finally, in this regime, an approximation for their second-order correlation function where the boundaries are far from the position of the particles is of the form:

$$g_2(z) = 1 - \frac{\sin^2(\pi n z)}{(\pi n z)^2}, \tag{3.13}$$

where n is the density of particles. These oscillations are a signature of strong correlations present in the gas where the motion of the particles will be strongly correlated with the motion of its two neighbours. Note how these oscillations are the ones described in our results from Fig. (3.4) for the cases of $c = 20, 2000$. The take away of this analysis is that the bosonic gas we are simulating, in the limit of $c \gg 1$ behaves as non-interacting Fermi particles. Moreover, in this limit, the energy density of the ground state is given only by the kinetic term. It will be interesting to see what is that kinetic term once we rewrite our matrices K and R in terms of cavity QED terms and how this fermionic behaviour could be recovered.

3.3 Alternative method

We want to compare our method with the procedure followed by [3, 6] to pinpoint some key differences at the moment of finding the energy of the ground state for the

Lieb-Liniger model. Although their method solves the problem, it may generate some confusion if we are not careful at the time of using the optimized variables to calculate the correlation functions. First of all, the expectation value they proposed to minimize is of the form:

$$E(c,\mu) = \langle\phi| \left[\frac{d\hat{\psi}^\dagger(x)}{dx}\frac{d\hat{\psi}(x)}{dx} + c\hat{\psi}^\dagger(x)\hat{\psi}^\dagger(x)\hat{\psi}(x)\hat{\psi}(x) - \mu\hat{\psi}^\dagger(x)\hat{\psi}(x) \right] |\phi\rangle, \tag{3.14}$$

this looks like the expectation value of the Lieb-Liniger Hamiltonian presented in Eq. (3.3) except for the last term that corresponds to the number of particle operator times the chemical potential μ. Thus using the same transformations for the expectation value respect to the cMPS $|\chi\rangle$ shown in section 1.2.2, in particular Eq. (1.52, 1.54 ,1.56) we obtain the expression:

$$\begin{aligned} E(c,Q,R,\mu) =& \mathrm{Tr}\left(\rho_{ss}\left[Q,R\right]^\dagger\left[Q,R\right]\right) + c\mathrm{Tr}\left(\rho_{ss}(R^\dagger)^2R^2\right) - \mu\mathrm{Tr}(\rho_{ss}R^\dagger R) && (3.15)\\ =& E_{LL}(c,Q,R) - \mu d, && (3.16) \end{aligned}$$

where $Q = -\frac{1}{2}R^\dagger R - iK$. For the following discussion in this section and to follow the notation on [3, 6] we will consider Q and R as our parameters so we denote $E_{LL}(c,Q,R)$ as the energy density of the Lieb-Liniger model as in Eq. (3.3), and without loss of generality, the chemical potential can be fixed to $\mu = 1$ and $d = \mathrm{Tr}(\rho_{ss}R^\dagger R) = \langle\hat{N}\rangle$ is the density of particles as derived from Eq. (3.8). We will use the symbol d to keep with the notation used in [6]. Next, they proceeded to minimize the function $E(c,Q,R,\mu)$ respect to the entries of the matrices Q and R without the use of any constraint. Once that is achieved, the energy density $E_{LL}(c,Q,R)$ with the optimal parameters Q and R can be expressed as:

$$E_{LL}(c,Q,R) = E(c,Q,R,\mu=1) + d. \tag{3.17}$$

Here we need to point out that in [3, 6] it is implicitly assumed that the optimal parameters that minimize the function $E(c,Q,R,\mu=1)$ are the same parameters that simultaneously optimize the expressions $E_{LL}(c,Q,R)$ and $d = \mathrm{Tr}(\rho_{ss}R^\dagger R)$ separately which is not immediately obvious but can be shown to be the case for this problem. The reasoning to propose the expression $E(c,\mu)$ in [6], was to maintain the density of particles constant and equal to unity. In the following we explain how it is done. Firstly,

since Eq. (3.17) is valid for all values of the parameter c, then it also applies for the particular value cd, so we have:

$$E_{LL}(cd, Q, R) = E(cd, Q, R, \mu = 1) + d, \tag{3.18}$$

this change will make sense below, and it will simplify the final result. The next step will be to introduce the following scaling transformation for the energy density of the Lieb-Liniger model $E_{LL}(c, Q, R)$:

$$E_{LL}(c, Qx, R\sqrt{x}) = x^3 E_{LL}\left(\frac{c}{x}, Q, R\right). \tag{3.19}$$

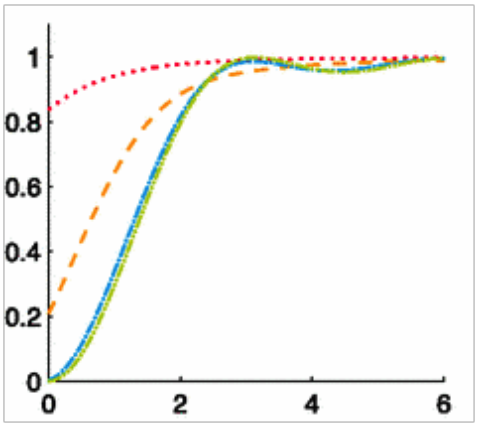
This is valid for any value of x and comes due to the functional dependency of $E_{LL}(c, Q, R)$ on Q and R. Replacing this expression back into Eq. (3.18) with the value $x = \frac{1}{d}$ we can rewrite the energy density as:

$$E_{LL}\left(c, \frac{Q}{d}, \frac{R}{\sqrt{d}}\right) = \frac{E(cd, Q, R, 1) + d}{d^3}. \tag{3.20}$$

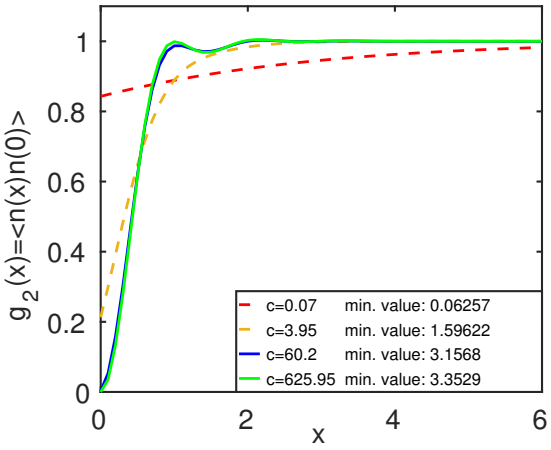
This relationship means that the optimal parameters that optimize the energy density of the Lieb-Liniger model, will be redefined such as $Q \to \frac{Q}{d}$ and $R \to \frac{R}{\sqrt{d}}$. The whole point of using this rescaling is to ensure that the density of particles $\langle N \rangle$ remains a constant. This can be seen by transforming $\langle N \rangle = \langle \hat{\psi}^\dagger(x)\hat{\psi}(x) \rangle$ into its cMPS counterpart and using the rescaled values $\frac{Q}{d}$ and $\frac{R}{\sqrt{d}}$ as follows:

$$\langle N \rangle = \mathrm{Tr}\left[\rho_{ss} \frac{R^\dagger}{\sqrt{d}} \frac{R}{\sqrt{d}}\right] = \frac{\mathrm{Tr}\left[\rho_{ss} R^\dagger R\right]}{d} = \frac{d}{d} = 1. \tag{3.21}$$

Note that from the equation of the density matrix in the steady state Eq. (3.5), $\rho_{ss}(K, R)$ is invariant under the rescaling. This procedure will ensure that the energy density E_{LL} will not go to zero for the trivial case $\langle N \rangle = 0$. The resulting Eq. (3.20) shows that the minimum value of the energy density $E_{LL}\left(c, \frac{Q}{c}, \frac{R}{\sqrt{d}}\right)$ for a particular value of c now depends on the parameters $\frac{Q}{d}$ and $\frac{R}{\sqrt{d}}$ and that minimum value will be obtained by minimizing $E(cd, Q, R, 1)$ for the parameter cd instead of c. This will ensure that the density of particles $\langle N \rangle$ remains a constant equal to one. Regarding the correlation functions, and in particular to plot the second correlation function $g_2(x)$, one just needs



(a) Second correlation function $g_2(x)$ extracted from [3] using cMPS with matrices of dimension $D = 14$ (392 variables) for the values of $c = 0.07$, 3.95, 60.2 and 625.95 in red, orange, blue and green respectively.

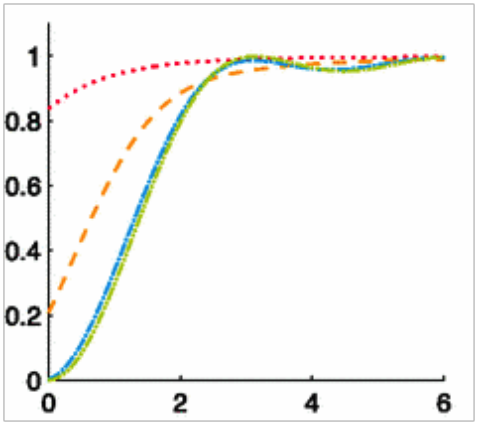


(b) Our method for $g_2(x)$, with $D = 4$, (32 variables) for $c = 0.07$, 3.95, 60.2 and 625.95 in the same colours. Although $D = 4$, most of the minimum values of the energy density shown are bounded by $\pi^2/3 \sim 3.2898$, corresponding to the energy of free fermions as predicted by [4]

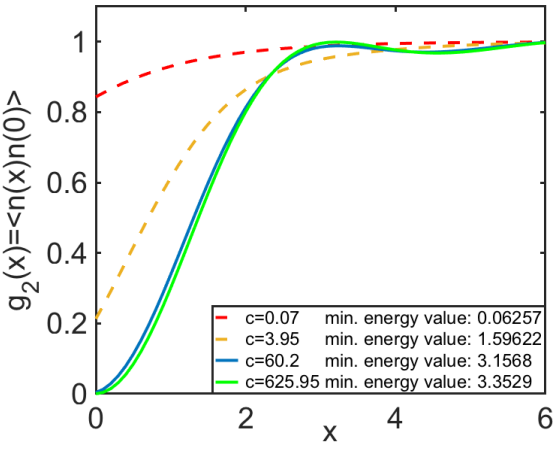
Figure 3.6: Comparison of $g_2(x)$ functions. Our method discused in 3.2 has proven to reproduce the $g_2(x)$ plots of [1] but it shows a discrepancy with [3]. This is explained when we note that they should have used the rescaled values: $\frac{Q}{d}$ and $\frac{R}{\sqrt{d}}$ we just discussed.

to replace the rescaled parameters $\frac{Q}{d}$ and $\frac{R}{\sqrt{d}}$ corresponding to the parameter c of interest, into the expression for the second correlation function $g_2(x) = \langle\hat{\psi}^\dagger(0)\hat{\psi}^\dagger(x)\hat{\psi}(x)\hat{\psi}(0)\rangle$ depicted in Eq. (3.9). In the following discussion, we want to raise awareness of some complications that may occur with this method so we proceed to compare in Fig. (3.6)[5] the function $g_2(x)$ for the bosonic system of the Lieb-Liniger model extracted from [3] with our own version. In Fig. (3.6a) Barrett et al [3], use cMPS, with matrices Q and R of dimensions $D = 14$. Both plots are normalized functions where $g_2(x) \to 1$ for large values of x, showing the usual oscillations for large values of the interaction strength parameter c for $c = 60.2$ (in blue) and $c = 625.95$ (in green) as discussed in the previous section. However the oscillations occur for $x \in (2, 6)$ while in our method, Fig.(3.6b) they occur for $x \in (0, 2)$. Furthermore $g_2(x)$ for the cases of $c = 007$ (in red) and $c = 3.95$ (in orange) for Fig. (3.6b) intersect at a point $\in (0, 2)$ while in Fig. (3.6a) there is no intersection in that region. Finally in the same figure, note that $g_2(x)$ for the value $c = 0.07$ is always above the other plots which does not happen in Fig. (3.6b). These discrepancies with both figures, are due to a small omission made in [3], where

[5] "Reprinted figure with permission from Sean Barrett et al., Simulating Quantum Fields with Cavity QED, Volume 110, Issue 9, pags. 1-7, 2013 Copyright (2013) by the American Physical Society.



(a) Second correlation function $g_2(x)$ extracted from [3] using cMPS with matrices of dimension $D = 14$ (392 variables) for the values of $c = 0.07$, 3.95, 60.2 and 625.95 in red, orange, blue and green respectively.



(b) Second correlation function $g_2(x)$ using cMPS with matrices Q and R of dimension $D = 4$, (32 variables). We are able to reproduce the same graphs profiles as [3] using only the optimized values Q and R without rescaling. Note that the energy values match those of Fig. (3.6b).

Figure 3.7: Reproducing $g_2(x)$ extracted from [3] using the alternate method described in section(3.3).

they should have used the rescaled values of $\frac{Q}{d}$ and $\frac{R}{\sqrt{d}}$ instead of the bare optimized values Q and R. On the other hand, the plots shown in Fig. (3.6b) were created using the same technique that reproduced the work of Cirac et.al. [1] as illustrated in Fig. (3.5) so we are confident that our method is correct. To understand what is happening, we optimized the expression $E(c, Q, R, \mu)$ shown in Eq. (3.16) for the parameter $c \to cd$ respect to the variables contained in the entries of Q and R. If the minima obtained is substituted in Eq. (3.20), the result should provide us with the minima of the energy density for the Lieb Liniger model $E_{LL}\left(c, \frac{Q}{d}, \frac{R}{\sqrt{d}}\right)$ for the parameter c respect to the rescaled variables $\frac{Q}{d}$ and $\frac{R}{\sqrt{d}}$. The values obtained are shown in the label of Fig. (3.7b) and they correspond to the values of energy shown in the label of Fig. (3.6b) where we used our own method. However, if we substitute not the rescaled variables but Q and R in the expression $g_2(x)$ for the second correlation function, Eq. (3.9) and plot respect to the position x we manage to reproduce [3] as shown in Fig. (3.7b). We want to stress that this alternative method works perfectly well. If we take into account the rescaled variables $\frac{Q}{d}$, $\frac{R}{\sqrt{d}}$ and substitute into the second correlation function, Eq. (3.9) we can reproduce the plots of our method. However, this shows the inconvenience of keeping track of the optimized variables for rescaling every time we need to calculate a

different correlation function. In contrast, our method to find the ground state energy is straightforward since we just use the expression for the energy density of the Lieb Liniger model in terms of the cMPS, Eq. (3.3) and minimize it under the constraint of the density of particles equal to a constant, Eq. (3.8). Moreover, the method does not depend on any scaling property of the field theory Hamiltonian such as Eq. (3.20) thus the minimization can be applied to even more complicated models.

3.4 Luttinger parameters

In this section we want to show some applications of the cMPS beyond the calculation of correlation functions, this will show the versatility and predictive power of the method.

One-dimensional models have been used to get intuition into more complex systems. These solvable models are usually more tractable with solutions that provide of valuable insight like the Lieb-Liniger model[4]. Furthermore, when they became feasible experimentally in the late 60's and 70's and after experimental developments that allowed the possibility of engineering almost any desired interaction and geometry, the research focused on understanding their correlation properties to characterize this models experimentally. In particular, we direct our attention to the concept of Luttinger liquids, an effective theory that study low energy one-dimensional systems. The approach developed by Haldane [40] as he realised that many one-dimensional models exhibiting gapless excitations with a linear spectrum can be described within the same framework which defined a universality class of systems coined Luttinger liquids in analogy to higher dimensional fermionic systems. The Bosonization (or Luttinger liquids approach or harmonic-fluid approach) technique consists of expressing the original degrees of freedom of one-dimensional models in terms of new fields that describe the dynamics of the system in terms of the collective behaviour that characterizes the low-energy regime[41]. This is possible since the effect of long wave-length thermal and quantum fluctuations is enhanced by reduced dimensionality since scattering is unavoidable and thus excitations acquire a collective nature [27]. Thus to derive a low-temperature description, we need to identify a set of variables that describe the low-energy fluctuations of the system. For a bosonic system $\hat{\psi}$, these are the density and the phase. These variables can be defined

by introducing the density-phase representation [41]

$$\hat{\psi}(x) = \sqrt{\hat{\rho}(x)}e^{-i\hat{\theta}(x)}, \tag{3.22}$$

where $\hat{\rho}(x) = \hat{\psi}^\dagger(x)\hat{\psi}(x)$ is the particle density field and $\hat{\theta}(x)$ is the phase field. Furthermore the density operator when close to the ground state can be approximated by

$$\hat{\rho}(x) \sim \rho_0 - \frac{1}{\pi}\partial_x\hat{\phi}(x), \tag{3.23}$$

where ρ_0 is the ground state density and $\hat{\phi}$ describes the fluctuations over the ground state. From the usual commutation relations for bosonic fields $\left[\psi(x), \psi^\dagger(x')\right] = \delta(x-x')$ we have he commutation relations for the fields $\hat{\theta}$ and $\hat{\phi}$:

$$\left[\frac{1}{\pi}\partial_x\hat{\phi}(x), \hat{\theta}(x')\right] = -i\delta(x-x'). \tag{3.24}$$

With these definitions, the effective Hamiltonian describing low energy behaviour for the Lieb Liniger model Eq. (1.99) becomes [28, 41]:

$$\hat{H}_{\text{eff}} = \frac{v_{\text{s}}}{2\pi}\int_0^L dx\, K\left[\partial_x\hat{\phi}(x)\right]^2 + \frac{1}{K}\left[\partial_x\hat{\theta}(x)\right]^2, \tag{3.25}$$

where the Luttinger parameters $\frac{v_{\text{s}}}{v_{\text{F}}}$ and K completely characterize the Hamiltonian. v_{s} refers to the phase velocity of the low-energy excitations, v_{F} is the Fermi velocity of a gas of free spinless fermions of density ρ_0 and the dimensionless parameter K is related to the strenght of the quantum fluctuations [41]. These parameters can be related to the ground state energy density of the Lieb-Liniger model $e(\rho, c)$ for a fixed parameter c as:

$$\left(\frac{v_{\text{s}}}{v_{\text{F}}}\right)^2 = \frac{M}{\pi^2\rho_0}\left(\frac{\partial^2 e(\rho,c)}{\partial^2\rho}\bigg|_{\rho_0=1}\right) \quad \text{and} \quad K^2 = \frac{\pi^2\rho_0}{M}\left(\frac{\partial^2 e(\rho,c)}{\partial^2\rho}\bigg|_{\rho_0=1}\right)^{-1}, \tag{3.26}$$

with ρ the density of particles, and M is the mass of the bosons which for simplicity will be taken to be equal to 1. These expressions have analytical approximations for

extremes values of c [41], for instance for small c:

$$\frac{v_s}{v_F} = \frac{\sqrt{c}}{\pi}\left(1 - \frac{\sqrt{c}}{2\pi}\right)^{1/2} \quad \text{and} \quad K = \frac{\pi}{\sqrt{c}}\left(1 - \frac{\sqrt{c}}{2\pi}\right)^{-1/2}, \tag{3.27}$$

and the corresponding approximations for big $c \gg 1$:

$$\frac{v_s}{v_F} = \left(1 - \frac{4}{c}\right) \quad \text{and} \quad K = \left(1 + \frac{4}{c}\right). \tag{3.28}$$

In Fig. (3.8) we compare the Luttinger parameters we calculated with our cMPS for

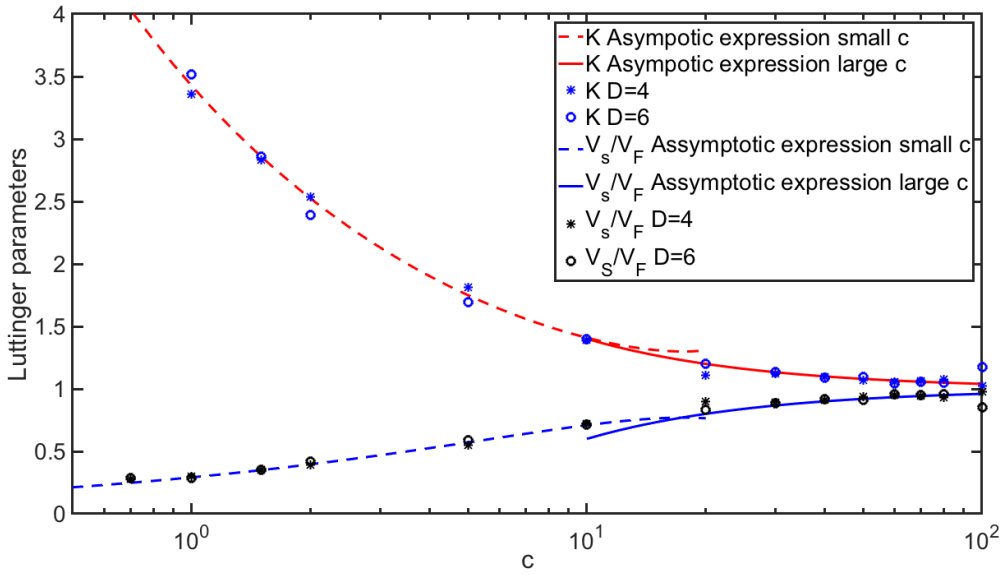


Figure 3.8: Luttinger parameters K and v_s/v_F as a function of the interaction strength c of the Lieb-Liniger model. The isolated asterisks and circles represent our own calculation of Eq. (3.26) using cMPS to find the energy density $e(\rho, c)$ at different density of particles ρ for each selected value of the parameter c. The continuous and dashed lines represent the asymptotic approximations for small and large c.

matrices of dimensions $D = 4$ and $D = 6$ where both reproduce very well the the assypmtotic cases for K and v_s/v_F as reported by [36]. As c increases from 0 to larger values, the parameter K varies from infinity to 1, where $K \to \infty$, $(c \to 0)$ corresponds to free bosons, which are not stable in one-dimension [27], for the cases where K has a finite value it represents repulsive bosons where in particular for the limit $K = 1$, $(c \to \infty)$ is the Tonks-Girardeau limit of perfectly repulsive bosons which also corresponds to the value for K for non interacting fermions. While also for $v_s/v_F = 1$ for the case $c \to \infty$ tells us that the phase velocity v_s is the same as the velocity v_F of free fermions

[27]. Up to this stage we have only considered the parameters that minimize the energy density as the entries of the matrices K and R that describe the auxiliary system. It was proposed in [3] to promote the matrix K to represent the Hamiltonian that describes a Jaynes-Cummings Hamiltonian and R the intracavity annihilation operator $\hat{a}$. Although they managed to describe some features of the Lieb-Liniger gas, it is still not clear why this particular Hamiltonian works with so little parameters. That is why in the next sections we will analyse deeply some characteristics of some cavity QED systems and try to improve the previous results obtained and try to, to uncover the physics behind this successful numerical simulation.

CHAPTER 4

OPTIMIZATION OF THE ENERGY DENSITY OF THE GROUND STATE OF THE LIEB-LINIGER MODEL USING A CAVITY QED

In the previous chapter, we introduced the concept of continuous matrix product states (cMPS) as a numerical tool to calculate the minimum of the expectation value of the energy density of the Lieb-Liniger model. Furthermore, we calculated the second correlation function and the Luttinger parameters of the system. The whole process depended on finding the optimal parameters that minimized the expectation value of the Hamiltonian of the Lieb-Liniger model. These parameters correspond to the entries of the matrices K and R. Currently, the only restriction of K is to be hermitian and R is to be real valued. Based on [3] Barrett et al. we argue that these matrices can be related to operators that describe physical systems. In particular, the matrix K can be related to a Hamiltonian and R to an operator involved in the loss of particles in a physical system. One possible candidate could be the Hamiltonian describing a cavity QED system. Thus in the following sections, we will familiarize with the dynamical properties of a laser-driven two-level atom and its interaction with a cavity. This understanding will enable us to establish a connection between the matrices K, R and the operators describing the cavity QED system. Finally, we will try to generalize to a three-level atom and discuss the results.

4.1 Atom inside the cavity

4.1.1 Two level atom

As a starting point we consider a driving classical laser of the form:

$$\vec{E}(t) = \hat{\epsilon} E_0 \cos(\omega_l t) = \frac{\hat{\epsilon} E_0}{2} \left(e^{-i\omega_l t} + e^{i\omega_l t} \right), \tag{4.1}$$

where E_0 is the laser amplitude, ω_l the frequency of the laser and $\hat{\epsilon}$ the polarization vector. We assume it drives a two-level atom with an atomic transition frequency ω_0 such that $\hbar\omega_0 = E_2 - E_1$ with E_1 is the energy of the ground state $|g\rangle$ and E_2 is the energy of the excited state $|e\rangle$. Although an atom has many energetic levels, assuming a model with only two levels is a good approximation when the frequency of the light beam ω_l is comparable with the energy difference of the two energy levels in question such as:

$$\hbar\omega_l \sim E_2 - E_1, \tag{4.2}$$

in that case, we can ignore other optical transitions since their occurrence is lower than in the resonant case. Following [25], the total Hamiltonian will be the sum of the free Hamiltonian H_{A} of the atom plus the Hamiltonian describing the atom-field interaction H_{AF}:

$$H = H_{\mathrm{A}} + H_{\mathrm{AF}}, \tag{4.3}$$

where the Hamiltonian of the free atom is given by:

$$H_{\mathrm{A}} = \hbar\omega_0 |e\rangle\langle e|, \tag{4.4}$$

on the other hand, for the conditions where the wavelength of the laser is much larger than the size of an atom, $\lambda \gg 1\text{Å}$, we can make use of the dipole approximation that allows us to use Eq. (4.1) for the atom-field interaction Hamiltonian which up to a constant is given by:

$$H_{\mathrm{AF}} = -\vec{d} \cdot \vec{E}, \tag{4.5}$$

where $\vec{d} = -e\vec{r}_0$ with e the electric charge of the electron and $\vec{r}_0$ the atomic electron vector position. If we apply the identity on the right and left of $\vec{d}$ given by $\mathbb{1} = |e\rangle\langle e| +$

$|g\rangle\langle g|$ we can rewrite the dipole operator as:

$$\vec{d} = \langle g|d|e\rangle\{\hat{\sigma}^\dagger + \hat{\sigma}\}, \tag{4.6}$$

where the diagonal terms are zero due to the parity of r_0 and since $\vec{d}$ is a physical quantity, it can be measured thus $\langle g|d|e\rangle = \langle g|d|e\rangle^*$. Also we define the atomic annihilation operator as $\hat{\sigma} = |g\rangle\langle e|$. Finally, combining equations Eq. (4.1) and Eq. (4.6) into the atom-field interaction Hamiltonian Eq. (4.5) we obtain:

$$H_{\mathrm{AF}} = \frac{\hbar\Omega_{\mathrm{R}}}{2}\left(\hat{\sigma}^\dagger + \hat{\sigma}\right)\left(e^{-i\omega_l t} + e^{i\omega_l t}\right), \tag{4.7}$$

where $\Omega_{\mathrm{R}} = -\frac{E_0\langle g|\hat{\epsilon}\cdot\vec{d}|e\rangle}{\hbar}$ is the Rabi frequency where the phase of the dipole matrix element is generally chosen to be positive. Finally, if we change H to the rotating frame by means of the unitary transformation $U = \exp\left(i\hbar\omega_0\hat{\sigma}^\dagger\hat{\sigma}t\right)$ the temporal evolution of the annihilation operators are of the form $\hat{\sigma} \sim e^{-i\omega_0 t}$ and $\hat{\sigma}^\dagger \sim e^{i\omega_0 t}$ so the time evolution of the cross terms in Eq. (4.7) of the form $e^{\pm i(\omega_l+\omega_0)t}$ oscillate rapidly while the terms $e^{\pm i(\omega_l-\omega_0)t}$ oscillate slowly, so assuming $|\omega - \omega_0| \ll \omega + \omega_0$ we make use of the rotating wave approximation, and eliminate the fast rotating terms leaving us with a simpler expression for the Hamiltonian of the atomic two level system driven by a laser:

$$H = \omega_0\hat{\sigma}^\dagger\hat{\sigma} + \frac{\Omega_{\mathrm{R}}}{2}(\hat{\sigma}^\dagger e^{-i\omega_l t} + \hat{\sigma}e^{i\omega_l t}), \tag{4.8}$$

from now on $\hbar = 1$ for convenience, and as a reminder, ω_l is the frequency of the laser, ω_0 is the atomic transition frequency related to the energy difference of the atomic energy levels in the two-level atom $\omega_0 = E_2 - E_1$, ω_l is the frequency of the laser, Ω_{R} is the Rabi frequency and $\hat{\sigma}$ the annihilation operator of the atom. This Hamiltonian, allow us to calculate the state of the system at any time. In particular, we are interested in the time evolution of the probabilities of the atom being in the ground and excited state since they will help us to understand the dynamics of the system and as we will see in the Jaynes-Cummings model, they will give us information of the amount each mode contributes to the dynamics of the system. This will help us to argue that we don't need all the information on each mode but only the ones that contribute the most to the dynamics of the system. That will justify the truncation of some operators to compute

them numerically. Following [42] we solve the time-dependent Schrödinger equation

$$H|\Psi\rangle = i\hbar\frac{\partial|\Psi\rangle}{\partial t}. \tag{4.9}$$

Using a state which is a general solution of Eq. (4.9) of the form:

$$|\Psi(r,t)\rangle = c_{\rm g}(t)|g\rangle e^{-iE_1 t} + c_{\rm e}(t)|e\rangle e^{-iE_2 t}, \tag{4.10}$$

where the $|g\rangle$ and $|e\rangle$ are the eigenstates of $H_{\rm A}$

$$H_{\rm A}|g\rangle = E_1|g\rangle, \tag{4.11}$$

$$H_{\rm A}|e\rangle = E_2|e\rangle, \tag{4.12}$$

which contain information of the ground and excited stated of the atom respectively. Using the general solution Eq. (4.10) in the time dependent Schrödinger equation with the Hamiltonian of Eq. (4.8) we arrive to the relations:

$$\dot{c}_{\rm g}(t) = \frac{i}{2}\Omega_{\rm R} e^{i(\omega_l-\omega_0)t} c_{\rm e}(t), \tag{4.13}$$

$$\dot{c}_{\rm e}(t) = \frac{i}{2}\Omega_{\rm R} e^{-i(\omega_l-\omega_0)t} c_{\rm g}(t), \tag{4.14}$$

which describe the limit where the light-atom interaction is strong such as in the case of laser beams. Note that these expressions already take into account the rotating wave approximation performed on the Hamiltonian Eq. (4.7) which simplifies the equations. Furthermore, if we choose the resonant case ($\omega_l - \omega_0 = 0$), and assuming the initial conditions $c_{\rm g}(0) = 1$ and $c_{\rm e}(0) = 0$, for the probability amplitudes, the solution for the probabilities of the atom being in the ground and excited state yields:

$$P_{\rm g} = |c_{\rm g}(t)|^2 = \cos^2(\Omega_{\rm R} t/2), \tag{4.15}$$

$$P_{\rm e} = |c_{\rm e}(t)|^2 = \sin^2(\Omega_{\rm R} t/2). \tag{4.16}$$

The temporal evolution of the probabilities is shown in Fig. (4.1) where their values oscillate at the Rabi frequency $\Omega_{\rm R}$, a phenomenon known as Rabi oscillations. The maximum and minimum values alternate in the range $P_{\rm e}, P_{\rm g} \in [0,1]$ where for instance,

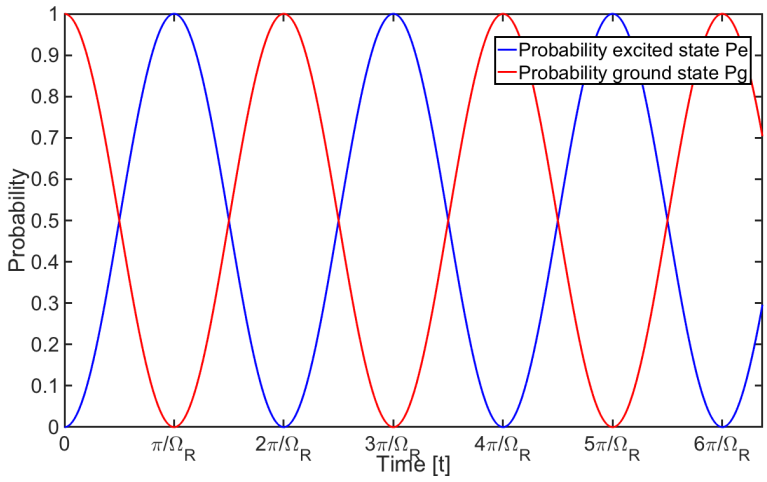


Figure 4.1: Probabilities for the ground state and excited state for the driven two level atom system in the resonant case $\omega_l - \omega_0 = 0$. The zeros in ground state are in: $2\pi n/\Omega_{\mathrm{R}}$ for $n \in \mathbb{Z}$

for the excited state probability, the minimum value $P_{\mathrm{e}} = 0$ occur for integer multiples of $2\pi/\Omega_{\mathrm{R}}$ while for the ground state, the minimum value $P_{\mathrm{g}} = 0$ occur for odd integer multiples of π/Ω_{R}. Note that the total probability is conserved at all times as we have explicitly $P_{\mathrm{g}} + P_{\mathrm{e}} = 1$. For the off-resonant case ($\omega_l - \omega_0 \neq 0$), and using Eq. (4.14)

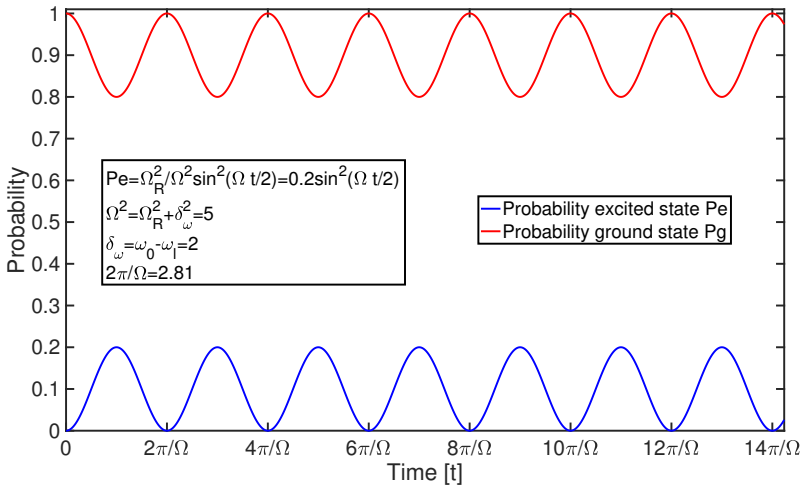


Figure 4.2: Probabilities for the ground state and excited state for the driven two level atom system in the off-resonant case $\delta_\omega = \omega_l - \omega_0 \neq 0$. The zeros in ground state are in: $2\pi n/\Omega$ for $n \in \mathbb{Z}$ where $\Omega_{\mathrm{R}} = 1$, $\delta_\omega = 2$, $\Omega = \sqrt{5}$.

and Eq. (4.13), the differential equation for c_{e} will be:

$$\ddot{c}_{\mathrm{e}}(t) + i\delta_\omega \dot{c}_{\mathrm{e}} + \frac{\Omega_{\mathrm{R}}^2}{4} c_{\mathrm{e}} = 0, \tag{4.17}$$

where $\delta_\omega = \omega_0 - \omega_l$ is the detuning. Solving for the initial conditions $c_{\rm g}(0) = 1$, and $c_{\rm e}(0) = 0$ the probability of the excited state $P_{\rm e}$ becomes:

$$P_{\rm e} = |c_{\rm e}(t)|^2 = \frac{\Omega_{\rm R}^2}{\Omega^2} \sin^2(\Omega t/2), \tag{4.18}$$

where $\Omega^2 = \Omega_{\rm R}^2 + \delta_\omega^2$ and $P_{\rm g}$ can be obtained from the conservation of the probability $P_{\rm e}+P_{\rm g} = 1$. Depicted in Fig. (4.2), the probabilities do not cross and in our example, the maximum amplitude for the probability in the excited state $P_{\rm e}$ is given by $\Omega_{\rm R}^2/\Omega^2 = 0.2$. In general, given the definition of Ω, as the laser increases the detuning δ_ω, the amplitude of the probability will decrease while the frequency of oscillation Ω will increase above the Rabi frequency defined in the resonant case. Physically this means that as the laser goes away from resonance, the frequency needed to stimulate the emission of a photon is less likely to occur. Thus in our example, with the initial condition that the atom is in the ground state, it will remain there with a probability oscillating, between 0.8 and 1. For the case where we include decay in the two-level atom system in the form

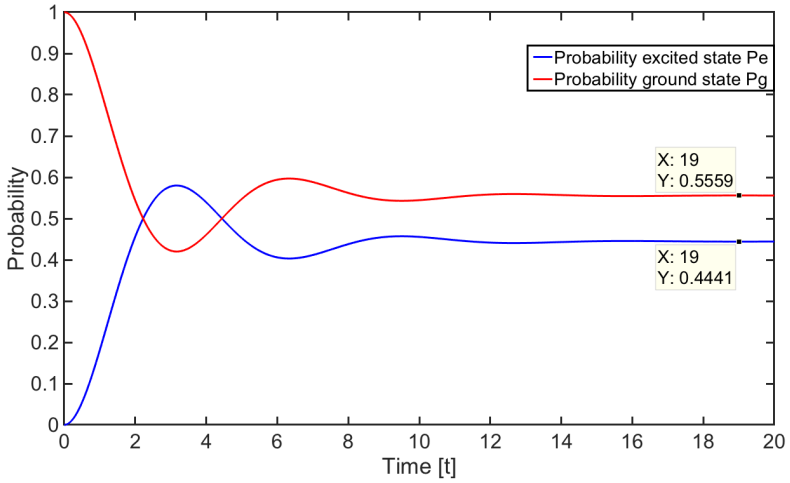


Figure 4.3: Probabilities for the ground state and excited state for the driven two level atom system that includes decay in the form of spontaneous emission in the resonance case. $\Omega_{\rm R} = 1$, $\omega_0 - \omega_l = 0$ and $\gamma = 0.5$. The total probability is conserved for all times even in the steady state. We still have an oscillatory behaviour but damped by γ.

of spontaneous emission, we follow [32, 43]. We focus on the equations for the matrix elements of the density matrix ρ for a two-level atom since they contain information of the probabilities. These relations are derived from the Bloch equations studied in [32]

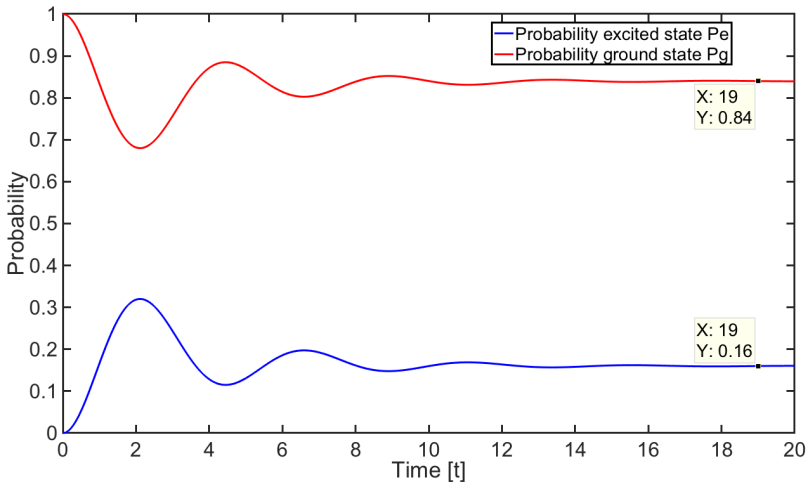


Figure 4.4: Probabilities for the ground state and excited state for the driven two level atom system that includes decay in the form of spontaneous emission in the off resonance case. $\Omega_{\mathrm{R}} = 1$ $\omega_0 - \omega_l = 1$, $\gamma = 0.5$. The total probability is conserved at all times as shown for the points near the steady state.

but we only need to analyse the final results as follows:

$$\frac{d\rho_{\mathrm{ee}}}{dt} = -\frac{d\rho_{\mathrm{gg}}}{dt} = -\frac{1}{2}i\Omega_{\mathrm{R}}(\rho_{\mathrm{eg}} - \rho_{\mathrm{ge}}) - 2\gamma\rho_{\mathrm{ee}}, \tag{4.19}$$

$$\frac{d\rho_{\mathrm{ge}}}{dt} = \frac{d\rho^*_{\mathrm{eg}}}{dt} = \frac{1}{2}i\Omega_{\mathrm{R}}(\rho_{\mathrm{gg}} - \rho_{\mathrm{ee}}) + [i(\omega_0 - \omega_l) - \gamma]\,\rho_{\mathrm{ge}}, \tag{4.20}$$

where ρ_{ij} are the matrix elements of the density matrix and γ represents the spontaneous emission decay. Notice from Eq. (4.19) and Eq. (4.20) there are still oscillatory terms involved but with a term proportional to γ that involves an exponential decay. On the other hand from Eq. (4.19) since ρ_{ee} and ρ_{gg} represent the probability of excited and ground state respectively, then $\frac{d(\rho_{\mathrm{ee}}+\rho_{\mathrm{gg}})}{dt} = 0$ implies that the total probability is still conserved. Finally, if we solve for the steady state, $\frac{d\rho_{\mathrm{ee}}}{dt} = -\frac{d\rho_{\mathrm{ge}}}{dt} = 0$, Eq. (4.19) and Eq. (4.20) yield:

$$\rho_{\mathrm{ee}}(\infty) = \frac{1}{2 + \xi^2 + 4(\omega_0 - \omega_l)^2/\Omega_{\mathrm{R}}^2}, \tag{4.21}$$

where $\xi = \gamma/\Omega_{\mathrm{R}}$. In Fig. (4.3) we can appreciate the previous discussion where despite the damping there are a few oscillations where the plots cross before taking a fixed value for the steady state. In our case for the values of $\Omega_{\mathrm{R}} = 1$, $\omega_0 - \omega_l = 0$ and $\gamma = 0.5$ Eq. (4.21) give us the probability of the excited state in the steady state to be $\rho_{\mathrm{ee}}(\infty) \sim 0.4444$ as can be seen in Fig. (4.3) to be the case for even small values

such as $t = 19$ whereas for Fig. (4.4) the steady state gives a probability of the excited state of $\rho_{\rm ee}(\infty) \sim 0.16$, this is a smaller value than in the resonant case, which makes sense given the inverse dependence of the detuning $\omega_0 - \omega_l = 1$ in Eq. (4.21). In general the amplitudes of oscillation will be reduced which again is a consequence of a non zero detuning just as in the non decaying case. With these simple examples we have learnt more about the roles each physical variable such as the decay rate γ, the Rabi frequency $\Omega_{\rm R}$ and the detuning δ_ω play in the dynamics of a laser interacting with a 2-level atom. Now we are ready to increase the complexity by introducing into the mix a cavity that will contain this 2-level atom.

Jaynes-Cummings model

Proceeding in a similar way as in the previous section, and following [25] the total Hamiltonian for a atom interacting with a cavity mode is of the form:

$$H = H_{\rm A} + H_{\rm F} + H_{\rm AF}, \tag{4.22}$$

where the uncoupled Hamiltonian for a two-level atom and cavity with a single mode is of the form:

$$H_{\rm A} + H_{\rm F} = \hbar\omega_0 \hat{\sigma}^\dagger \hat{\sigma} + \hbar\omega_c \left(\hat{a}^\dagger \hat{a} + \frac{1}{2} \right), \tag{4.23}$$

like in the previous section, ω_0 is the atomic transition frequency, $\hat{\sigma}$ is the atomic annihilation operator and ω_c is the cavity resonance frequency of the field mode. The atom field interaction Hamiltonian is the same as in Eq. (4.5) $H_{\rm AF} = -\vec{d} \cdot \vec{E}$ with the atomic dipole operator as previously defined in Eq. (4.6) as $\vec{d} = \langle g|d|e\rangle\{\hat{\sigma}^\dagger + \hat{\sigma}\}$. However in this case the electric field $\vec{E}$ is of the form:

$$\vec{E}(r,t) = -\sqrt{\frac{\hbar\omega_c}{2\epsilon_0}} \left[f(\vec{r})\hat{a} + \vec{f^*}(r)\hat{a}^\dagger \right], \tag{4.24}$$

where $f(\vec{r})$ is the normalized spatial mode profile, a is the annihilation operator of the cavity mode and ϵ_0 is the electric permittivity in the vacuum. This means that the interaction Hamiltonian takes the form:

$$H_{\rm AF} = \hbar \left(\hat{\sigma}^\dagger + \hat{\sigma} \right) \left[g(r)\hat{a} + g(r)^*(r)\hat{a}^\dagger \right], \tag{4.25}$$

where we define the atom-field coupling energy as:

$$\hbar g(r) = -\sqrt{\frac{\hbar\omega_c}{2\epsilon_0}}\vec{d}\cdot\vec{f}(r), \tag{4.26}$$

with $g(r)$ as the cavity QED coupling constant. Similarly, as with the driven two-level atom, we will use the dipole approximation which is valid since the shortest wavelengths of interest for quantum optics are in the extreme ultraviolet so we are assuming $\lambda >$ 100nm, whereas typical atoms have diameters $a \approx 0.1$nm we can conclude that is safe to use due to the large disparity between atomic diameters and optical wavelengths [26]. Furthermore, we are using the rotating wave approximation to get rid of fast-rotating terms, dropping the constant vacuum-field energy and $g(r) = g/2$ for a fixed position $\vec{r}$ due to the dipole approximation, and for simplicity assuming $\hbar = 1$. Thus the Jaynes-Cummings Hamiltonian takes the final form:

$$H = \omega_0\hat{\sigma}^\dagger\hat{\sigma} + \omega_c\hat{a}^\dagger\hat{a} + \frac{g}{2}(\hat{a}^\dagger\hat{\sigma} + \hat{a}\hat{\sigma}^\dagger). \tag{4.27}$$

In the next section, we will consider losses of photons due to a lossy cavity thus to compensate for the loss of photons inside the cavity through the semitransparent wall and to avoid that the number of photons goes to zero, we drive the atom with a coherent source, a laser of frequency ω_l. Following [25] the Hamiltonian of the driving atom under the Jaynes-Cummings model is depicted as follows:

$$H = \omega_0\hat{\sigma}^\dagger\hat{\sigma} + \omega_c\hat{a}^\dagger\hat{a} + \frac{g}{2}(\hat{a}^\dagger\hat{\sigma} + \hat{a}\hat{\sigma}^\dagger) + \frac{\Omega}{2}(\hat{\sigma}^\dagger e^{-i\omega_l t} + \hat{\sigma}e^{i\omega_l t}), \tag{4.28}$$

where Ω is the Rabi frequency of the laser. Our goal is to obtain the probabilities in the ground and excited state to understand how the different modes affect the dynamics of the system and with that in mind, if we express a general state as a summation of the states $|g,n\rangle$ and $|e,n\rangle$

$$|\Psi\rangle = \sum_{n=0}^{\infty}\left[C_{g,n}|g,n\rangle + C_{e,n}|e,n\rangle\right], \tag{4.29}$$

and rewrite Eq. (4.28) in the rotating frame of $U = \exp(i\omega_l\hat{\sigma}^\dagger\hat{\sigma}t)\exp(i\omega_l\hat{a}^\dagger\hat{a}t)$

$$H = (\omega_0 - \omega_l)\hat{\sigma}^\dagger\hat{\sigma} + (\omega_c - \omega_l)\hat{a}^\dagger\hat{a} + \frac{g}{2}(\hat{a}^\dagger\hat{\sigma} + \hat{a}\hat{\sigma}^\dagger) + \frac{\Omega}{2}(\hat{\sigma}^\dagger + \hat{\sigma}), \tag{4.30}$$

then we can solve the time dependent Schrödinger equation in that rotating frame

$$H_{\mathrm{R}}|\Psi\rangle_{\mathrm{R}} = i\hbar\frac{\partial|\Psi\rangle_{\mathrm{R}}}{\partial t}, \tag{4.31}$$

which gives the coupled equations:

$$\dot{C}_{e,n} = -i(\omega_0-\omega_l)C_{e,n} - i(\omega_c-\omega_l)nC_{e,n} - i\frac{g}{2}\sqrt{n+1}C_{g,n+1} - i\frac{\Omega}{2}C_{g,n}, \tag{4.32}$$

$$\dot{C}_{g,n+1} = -i(\omega_c-\omega_l)(n+1)C_{g,n+1} - i\frac{g}{2}\sqrt{n+1}C_{e,n} - i\frac{\Omega}{2}C_{e,n+1}. \tag{4.33}$$

If we turn off the driving we just end up with the usual coupled differential equations between $C_{e,n}$ and $C_{g,n+1}$ that define a 2 dimensional Hilbert space for each n value in the Jaynes-Cummings model as:

$$\dot{C}_{e,n} = -i(\omega_0+n\omega_c)C_{e,n} - i\frac{g}{2}\sqrt{n+1}C_{g,n+1}, \tag{4.34}$$

$$\dot{C}_{g,n+1} = -i\omega_c(n+1)C_{g,n+1} - i\frac{g}{2}\sqrt{n+1}C_{e,n}. \tag{4.35}$$

Following [25], a closer look into Eq. (4.32) and Eq. (4.33) for the case of $\Omega = 0$ and $\omega_l = 0$ shows that the differential equations Eq. (4.34) and Eq. (4.35) are formally equivalent to the semiclassical equations of motion for the atom-field interaction that we previously solved. If we had obtained them in the interaction frame, we would have found exactly the same equations as in Eq. (4.13) and Eq. (4.14) thus the equivalent Rabi frequency is of the form: $g\sqrt{n+1}$ and if we include the detuning $\omega_c - \omega_0$ the generalised Rabi frequency reads:

$$\Omega_n = \sqrt{g^2(n+1) + (\omega_c-\omega_0)^2}. \tag{4.36}$$

Fig. (4.5) illustrates these equivalences since the temporal evolution of the probabilities is exactly the same as the driven 2 level atom counterpart Fig (4.1) however the zeros for the ground state are in terms of the equivalent Rabi frequency $g\sqrt{n+1}$ as multiples of $\frac{2\pi}{(g\sqrt{n+1})}$. Similarly, for the off-resonant case, Fig. (4.6) has the same behaviour as in the off-resonant case in the absence of a cavity Eq. (4.2). The range of the probabilities for the ground state and excited state are reduced due to the increase of the detuning now between the frequency of the cavity and the natural frequency of the atom $\omega_c - \omega_0 \neq 0$

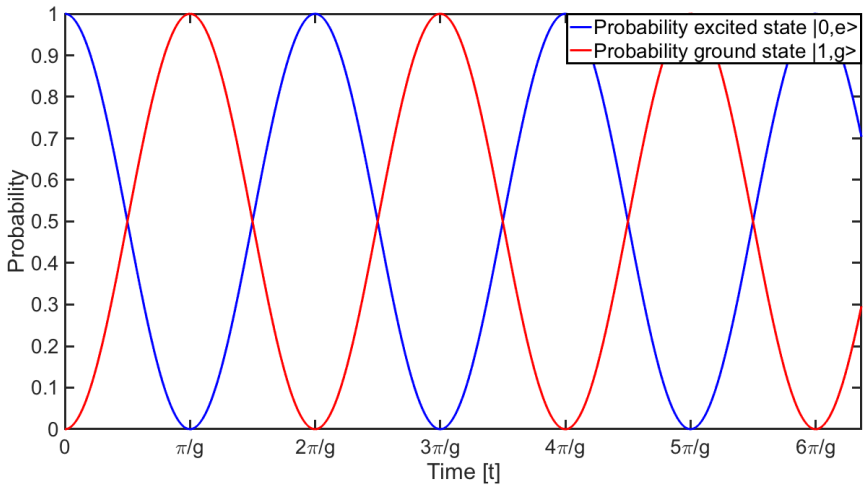


Figure 4.5: Cavity with 2 level atom, zeros in ground state are of the form $\frac{2\pi}{(g\sqrt{n+1})}k$ for $k \in \mathbb{Z}$ for our values: $g = 1$, $\omega_0 - \omega_l = 0$ and Initial state $|n = 0, e\rangle$ this means multiple integers of $2\pi/g$ similarly the zeros for the excited state are in the multiples of odd integers of π/g.

where the zeros for the probability in the ground state are for the multiples of $\frac{2\pi}{\Omega_n}$ Finally,

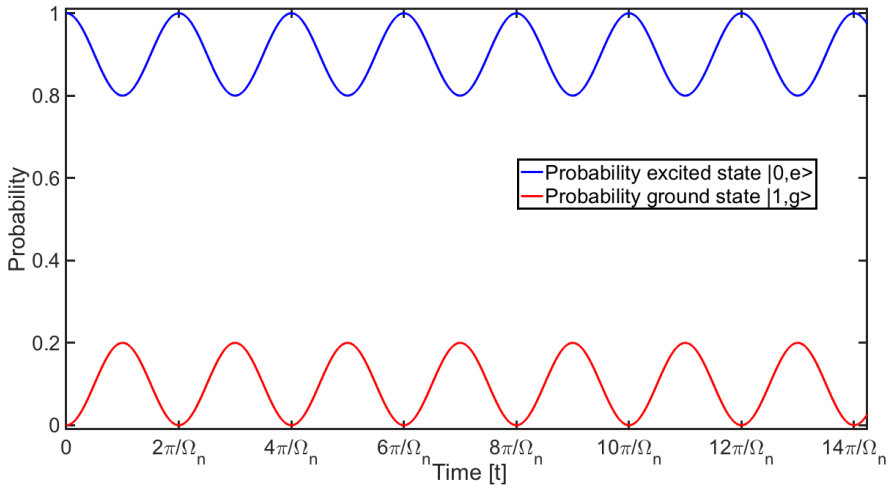


Figure 4.6: Cavity with 2 level atom, zeros in ground state are of the form: $\frac{2\pi}{\Omega_n}k = \frac{2\pi}{\sqrt{g^2(n+1)+(\omega_0-\omega_l)^2}}k$ for $k \in \mathbb{Z}$ for our values: $g = 1$, $\omega_0 - \omega_l = 2$ and initial state $|n = 0, e\rangle$.

let us note that in the Jaynes-Cummings model, not all the states are coupled in pairs. The state for $|n = 0, g\rangle$ is not coupled. That is to say, the vacuum amplitude $C_{g,0}$ is not coupled to any other amplitude, since no absorption can occur in the absence of light quanta as illustrated in Fig. (4.7) (left) where for the state $|0, g\rangle$ and any state $|n, e\rangle$ if the atom is initially in the ground state and the cavity has no photons it will remain that

way for all times unlike the pair of states $|1, g\rangle$ and $|0, e\rangle$ Fig. (4.7) (right). So far we have

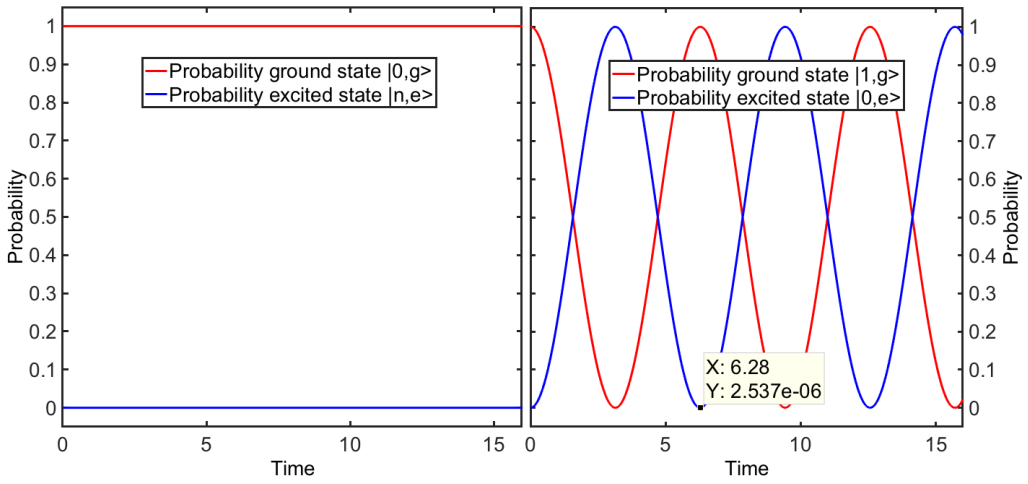


Figure 4.7: Cavity with 2 level atom . Left: Initial state $|n = 0, g\rangle$ is uncoupled as no absorption can occur in absence of light quanta. Right: Initial state is $|n = 1, g\rangle$ and zeros in ground state are in the multiple integers of: $\frac{2\pi}{(g\sqrt{n+1})} = 2\pi$ for our values: $g = 1$, $\omega_0 = 13$, $\omega_l = 13$, $\gamma = 0$ and initial state $|n = 0, e\rangle$.

learned how similar a driven atom-cavity system is to a driven atom. However, a few differences appear when the Jaynes-Cummings model reveals a more complex structure that couples pairs of eigenstates in a reduced subspace of its Hamiltonian. Physically this means that an excited atom can emit a photon into the cavity and reabsorb it but that is the extent of the energy transfer. A more interesting case will present when we start driving the atom so more modes will be involved in the dynamics.

Driving atom in cavity

We return our focus to the driving atom where $\Omega \neq 0$ in Eq. (4.32) and Eq. (4.33), as we start driving the atom, the separation into well-defined subspaces is not possible anymore. In that case, the probabilities from each of the cavity modes contribute to the total probability of the atom to be either in the ground or the excited state as shown in Fig. (4.8). The probabilities exhibit a behaviour much more complex due to the coupling of all the modes by the Rabi frequency of the laser. We want to show that not all modes contribute to the total probability in the same amount. As the number n of modes increase, the probability of that particular mode to be in the ground or the excited state will decrease. In Fig. (4.9) we obtained the temporal evolution of the probabilities for the ground and excited state for the first three modes $n = 0, 1, 2$ separately. While most

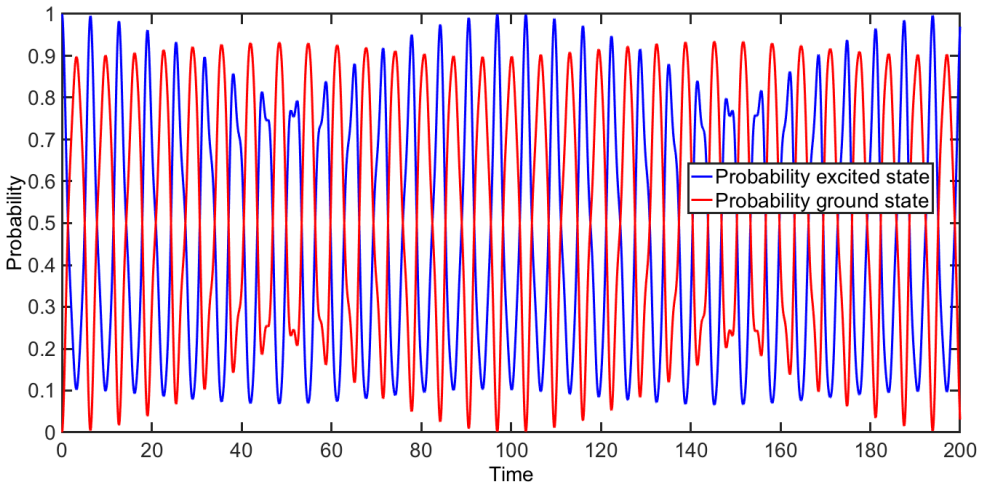


Figure 4.8: Driven 2 level atom in a cavity with $\Omega = 1$ g=1 $\omega_0 - \omega_l = 0$, $\omega_c - \omega_l = 2$, and initial state is $|n = 0, e\rangle$.

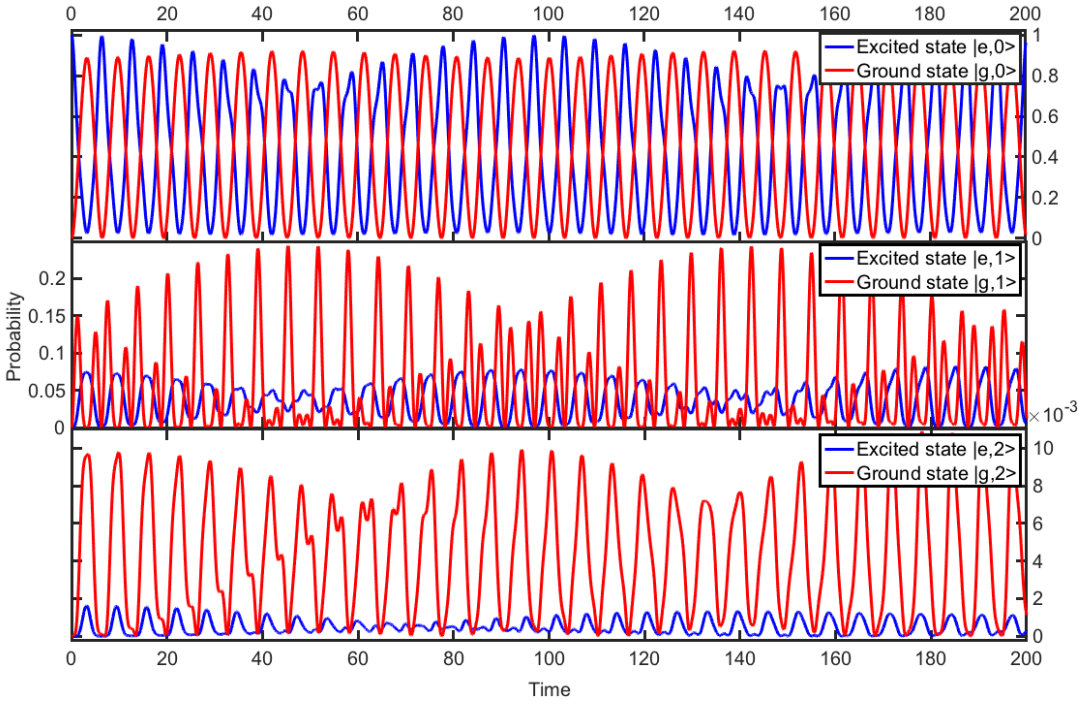


Figure 4.9: Driven 2 level atom in a cavity with $\Omega = 1$, g=1, $\omega_0 - \omega_l = 0$, $\omega_0 - \omega_c = 2$ and initial state $|n = 0, e\rangle$. Contribution of each mode. a) Probabilities for the mode n=0. b) Probabilities for the mode n=1. c) Probabilities for the mode n=2.

of the probability contribution comes from the mode $n = 0$, where $P_{e,0}(0) = 1$ and , $P_{g,0}(0) = 0$ and its maximum values are around ~ 0.85 for $n = 1$ there is a drop and the maximum probabilities are ~ 0.076 and ~ 0.24 for the excited state and the ground state respectively. Finally for $n = 2$ the maximum probabilities are ~ 0.0097 and ~ 0.0015

for the ground state and the excited state respectively. This means that for higher values of n the contribution to the total probability and the dynamics of the system will be negligible. This fact will allow us to truncate the space of an otherwise infinite-dimensional intracavity annihilation operator a. Up to now, we have considered a closed system however, in a more realistic cavity system, the environment will cause loss of information through spontaneous emission and cavity loss of photons. Assuming that the dimensions of the cavity allow us to ignore spontaneous emission, we can describe the cavity loss using the master equation in the Lindblad form.

4.2 CMPS and cavity QED corrrespondence

In the following the formal relationship between the cMPS matrices K, R as well as the cavity-QED operators will be presented. First we will discuss their similarities, which will introduce an intuition for the formalisms proposed previously in [3]. These similarities can be made apparent by relating the measurable leaking field correlation functions to intra-cavity field correlations by use of the input-output theory described in section (2.1), following which these expectation values can be re-written to mimic the structure of the expectation values of the bosonic fields in terms of the cMPS Eq. (1.52 -1.54). Taking $\hbar$ as unity, the Langevin equation Eq. (1.70), describing the time evolution of the intra-cavity annihilation operator $\hat{a}$ can be written as:

$$\dot{\hat{a}} = -\frac{i}{\hbar}\left[\hat{a}, \mathcal{H}_{\text{sys}}\right] - \left[\hat{a}, \hat{a}^\dagger\right]\left[\frac{\kappa}{2}\hat{a} + \sqrt{\kappa}\hat{a}_{in}\right] + \left[\frac{\kappa}{2}\hat{a}^\dagger + \sqrt{\kappa}\hat{a}_{in}^\dagger\right]\left[\hat{a}, \hat{a}\right], \tag{4.37}$$

where $\hat{a}_{in}$ is the cavity input operator describing fields entering the cavity, κ is the decay rate and $\mathcal{H}_{\text{sys}}$ is the cavity-atom Hamiltonian describing the system. If we use the properties of the commutators, we can simplify the previous expressions to,

$$\dot{\hat{a}} = \left[\hat{a}, Q'\right] - \left[\hat{a}, \hat{a}^\dagger\right]\sqrt{\kappa}\hat{a}_{in} = \left[\hat{a}, Q'\right] - \sqrt{\kappa}\hat{a}_{in}, \tag{4.38}$$

where $Q' = -i\mathcal{H}_{\text{sys}} - \frac{\kappa}{2}\hat{a}^\dagger\hat{a}$. In a similar procedure we obtain an equivalent expression for $\dot{\hat{a}}^\dagger$. It then follows from the input-output relation Eq. (1.76) that an expression for the expectation values in Eq. (4.42) can be obtained, with the assumption of vanishing input fields i.e. $\forall\ t,\ \hat{a}_{in}(t)|0\rangle = 0$. The first equality just links the correlation function

of the output field $\hat{a}_o$ with the intracavity field $\hat{a}$ as discussed in Eq. (2.1). For the remaining equations, Eqs. (4.39 to 4.41), we simply used the relationships between the correlation functions of the output fields with the intra-cavity fields derived in Eq. (2.1) and the two-time averages derived for open quantum systems Eq. (1.86) and Eq. (1.88) to express the expectation values as the trace of the system:

$$\begin{aligned}
\langle \hat{a}_o^\dagger(t)\hat{a}_o(t)\rangle &= \kappa\langle \hat{a}^\dagger(t)\hat{a}(t)\rangle = \kappa \mathrm{Tr}_{\mathrm{sys}}\left\{\hat{a}^\dagger\hat{a}\rho_{ss}\right\}, && (4.39)\\
\langle \hat{a}_0^\dagger(0)\hat{a}_o^\dagger(t)\hat{a}_o(t)\hat{a}_o(0)\rangle &= \kappa^2\langle \hat{a}^\dagger(0)\hat{a}^\dagger(t)\hat{a}(t)\hat{a}(0)\rangle \\
&= \kappa^2 \mathrm{Tr}_{\mathrm{sys}}\left\{\hat{a}V(t,0)(\hat{a}\rho_{ss}\hat{a}^\dagger)\hat{a}^\dagger)\right\}, && (4.40)\\
\langle \hat{a}_o^\dagger(t)\hat{a}_o(0)\rangle &= \kappa\langle \hat{a}^\dagger(t)\hat{a}(0)\rangle = \kappa \mathrm{Tr}_{\mathrm{sys}}\left\{\hat{a}^\dagger V(t,0)\hat{a}\rho_{ss}\right\}, && (4.41)\\
\langle \dot{\hat{a}}_o^\dagger(t)\dot{\hat{a}}_o(t)\rangle &= \kappa\langle \dot{\hat{a}}^\dagger(t)\dot{\hat{a}}(t)\rangle = \kappa \mathrm{Tr}_{\mathrm{sys}}\left\{\left[Q',\hat{a}\right]^\dagger\left[Q',\hat{a}\right]\rho_{ss}\right\}. && (4.42)
\end{aligned}$$

We need to point out that for the equal time expectation values Eq. (4.39) and Eq. (4.42) we are implicitly assuming that $t \to \infty$ to achieve the steady state. However, for the different time expectation values Eq. (4.40) and Eq. (4.41) we imposed as an initial condition that the density matrix at the beginning of the measurement is already in the steady state $\rho(0) = \rho_{ss}$. In all the derivations, the input-output relation Eq. (1.76) was used with the assumption of vanishing input fields, $\hat{a}_{\mathrm{in}}^\dagger(t)|0\rangle = 0$. This means that all the information about the leaking field will come from the annihilation operator $\hat{a}$. Comparing these equations with the expectation values of the bosonic fields in terms of cMPS, Eqs. (1.52 to1.55) we notice that they have the same structure Table (4.1). Moreover, it is apparent that the matrix R, will be somehow related to the operator

$\langle \hat{a}_o^\dagger(t)\hat{a}_o(t)\rangle = \kappa \mathrm{Tr}_{\mathrm{sys}}\left\{\hat{a}^\dagger\hat{a}\rho_{ss}\right\}$	$\langle \hat{\psi}^\dagger(x)\hat{\psi}(x)\rangle = \mathrm{Tr}[R^\dagger R\rho_{ss}]$
$\langle \hat{a}_o^\dagger(0)\hat{a}_o^\dagger(t)\hat{a}_o(t)\hat{a}_o(0)\rangle = \kappa^2 \mathrm{Tr}_{\mathrm{sys}}\left\{\hat{a}V(t,0)(\hat{a}\rho_{ss}\hat{a}^\dagger)\hat{a}^\dagger)\right\}$	$\langle \hat{\psi}^\dagger(0)\hat{\psi}^\dagger(x)\hat{\psi}(x)\hat{\psi}(0)\rangle = \mathrm{Tr}\left[Re^{\tilde{T}x}(R\rho_{ss}R^\dagger)R^\dagger\right]$
$\langle \hat{a}_o^\dagger(t)\hat{a}_o(0)\rangle = \kappa \mathrm{Tr}_{\mathrm{sys}}\left\{\hat{a}^\dagger V(t,0)\hat{a}\rho_{ss}\right\}$	$\langle \hat{\psi}^\dagger(x)\hat{\psi}(0)\rangle = \mathrm{Tr}[R^\dagger e^{\tilde{T}x}(R\rho_{ss})]$
$\langle \dot{\hat{a}}_o^\dagger(t)\dot{\hat{a}}_o(t)\rangle = \kappa \mathrm{Tr}_{\mathrm{sys}}\left\{\left[Q',\hat{a}\right]^\dagger\left[Q',\hat{a}\right]\rho_{ss}\right\}$	$\langle \frac{d\hat{\psi}^\dagger(x)}{dx}\frac{d\hat{\psi}(x)}{dx}\rangle = \mathrm{Tr}\left[([Q,R])^\dagger[Q,R]\rho_{ss}\right]$
$Q' = -i\mathcal{H}_{\mathrm{sys}} - \frac{\kappa}{2}\hat{a}^\dagger\hat{a}$	$Q = -\frac{1}{2}R^\dagger R - iK$

Table 4.1: Comparison between the correlation functions of the cavity QED output field and the correlation functions of the bosonic fields in terms of the cMPS, with $Q = -\frac{1}{2}R^\dagger R - iK$, $Q' = -i\mathcal{H}_{\mathrm{sys}} - \frac{\kappa}{2}\hat{a}^\dagger\hat{a}$ and $V(t,0) = \mathcal{T}\exp\left\{\int_0^t dt' L(t')\right\}$ satisfies the master equation Eq. (1.77) for the superoperator L, in the same way for $e^{\tilde{T}x}$ satisfying a similar master equation.

$\sqrt{\kappa}\hat{a}$ and K will be as discussed previously, related to the Hamiltonian of the system. Note also that, the density matrix in the steady state ρ_{ss} for the cavity QED system, obeys the same kind of master equation as the density matrix of the auxiliary system for the cMPS case deduced in Eq. (1.49). Now that we have two sets of equations, we can discern the correspondence between the finite dimensional matrices Q, R, in which the bosonic field operators are expressed, with the cavity QED operators involved in the dynamics of the cavity system. Table (4.1) lists the correlation functions in the cavity-QED formalism on the left and on the right the equivalent functions in the cMPS model. The equivalence between cMPS and cavity-QED is now apparent, we summarize the equivalent operators from both formalisms in Table (4.2).

cQED	cMPS
$\hat{a}_o(t)$	$\hat{\psi}(x)$
$\hat{a}$	R
H_{sys}	K
t	x
$V(t,0) = \mathcal{T}\exp\left\{\int_0^t dt' L(t')\right\}$	$e^{\tilde{T}x}$

Table 4.2: Relationship between operators that describe the cavity QED system and the operators involved in the description of a field theory by means of the cMPS

4.3 Simulation with a cavity and a 2 level atom

We now consider the correspondence established in [3] between the finite dimensional matrices (K, R), the single-mode cavity annihilation operator a and the Hamiltonian $\hat{H}_{\text{JC}}$ of an externally driven atom coupled to that cavity are expressed as:

$$K = \frac{\hat{H}_{\text{JC}}}{s}, \tag{4.43}$$

$$R = \sqrt{\frac{\kappa}{s}}\hat{a}. \tag{4.44}$$

Here κ is the cavity decay rate while s is a scaling parameter that maps the distance x in the Lieb-Liniger model with the time t in the atom-cavity system. Its role will be discussed in detail later. The Jaynes-Cummings Hamiltonian $\hat{H}_{\text{JC}}$ is that of a driven 2

level atom interacting with a cavity and has the following form:

$$\hat{H}_{\mathrm{JC}} = \omega_0 \hat{\sigma}^\dagger \hat{\sigma} + \omega_c \hat{a}^\dagger \hat{a} + \frac{g}{2}(\hat{a}^\dagger \hat{\sigma} + \hat{a}\hat{\sigma}^\dagger) + \frac{\Omega}{2}(\hat{\sigma}^\dagger e^{-i\omega_l t} + \hat{\sigma} e^{i\omega_l t}). \tag{4.45}$$

However, using the rotating frame $U = \exp(i\omega_l \hat{\sigma}^\dagger \hat{\sigma} t) \exp(i\omega_l \hat{a}^\dagger \hat{a} t)$ to eliminate temporal dependencies we obtain:

$$\hat{H}_{\mathrm{JC}} = (\omega_0 - \omega_l)\hat{\sigma}^\dagger \hat{\sigma} + (\omega_c - \omega_l)\hat{a}^\dagger \hat{a} + \frac{g}{2}(\hat{a}^\dagger \hat{\sigma} + \hat{a}\hat{\sigma}^\dagger) + \frac{\Omega}{2}(\hat{\sigma}^\dagger + \hat{\sigma}), \tag{4.46}$$

where g, $\hat{\sigma}$ and Ω are respectively the atom-cavity coupling strength, the atomic lowering operator, and the Rabi frequency of the driving field. The frequency ω_0 is related to the energy necessary to excite the two-level atom, ω_l is the frequency of the excitation laser and ω_c the quantized cavity mode. When the cavity, atom and driving field are all resonant, and in a suitable rotating frame the Hamiltonian takes the form

$$\hat{H}_{\mathrm{JC}} = \frac{g}{2}(\hat{a}^\dagger \hat{\sigma} + \hat{a}\hat{\sigma}^\dagger) + \frac{\Omega}{2}(\hat{\sigma}^\dagger + \hat{\sigma}). \tag{4.47}$$

We remark that we have checked whether allowing extra variational parameters of non-zero detunings would improve the simulations but it does not appear to be the case. In order to find the density-density correlation function of our field theory in terms of the measurable quantities of the cavity system, we first notice that if we substitute the definitions of the matrices K, R Eq. (4.43) and Eq. (4.44) into the Liouvillian Eq. (1.50) we obtain

$$\mathcal{L}\rho(x) := \frac{-i\left[\hat{H}_{\mathrm{JC}}, \rho(x)\right] + \kappa \hat{a}\rho(x)\hat{a}^\dagger - \frac{1}{2}\kappa \hat{a}^\dagger \hat{a}\rho(x) - \frac{1}{2}\kappa \rho(x)\hat{a}^\dagger \hat{a}}{s}. \tag{4.48}$$

From this expression we can see that ρ_{ss} will not depend on the parameter s since in the steady state $\mathcal{L}\rho_{ss}(x) = 0$. Moreover the expression in the numerator corresponds to the Liouvillian for the cavity-atom system. Substituting the definition of R Eq. (4.44) into the density-density correlation function for bosonic operators defined in Eq. (3.9) and compare with the second correlation function of annihilation operators Eq. (4.40) we end up with an expression proportional to the second order correlation function for

the intra-cavity annihilation operators

$$\langle\hat{\psi}^\dagger(0)\hat{\psi}^\dagger(x)\hat{\psi}(x)\hat{\psi}(0)\rangle \;=\; \frac{4\kappa^2}{s^2}\langle\hat{a}^\dagger(0)\hat{a}^\dagger\left(\frac{x}{s}\right)\hat{a}\left(\frac{x}{s}\right)\hat{a}(0)\rangle, \tag{4.49}$$

where the parameter s introduced in Eq. (4.43) and Eq. (4.44) acts as an scaling constant for the dimension x. Furthermore, since the evolution of the annihilation operators describing the cavity-atom system depends on the time t, we can make the connection that $t = x/s$. Finally, substituting the definition of R Eq. (4.44) into the constrain for constant density of particles expressed in terms of cMPS, Eq. (3.8) we find that:

$$\mathrm{Tr}\left[\rho_{ss}\hat{a}^\dagger\hat{a}\right] = \frac{s}{2\kappa}. \tag{4.50}$$

Including this expression back into Eq. (4.49) we end up with the definition of the normalized second order correlation function for photons:

$$\frac{\langle\hat{a}^\dagger(0)\hat{a}^\dagger(\frac{x}{s})\hat{a}(\frac{x}{s})\hat{a}(0)\rangle}{\mathrm{Tr}\left[\rho_{ss}\hat{a}^\dagger\hat{a}\right]^2} = g_2\left(\frac{x}{s}\right), \tag{4.51}$$

thus

$$\langle\hat{\psi}^\dagger(0)\hat{\psi}^\dagger(x)\hat{\psi}(x)\hat{\psi}(0)\rangle = g_2\left(\frac{x}{s}\right), \tag{4.52}$$

which means that to obtain the relation of $\langle\hat{\psi}^\dagger(0)\hat{\psi}^\dagger(x)\hat{\psi}(x)\hat{\psi}(0)\rangle$ versus x we simply quantify $g_2(x/s)$ as a function of x. Moreover, in the previous paragraph we made use of the scaling factor s to define the time as $t = x/s$. Thus we have $g_2(x/s)$ versus the re-scaled "time" $x = st$.

4.3.1 Improved cQED/cMPS correspondence, analytical derivations

Truncation of the annihilation operators inevitably lead to uncertainties. From Eqs. (4.43) and (4.44), we see that cavity-QED equivalent of K and R are infinite dimensional operators, due to their dependence on the cavity creation and annihilation $a, a^\dagger$. However, in all previous simulations [3, 6] these operators were truncated to only four dimensions. In general, a $d-$dimensional truncation leads to a change in the commutation relation,

such that,

$$[\hat{a}, \hat{a}^\dagger] = \begin{pmatrix} 1 & 0 & 0 & 0 \\ 0 & 1 & 0 & 0 \\ \vdots & \vdots & \ddots & \vdots \\ 0 & 0 & 0 & 1-d \end{pmatrix} =: \tilde{\mathbb{1}}, \tag{4.53}$$

where the 'tilde' emphasizes that this is only approximately the identity matrix. In trying to find a way to mitigate the truncation error in simulations of the cavity-QED/cMPS correspondence, we discovered that the energy density for the cavity-QED/cMPS states under the correspondence given by Eqs. (4.43) and (4.44) can be rewritten as

$$e(c) = \mathrm{Tr}[\rho_{ss} \hat{H}^*_{\mathrm{JC}}], \tag{4.54}$$

where $\hat{H}^*_{\mathrm{JC}}$ is given by

$$\begin{aligned} \hat{H}^*_{\mathrm{JC}} =& \frac{\kappa g^2}{2s^3} \mathbb{1}_c \otimes \hat{\sigma}^\dagger \hat{\sigma} + \frac{2\kappa^3}{s^3} \hat{N} \otimes \mathbb{1}_a \\ & - \frac{i\kappa^2 g}{s^3} (\hat{a}\hat{\sigma}^\dagger - \hat{a}^\dagger \hat{\sigma}) \\ & + \frac{4\kappa^2}{s^2} c\hat{N}(\hat{N}-1) \otimes \mathbb{1}_a, \end{aligned} \tag{4.55}$$

with $\mathbb{1}_a$ the identity of the Hilbert space describing the atom and $\mathbb{1}_c$ the identity of the Hilbert space describing the cavity, we refer the reader to Appendix 5.1 for the full derivation. This form shows that, somewhat remarkably, the energy density of our simulated Lieb-Liniger model is given by the energy expectation value of a new, undriven, "Jaynes-Cummings-like" Hamiltonian, which we have denoted $\hat{H}^*_{\mathrm{JC}}$. This new Hamiltonian is non-trivially related to the original $\hat{H}_{\mathrm{JC}}$ as evidenced by the fact that the atom-cavity coupling and cavity decay rates enter even into the first two "free Hamiltonian" terms of $\hat{H}^*_{\mathrm{JC}}$. More over as shown in Appendix 5.1, this effective Hamiltonian, doesn't depend on Ω, the Rabi frequency. It is the last term of $\hat{H}^*_{\mathrm{JC}}$ as written above which is non-standard for a Jaynes-Cummings model. This term is normally encountered in Bose-Hubbard models, where it corresponds to an "on-site repulsion". Here there is only one site, and this term corresponds to an energy penalty as the number of photons in the cavity grows. Note that it is only this term which depends on the Lieb-Liniger interaction energy c. We can obtain an alternative interpretation if we use

the second correlation function for photons Eq. (4.51) and the constraint Eq. (4.50), where we will notice that this term is none other than $cg_2(0)$. It will be apparent in the next sections, from Fig. (4.14) that for strongly interacting particles $c \gg 1$ the second correlation function $g_2(0) \to 0$ thus the probability of finding 2 particles close to each other tends to zero meaning that for high values of c the interaction potential will be negligible and the kinetic energy will be given by the remainder terms of this "effective Jaynes-Cummings Hamiltonian". This effect was illustrated in Fig. (3.3) by the plot of energies obtained using cMPS in section 3.2. It should be emphasized that the minimum for $e(c)$ is not the expectation value of the ground state energy $\hat{H}^*_{\mathrm{JC}}$, since ρ_{ss} in Eq. (4.54) is the steady state density matrix of the atom-cavity system for the original Hamiltonian $\hat{H}_{\mathrm{JC}}$. As we mentioned at the end of section 3.1, the use of the cMPS, allow us to describe the expectation value of the density Hamiltonian describing the Lieb-Liniger model in terms of the expectation value of an auxiliary system, in this case the driven two level atom contained in a lossy cavity, where the unknown operator turned out to be $\hat{H}^*_{\mathrm{JC}}$.

With the following analogy, we attempt to explain the above phenomenon where an open system represented by the bosonic gas, is described by an open system given by the cavity-atom. Consider a driven damped harmonic oscillator, this represents an open system since it is losing energy through friction but at the same time is gaining energy through a sinusoidal driving force. This means that for $t \to \infty$ this open system will tend to a steady-state and effectively will behave like a simple harmonic oscillator. Thus in principle, we could use the open system in the steady-state to "describe" a simple harmonic oscillator, a closed system. We only need to select the right values of the force F_0 and driving frequency ω_d for $F(t) = F_0 \cos(\omega_d t)$ to adjust to the amplitude A and natural frequency ω_0 of the simple harmonic oscillator $A\cos(\omega_0 t)$. In the same sense, the cMPS formalism allows us to describe an uni-dimensional bosonic gas constrained to a ring (a closed system) by using an open system, the driven atom inside the lossy cavity. Thus the density matrix of the cavity in the steady state seeks to behave as a closed system and the effective Hamiltonian would represent the non-trivial transformation that its parameters need to fulfil to describe the bosonic gas efficiently. Using this new form of $e(c)$ automatically corrects the truncation error mentioned above. Specifically,

the term $\frac{\kappa g^2}{2s^3}\mathbb{1}_c \otimes \hat{\sigma}^\dagger\hat{\sigma}$ corrects for the originally approximated term $\frac{\kappa g^2}{2s^3}\tilde{\mathbb{1}}^2 \otimes \hat{\sigma}^\dagger\hat{\sigma}$. If we subtract the corrected expression for the expectation value of the energy density Eq. (4.54) to the uncorrected expression for the energy density, the difference would correspond to an error in the simulated energy of:

$$\Delta e(c) = \frac{\kappa g^2}{2s^3}\mathrm{Tr}[\rho_{ss}((\tilde{\mathbb{1}}^2 - \mathbb{1}_c) \otimes \hat{\sigma}^\dagger\hat{\sigma}]. \tag{4.56}$$

Although this effect will be somehow noticeable in the calculation of the energy density Fig. (4.12), it will prove to be important for determining the values of the physical variables that we will use as parameters (g, Ω, s) Fig. (4.13). It is worth mentioning that $\hat{H}^*_{\mathrm{JC}}$ depends on the form of the cavity-QED Hamiltonian used for K, thus it is possible to derive different forms of $\hat{H}^*_{\mathrm{JC}}$ for different initial energy structures of the system e.g. two levels or three levels systems, chapter 5 will explore this further.

4.3.2 Improved simulation results: Energy density

So far we have a simplified expression for the energy density, in terms of the interaction parameter of the delta potential c, shown in Eq. (4.54). Without further calculations this is the most meaningful expression of the gas energy one could obtain. In order to improve this, hence obtaining a better understanding of the energy density, numerical optimization is now required, specifically we must minimize Eq. (4.54) (over g, Ω and s). To begin with, the energy density has two terms, the first of which relates to the steady state of the cavity ρ_{ss}, while the second refers to the effective Hamiltonian H^*_{JC}. Treating this problem by parts we first calculate the steady state of the density matrix ρ_{ss}, which is given by the Lindblad equation Eq. (1.50). On substitution of the matrices K Eq. (4.43) and R Eq. (4.44) into the Lindblad equation Eq. (1.50) we immediately realise that ρ_{ss} is independent of s. In other words, s is constant as far as the density matrix is concerned. Next, we fix the Boson number Eq. (3.8) and proceed to minimize Eq. (4.54). It is worth nothing that upon writing the Boson number in terms of the cavity operators, Eq. (4.50) we can obtain the following expression for s consistent for all given ρ_{ss}

$$s = 2\kappa\mathrm{Tr}[\rho_{ss}\hat{a}^\dagger\hat{a}]. \tag{4.57}$$

This could reduce the amount of minimization we need to do (although the value of s still needs to be found numerically). In Refs. [3, 44] the minimizations were performed incorporating a symmetry of the Lieb-Liniger model, namely as explained in Section 3.3. In addition to reducing the truncation error, we performed our simulations without incorporating this symmetry, which, not only seemed to have improved the quality of the simulation but allowed a general, symmetry-free method to take shape. The results for the minimum value of energy for each c from 0 to 200, obtained by [3] as well as our values obtained in our simulations are shown in Fig. (4.10). As a reminder, c describes the delta

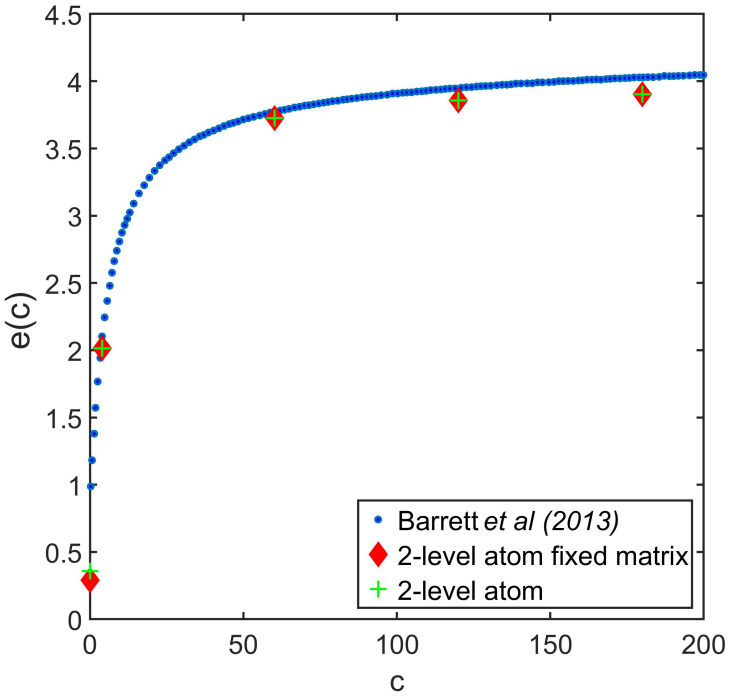


Figure 4.10: Minimum value for the energy density in the Lieb-Liniger Hamiltonian using a 2 level atom inside a cavity as simulator. In blue, extracted values from Barrett et al [3, 6] using a two level atom. In green our take on the simulation also using a 2 level atom showing the ground state energy density for values of $c = 0.07$, 3.95, 60.2, 120 and 180. On red same simulation but correcting for normal ordering of the annihilation operators. The small corrections for $c < 2$ will prove to be of importance at the moment of simulating second order correlation functions since will describe g_2 for smaller values of c much better than previous research. All plots use the same dimension for the truncated annihilation operator. $N = 4$

potential bosonic interaction. It can be seen that as c increases, the energy minimum increases and saturates at high c. This behaviour is largely reproducible regardless of the method used to calculate the cMPS. Our results are qualitatively similar to the ones obtained by [3] however for $c = 0$ we notice our simulation is closer to zero (green

cross) and even closer by a small margin our fixed simulation that avoids the truncation problem. (red diamonds). These and other yet, subtle differences do appear if we look closely, in particular for $c : [0, 4]$ Fig. (4.11). At this stage it should be emphasized that in a genuine quantum simulation that is, if we are using an actual cavity QED system to do the optimization, there is no truncation error, the "effective d" is $d = \infty$.

We want to discuss the consequences of the seemingly small variations that appear for small values of c between the simulation that fix the truncation error and the simulation that ignore this error. On correcting the truncation error, we see that the minimization yields as much as 20% lower values ($c = 0$) compared to the model without error correction. This shift reduces for increasing values of c and vanishes near $c = 1.5$, Fig. (4.11). For larger values of c, the shift between the error corrected and uncorrected models is negligible. With cMPS of dimension $D = 2$, only 8 variables were allowed in the simulation and clearly, had been insufficient as we recall from Fig. (3.1), where it crosses the Tonks-Girardeau gas limit of the Lieb-Liniger model at $\pi^2/3$, hence when simulating a large system we should expect, for a given parameter space, the energy density in the limit of $c \to \infty$ to be bounded by that value.. How quickly the energy density reaches the limit determines the accuracy of the simulation. Clearly we should configure the simulation to consider as higher dimension as possible, but we have shown, improvement to the simulation is negligible for $D > 4$. The results from our simulations, subsequently refereed as physical cMPS, the mathematical cMPS and the extracted data points from Barrett et al, are plotted together in Fig.(4.11). Immediately we see that the mathematical cMPS curves crosses the origin for $c = 0$. However the physical cMPS as well as Barrett et al data points fail to reproduce that behaviour. This could be explained If we recall that the energy density that we are minimizing Eq. (4.54) is the expectation value of an effective Jaynes-Cummings Hamiltonian Eq. (4.55) not of its ground state but a steady state ρ_{ss}. As the mathematical cMPS shows the expected behaviour at $c = 0$, physical models, such as the simulations from this work and from Barrett et al should approach the mathematical cMPS as much as possible maybe by increasing the dimension of the truncated operators. Clearly, from this perspective, the minimization from this work shows improved accuracy compared to the methods used by Barrett et al. The improvement may be attributed to the fact that the method

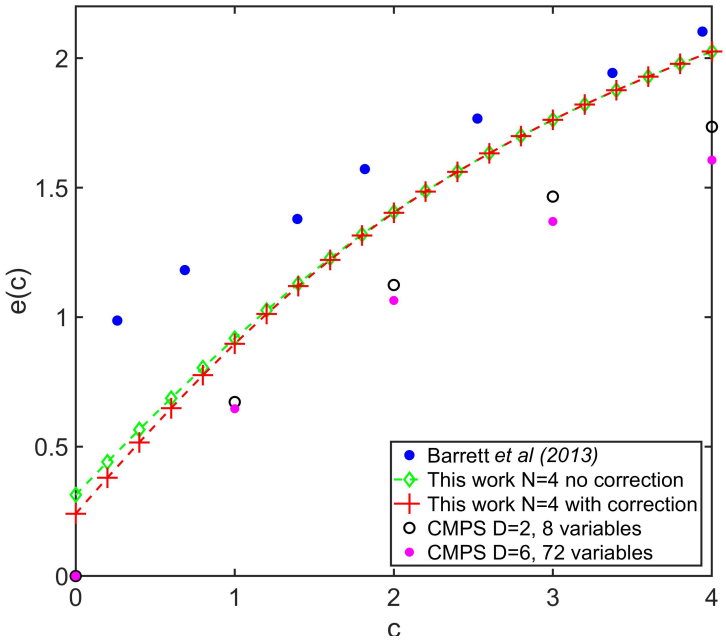


Figure 4.11: Comparing energy densities, in blue, the values obtained by Barrett et.al [3, 6], in green and red our minimization using a 2 level atom for the uncorrected and corrected values of the energy. In black and pink simulations done with the mathematical cMPS for K and R matrices of dimensions $D = 2, 6$ respectively.

used here does not assume symmetry, nor does it apply re-scaling to variables in the minimization, as this may cause unintended mistakes. However note, that as the data points for Barrett et al were not the original data produced by the authors but extracted from the figure, the argument made here only compares the qualitative difference, not the quantitative difference. The first impression from the results shown in Fig.(4.11), is that the relative changes observed on correcting the truncation error is small. However if we delve deeper and investigate the impact this has on the variables s, g, Ω, we will find the true significance of this error correction. Another factor that affects the simulation accuracy is the dimension of the truncated annihilation operator. For larger dimensions, more modes will be involved in the simulation, leading to a richer description of the reality. From the perspective of the cMPS, the higher the dimensions of the matrices K and R, the more accurate we can describe the energy of a bosonic field. In the physical cMPS simulation, the matrix R is proportional to the annihilation operator a, hence more accurate descriptions of the bosonic field will result from R with higher dimensionality. In Fig.(4.12) we show the energy density for $c \in [0 : 2]$, with both corrected and uncorrected cases of $N = 4, 6, 8$. To interpret this figure we consider now

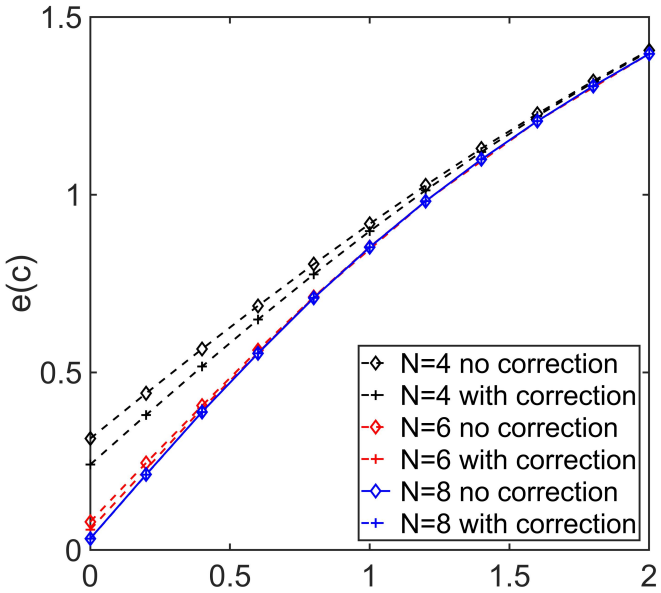


Figure 4.12: Comparing energy densities with and without corrections on the annihilation operators. Increasing the dimension of the annihilation operators while keeping the number of parameters constant, also proves to improve the simulations. The major change comes from using a dimension of $N = 6$ while no significant change seems to be produced is we calculate for $N = 8$.

the energy density "shift between corrected and uncorrected cases as a possible source of simulation inaccuracy for the uncorrected cases. We can see that the shift is the most significant for $0 \leq c \leq 1.5$, in particular the energy density offset increases for smaller dimensions. For larger values of $N > 4$, the shift improves with diminishing returns. Ideally we would choose $N = 6$ or above to maximize the simulation accuracy, but for computational simplicity, we will take $N = 4$, corresponding to the largest shift, to illustrate the effects of the correction on variables s, g and Ω. Since the energy density depends on c, s, Ω and g, minimizing Eq. (4.54) with respect to g, s, Ω allows us to extract a set of optimal values g, s and Ω, for each value of the parameter c. We plot the resulting curves in a)-c) Fig. 4.13. We notice that as c increases, all the variables, c, s, Ω and g decrease. We can provide an explanation of this behaviour if we notice that the second correlation function associated with the cavity-atom system $g_2(0) \to 0$ as c increases Fig.(4.14).That means that the probability of finding 2 photons leaking out of the cavity at the same time should decrease. That can be attained if the Rabi frequency Ω and the coupling g decrease to reduce the number of available photons inside the

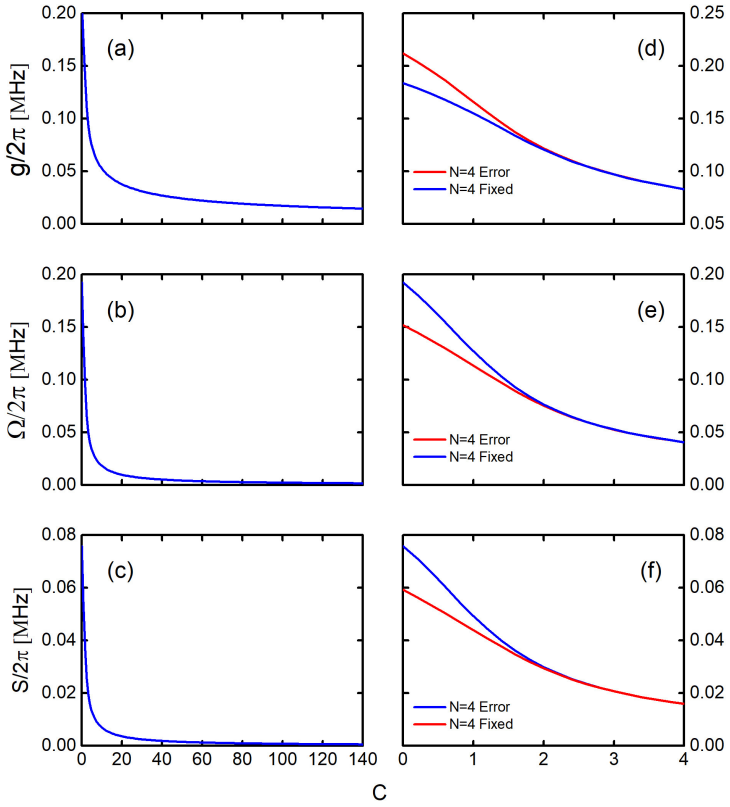


Figure 4.13: a)-c) Values of the three parameters used in the optimization of the energy density of the L.L. model tend to decrease as the interaction strength increases. In this optimization we implemented the corrections for the annihilation operators of dimension $N = 4$. d)-f) Effect of the corrections made on the three variables used in the optimization of the energy density for a truncated annihilation operator of dimension $N = 4$. Notice that these corrections affect mainly the sector of weak gas interactions, that is to say, values of $c \ll 2$. Increasing the dimension of the truncated operators will improve even more the results but as we have shown, only up to dimension of the order of 6 there will be noticeable changes.

cavity. Finally, the behaviour of s is related to the constraint that the Boson number density should be a constant at all times and equal to unity. It follows that s should be equal to the mean number of photons leaking out of the cavity Eq. (4.57), but as the number of photons leaking out of the cavity decreases hence s decreases. Similar arguments may be made for the increase of all three variables (s, g and Ω) as c tends to zero. Moving our attention now to d)-f) Fig(4.13) we are comparing the optimized variables (Ω, s, g) for the the corrected and the error case. While the corrections to the energy of the one-dimensional bosons, $e(c)$ are small, the values of s, Ω, g that yield the optimum values are significantly different . We see the bigger discrepancies for the regions of the c between 0 and 2 and no difference for $c > 2$. This suggest that the

optimal variables will increase faster than originally thought. For example, at $c = 0.2$, we find using our improved methods that the optimal values of s, Ω, g are 21%, 20%, 12% larger than those obtained without using them.

4.3.3 Improved simulation results: Second order correlation function

After exploring the effect of our corrections on the optimal variables (g, s, Ω) we want to move our attention to understand how this changes will affect the measurable quantities that we can extract from of our cavity-atom simulator, for instance the second correlation function $g_2(t)$. In section 4.3, we managed to mathematically relate the density-density correlation function that describes the bosonic particles used in [1] with the second order correlation function that describes photons leaking out of our cavity simulator Eq. (4.52) . Thus a good understanding of $g_2(t)$ will provide us with valuable insights in the description of the one dimensional bosonic gas. To calculate the plots in Fig.(4.14), we focused on equation Eq. (4.51) that relates $g_2(t)$, for $t = x/s$ with the annihilation operators. First, for each value of c we use the optimal parameters (g, s, Ω) to calculate the steady state ρ_{ss} using the vectorization procedure discussed in section 3 Eq. (3.12) that transforms the Lindblad operator Eq. (4.48) into a superoperator of the form $\mathcal{L}\rho_{ss} = 0$ in that way we calculate the evolution operator $V(t, 0) = \exp(\mathcal{L}t)$ that describes the temporal evolution of the correlation function Eq. (4.40) as:

$$\langle \hat{a}^\dagger(0)\hat{a}^\dagger(t)\hat{a}(t)\hat{a}(0)\rangle = \mathrm{Tr}_{\mathrm{sys}}\left\{\hat{a}V(t,0)(\hat{a}\rho_{ss}\hat{a}^\dagger)\hat{a}^\dagger)\right\}, \tag{4.58}$$

with that expression and knowledge of $\mathrm{Tr}\left[\rho_{ss}\hat{a}^\dagger\hat{a}\right]$ we obtained $g_2(x/s)$ for each value of c. Fig. (4.14)[1] shows our different attempts to improve the second correlation function $g_2(t)$. We note that the four plots have similar values for $g_2(0)$ for $c = 3.95, 60.2, 625.95$. However the most significant improvements are in the region for weakly interacting Bosons, $c < 1$ where $g_2(0)$ tends to 1. In particular from the cMPS simulations Fig. (3.6)b $g_2(0) = 0.8431$ for $c = 0.07$ so any simulation that properly describes this bosonic system should get closer to that value. In that regard, Fig. (4.14)b already shows and improvement with $g_2(0) = 0.6393$ respect to the plot obtained by Barrett et al. Fig.

[1] "Reprinted figure with permission from Sean Barrett et al., Simulating Quantum Fields with Cavity QED, Volume 110, Issue 9, pags. 1-7, 2013 Copyright (2013) by the American Physical Society.

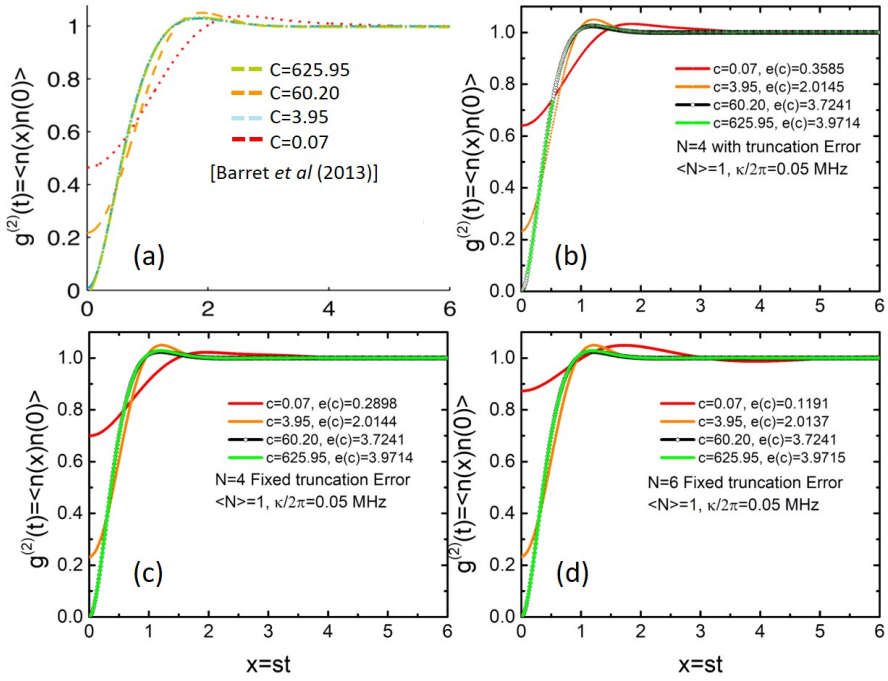


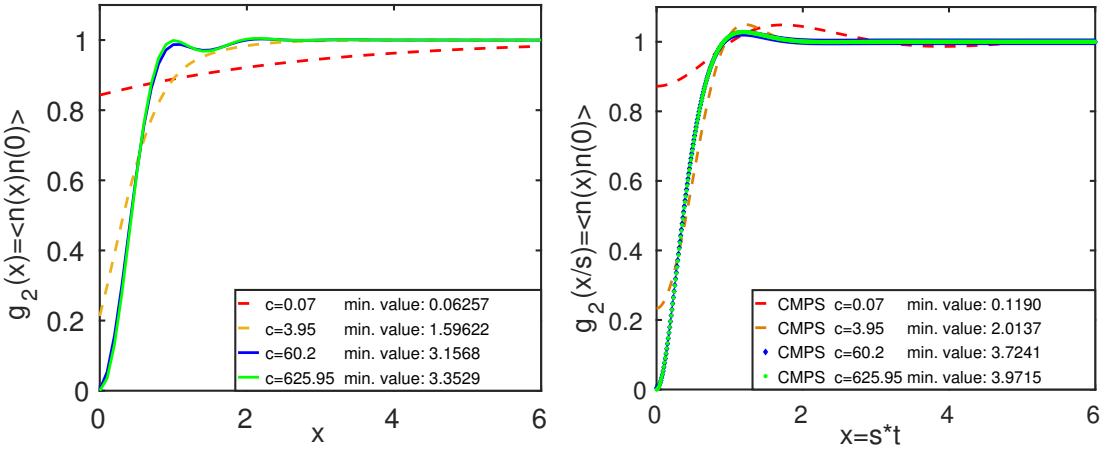
Figure 4.14: Second order correlation functions obtained from the physical cMPS where the matrices K and R are proportional to the Hamiltonian of a driven cavity-QED system and the intracavity annihilation operator a respectively. All the plots describe the values $c = 0.07, 3.95, 60.2, 625.95$. a) Plot extracted from [3] where the dimension of the annihilation operator is $N = 4$ b) Our simulation for $g_2(t)$ with the truncation error for $N = 4$. c) $g_2(t)$ for $N = 4$ using the energy density that fixes the truncation error Eq. (4.54). d) $g_2(t)$ with no truncation error and dimension of the annihilation operator $N = 6$

(4.14)a for the same value of c where $g_2(0) < 0.6$. In both cases the the truncation error is present, the discrepancy maybe due to the optimization method they used that included taking advantage of the Lieb-Liniger model symmetry or due to problems with the rescaling as discussed in section 3.3. Once the truncation is fixed and for $N = 4$ $g_2(0) = .6996$ Fig.(3.6)c and finally for the case where we also increase the dimension of the intracavity annihilation operator to $N = 6$ we see a major improvement with $g_2(0) = 0.8724$ Fig.(3.6)d. The fact that we are slightly above the cMPS value only reflects that these simulations are only using three variables (g, s, Ω) versus the 32 variables that the cMPS can access Fig.(3.6)b.

.

4.4 Discussion of results

One question we want to answer is, why the chosen quantum electrodynamic system, a driven two-level atom inside a lossy cavity, surprisingly acts as a good simulator for the one-dimensional bosonic gas Fig. (4.15). This could allow us to understand the limitations and potential improvements for future simulations. As a first step, we need to understand the physics behind each system so we can find the similarities that both systems share. On the one hand, Fig. (4.15a) describes the second order correlation



(a) Simulation of the Lieb-Liniger model using cMPS. The dimension of the matrices K and R given by dim(K)=dim(R)=4 for a total of 32 variables.

(b) Density-density correlation functions of the Lieb-Liniger model using a 2 level atom. The dimension of the anihilation operator is dim(a)=6.

Figure 4.15: The g_2 functions a) bosonic gas simulated using the cMPS and b) simulation of the bosonic gas using a cavity QED system.

function of bosonic particles for the Lieb-Liniger model in the one-dimensional position space for different values of the interaction strength c. According to chapter 3, this was an accurate description obtained using the cMPS as variational states with 32 variables. On the other hand, Fig. (4.15b) showcases the most improved simulation of the same bosonic unidimensional gas but using a driven atom in a lossy cavity as a simulator. This simulation is characterised by the second order correlation function g_2 rescaled by the parameter s. If for a moment we ignore the simulation and focus on the physics that it describes, Fig. (4.15b) only represents the second correlation function $g_2(t)$ of a driven 2 level atom inside a lossy cavity, only rescaled in the time dimension by the parameter s. What we would like to argue in the following analysis is that the physics that describes the dynamics of the photons produced by a driving atom in a cavity already possesses

Interaction c	$g_2(0)$ cMPS	$g_2(0)$ cavity simulation	optimized cavity variables $[MHz]$
0.07	0.8431	0.8724	$\Omega = .349288$, $g = 0.347690$
3.95	0.2129	0.2332	$\Omega = 0.041179$, $g = 0.083865$
60.2	0.003434	0.004217	$\Omega = 0.003427$, $g = 0.022154$
625.95	0.0000349	0.0000467	$\Omega = 0.000344$, $g = 0.006975$

Table 4.3: $g_2(0)$ of the one dimensional bosonic gas using cMPS with 32 variables and using the Jaynes Cummings model as a simulator of the bosonic gas. We see that for each interaction value c, in the Lieb-Liniger model, there is a corresponding set of variables Ω, g in the cavity model. Moreover the value of $g_2(0)$ are very close to each other

characteristics that mimic the corresponding physics of unidimensional gases. In other words, we are using a simulator with equivalent physical traits to the system we want to simulate. For starters, the delta-potential interaction in the Lieb-Liniger model is responsible for the free particle-like behaviour for long distances, thus the probability of finding another particle within an infinite distance is naturally 1. Similarly, for the cavity-atom, the probability of emitting a second photon after one was emitted within an infinity time is 1. Thus for all values of c, both correlation functions will behave similarly as

$$g_2(x \to \infty) = g_2(\tau \to \infty) = 1. \tag{4.59}$$

If we focus on $g_2(0)$ as the repulsive interaction strength c decreases, then the probability of finding two bosons in the same place increases towards 1, which is the limit of the ideal gas for non-interacting particles. Meanwhile, in the cavity QED case, $g_2(0) \to 1$ occurs when the couplings Ω and g are bigger than the decay rate κ thus the production of photons inside the cavity increases making more likely to encounter a pair of them at the same time. Thus for both cases, in the limit of $c \to 0$:

$$g_2(x \to 0) = g_2(t \to 0) \sim 1. \tag{4.60}$$

On the other hand for $c \to \infty$ we are close to the Tonks-Girardeau limit where the one-dimensional bosons separate from each other as much as possible furthermore, they can not cross each other nor be in the same place at the same time, behaving as non-interacting fermions [5]. In that limit, the probability of finding two bosons at the same point in space (i.e. at a distance zero) is zero creating an antibunching effect. Similarly, a two-level atom is only capable of absorbing a photon from the driving electromagnetic

field after a certain time even though the atom is ready to be excited as soon as it releases its previous photon. However, the electromagnetic field induced by the laser requires time to excite the atom. Thus in those conditions, the probability for the cavity to emit two photons simultaneously reduces to zero producing the antibunching effect. Thus for both cases, in the limit $c \to \infty$

$$g_2(x \to 0) = g_2(t \to 0) \sim 0. \tag{4.61}$$

Furthermore, not only for the extreme values but for intermediate values of c, there is good agreement in both correlation functions. For instance for $g_2(0)$ we can see from the second and third column in Table (4.3) they are very similar where the percentage errors in $g_2(0)$ for the cavity simulation are: 3.4%, 9.53%, 22.8%, and 33.8% for $c =$ 0.07, 3.95, 60.2 and 625.95 respectively which still is surprising considering we only used 3 variables for the cavity simulation versus 32 variables with the cMPS thus confirming that there is a certain equivalence between both systems. These similarities tells us that by themselves that the cavity atom system, has an inherent structure similar to the bosonic gas. Furthermore, from the effective Hamiltonian derived analytically using the physical cMPS Eq. (4.55) we can also compare the Hamiltonian of the one-dimensional gas with the equivalent effective Hamiltonian that describes a cavity QED system. As we previously mentioned, we are modelling a closed system (the bosonic gas) and using an open system (a driven atom inside a cavity with leaking photons) to describe it. We already tried to argue why it makes sense using an analogy with the harmonic oscillator. However, we need to understand succinctly the underlying mechanism that makes it possible. For instance, looking at the effective Hamiltonian, we can relate the contact interaction potential of the Lieb-Liniger model with a term proportional to the second correlation function g_2 meanwhile the dynamics of a Jaynes-Cummings type-Hamiltonian mimics the kinetic energy of the gas.

CHAPTER 5

GENERALIZATION FOR DIFFERENT HAMILTONIANS

5.1 Jaynes-Cummings Hamiltonian in a two level atom

We will explore how different Hamiltonians modify the final expression for the energy density $e(c)$ in terms of the cMPS. And will show that the terms of the form $[Q,R]^\dagger[Q,R]$ that represent the kinetic energy in the cMPS description of a field theory, will produce an effective Hamiltonian that has the same structure as the physical cavity q.e.d. Hamiltonian used to parametrize the cMPS. Departing from the expression for the energy density of the Lieb-Liniger model in terms of the cMPS:

$$e(c) = \mathrm{Tr}\left(\rho_{ss}\left[Q,R\right]^\dagger\left[Q,R\right]\right) + c\mathrm{Tr}\left(\rho_{ss}(R^\dagger)^2R^2\right), \tag{5.1}$$

with $Q = -iK - \frac{R^\dagger R}{2}$ and c the interaction strength. The second term describes in the cMPS representation the interaction between the atoms in the gas. Parametrizing the matrices K and R with operators that describe a physical system, we have the following identifications:

$$K = \frac{\hat{H}_{\mathrm{sys}}}{s}, \tag{5.2}$$

$$R = \sqrt{\frac{2\kappa}{s}}\hat{a}. \tag{5.3}$$

$\hat{H}_{\text{sys}}$ corresponds to the Hamiltonian of a suitable system, which variables we can control. For the case of $\hat{H}_{\text{sys}}$ being the Jaynes-Cummings Hamiltonian we have:

$$\hat{H}_{\text{sys}} = \frac{g}{2}(\hat{a}^\dagger\hat{\sigma} + \hat{a}\hat{\sigma}^\dagger) + \frac{\Omega}{2}(\hat{\sigma}^\dagger + \hat{\sigma}), \tag{5.4}$$

where $\hat{a}$ and $\hat{\sigma}$ represent the annihilation operators of the cavity and the atom respectively. The constants g and Ω are the coupling interaction and the Rabi frequency respectively. We can separate the terms that describe the interaction with the cavity from the ones only referring to the atom

$$\hat{H}_{\text{sys}} = \hat{\mathcal{H}}_{\text{atom}} + \hat{\mathcal{H}}_{\text{ca}}, \tag{5.5}$$

where

$$\hat{\mathcal{H}}_{\text{atom}} = \left(\frac{\Omega}{2}(\hat{\sigma}^\dagger + \hat{\sigma})\right), \tag{5.6}$$

$$\hat{\mathcal{H}}_{\text{ca}} = \frac{g}{2}(\hat{a}^\dagger\hat{\sigma} + \hat{\sigma}^\dagger\hat{a}). \tag{5.7}$$

For simplicity we are omitting the exterior product symbol between the annihilation operator a and the atomic annihilation operator $\hat{\sigma}$. Then we can rewrite Q as:

$$Q = -i\frac{\hat{\mathcal{H}}_{\text{atom}}}{s} - i\frac{\hat{\mathcal{H}}_{\text{ca}}}{s} - \frac{1}{2}R^\dagger R = -i\frac{\hat{\mathcal{H}}_{\text{atom}}}{s} + Q_{\text{ca}}, \tag{5.8}$$

but note that $[\hat{\sigma}, R] = 0$ since both operators act on different spaces, thus $[\mathcal{H}_{atom}, R] = 0$. This implies

$$[Q, R] = [Q_{\text{ca}}, R], \tag{5.9}$$

with $Q_{\text{ca}} = -i\frac{\mathcal{H}_{\text{ca}}}{s} - \frac{1}{2}R^\dagger R$. Reducing the energy density to:

$$e(c) = \text{Tr}\left(\rho_{ss}\left[Q_{\text{ca}}, R\right]^\dagger\left[Q_{\text{ca}}, R\right]\right) + c\text{Tr}\left(\rho_{ss}(R^\dagger)^2R^2\right) \tag{5.10}$$

$$= \text{Tr}[\rho_{ss}M], \tag{5.11}$$

where the first term corresponds to the representation of the kinetic energy of a field theory. In the following calculations we will show how this term will provide us with an effective Hamiltonian that in some cases will reflect the structure of the Hamiltonian

$\hat{\mathcal{H}}_{\rm ca}$ used. Also note that M does not depend on the parameter Ω which is multiplying only operators acting on the atom. That is to say, even for a more complex atom with more energy levels, the new added terms that describe them, won't affect the value of M as long as those new terms don't interact with the cavity. Analysing the commutator,

$$[Q_{\rm ca}, R] = [-\frac{ig}{2s}(\hat{a}^\dagger\hat{\sigma} + \hat{a}\hat{\sigma}^\dagger) - \frac{1}{2}R^\dagger R, R], \tag{5.12}$$

where $[R, R^\dagger] = \frac{2\kappa}{s}[\hat{a}, \hat{a}^\dagger]$ we can see that the second term is reduced to,

$$\begin{aligned}[-\frac{1}{2}RR^\dagger, R] &= -\frac{1}{2}\left(\frac{2\kappa}{s}\right)^{3/2}[\hat{a}^\dagger, \hat{a}]\hat{a} &(5.13)\\ &= -\frac{1}{2}\left(\frac{2\kappa}{s}\right)^{3/2}\hat{a}. &(5.14)\end{aligned}$$

Note however that in the truncated space $[\hat{a}^\dagger, \hat{a}] = I_d$ where, I_d is a matrix of dimension d resulting from the commutation relation between the truncated annihilation and creation operators of the cavity. It contains ones in the main diagonal except for the last line that contains the matrix element $1 - d$ as follows:

$$I_d = \left[\hat{a}, \hat{a}^\dagger\right]_t = \begin{pmatrix} 1 & 0 & 0 & ... & 0 & 0 \\ 0 & 1 & 0 & ... & 0 & 0 \\ 0 & 0 & 1 & ... & 0 & 0 \\ \vdots & & & & & \vdots \\ 0 & 0 & 0 & ... & 0 & (1-d) \end{pmatrix}, \tag{5.15}$$

but $I_d\hat{a} = \hat{a}$, thus the Eq. (5.14) still stands. Meanwhile for the first term in Eq. (5.12),

$$-\frac{ig}{2s}[\hat{a}^\dagger\hat{\sigma} + \hat{a}\hat{\sigma}^\dagger, R] = -\frac{ig}{2s}\sqrt{\frac{2\kappa}{s}}\hat{\sigma}[\hat{a}^\dagger, \hat{a}]. \tag{5.16}$$

Thus Eq. (5.12) yields,

$$[Q_{\rm ca}, R] = -\frac{ig}{2s}\sqrt{\frac{2\kappa}{s}}\hat{\sigma}[\hat{a}^\dagger, \hat{a}] - \frac{1}{2}\left(\frac{2\kappa}{s}\right)^{3/2}\hat{a}, \tag{5.17}$$

giving for the kinetic energy in the cMPS representation,

$$\begin{aligned}[Q_{\rm ca},R]^\dagger[Q_{\rm ca},R] =& \frac{g^2\kappa}{2s^3}\hat{\sigma}^\dagger\hat{\sigma}[\hat{a}^\dagger,\hat{a}]^2 + \frac{2\kappa^3}{s^3}\hat{a}^\dagger\hat{a} \\ & -\frac{ig\kappa^2}{s^3}\hat{\sigma}^\dagger[\hat{a}^\dagger,\hat{a}]\hat{a} + \frac{ig\kappa^2}{s^3}\hat{a}^\dagger\hat{\sigma}[\hat{a}^\dagger,\hat{a}].\end{aligned} \tag{5.18}$$

Again, if we consider the truncated space, we realise the inclusion of I_d won't affect the last two terms of Eq. (5.18) thus

$$[Q_{\rm ca},R]^\dagger[Q_{\rm ca},R] = \frac{g^2\kappa}{2s^3}\hat{\sigma}^\dagger\hat{\sigma}I_d^2 + \frac{2\kappa^3}{s^3}\hat{a}^\dagger\hat{a} + \frac{ig\kappa^2}{s^3}(\hat{a}^\dagger\hat{\sigma} - \hat{\sigma}^\dagger\hat{a}), \tag{5.19}$$

and for the last term of Eq. (5.10)

$$R^{\dagger 2}R^2 = \frac{4\kappa}{s^2}\hat{a}^{\dagger 2}\hat{a}^2 = \frac{4\kappa^2}{s^2}N(N-1), \tag{5.20}$$

where the last equality is still valid even for the truncated case and $N = \hat{a}^\dagger\hat{a}$. Finally, making the correction $I_d \to I$ that accounts for the implicit error that the truncated operators produce in the commutation relations. The expression for the energy density in the cMPS representation parametrised with the Jaynes-Cummings Hamiltonian, takes the form:

$$e(c) = \mathrm{Tr}\left[\rho_{ss}\left(\frac{g^2\kappa}{2s^3}\hat{\sigma}^\dagger\hat{\sigma} + \frac{2\kappa^3}{s^3}N + \frac{ig\kappa^2}{s^3}(\hat{a}^\dagger\hat{\sigma} - \hat{\sigma}^\dagger\hat{a}) + c\frac{4\kappa^2}{s^2}N(N-1)\right)\right], \tag{5.21}$$

where as the first three terms correspond to the description of an effective Jaynes-Cummings Hamiltonian.

5.2 General case

From the Eq. (5.9) it is more evident that only terms that are coupled with the annihilation/creation operators of the cavity, will intervene in the operator M of Eq. (5.11) and ultimately, in the form of the effective resulting Hamiltonian. We now consider a Hamiltonian of the form

$$\hat{\mathcal{H}}_{\rm ca} = g'(\hat{a}^{\dagger n}B + \hat{a}^n B^\dagger), \tag{5.22}$$

for B an operator that acts only on the atomic space, i.e. $[B, \hat{a}] = 0$. We start our analysis with the commutator:

$$[Q, R] = [Q_{\mathrm{ca}}, R] = -\frac{i}{s}\sqrt{\frac{2\kappa}{s}}[\hat{\mathcal{H}}_{\mathrm{ca}}, \hat{a}] - \frac{1}{2}\left(\frac{2\kappa}{s}\right)^{3/2}\hat{a}, \tag{5.23}$$

and working out the terms in the commutator involving the Hamiltonian $\hat{\mathcal{H}}_{\mathrm{ca}}$ and assuming we are dealing with the truncated case, we have

$$[\hat{\mathcal{H}}_{\mathrm{ca}}, \hat{a}] = g'[\hat{a}^{\dagger n}B + \hat{a}^n B^\dagger, \hat{a}] = g'[\hat{a}^{\dagger n}, \hat{a}]B = -g'\left((n-1)I + I_d\right)\hat{a}^{\dagger n-1}B, \tag{5.24}$$

where we used the relation

$$[\hat{a}^{\dagger n}, \hat{a}] = -\left[(n-1)I + I_d\right]\hat{a}^{\dagger n-1}, \tag{5.25}$$

which can be proved using mathematical induction. This gives us:

$$[Q, R] = [Q_{\mathrm{ca}}, R] = -\frac{i}{s}\sqrt{\frac{2\kappa}{s}}\left(-g'\left[(n-1)I + I_d\right]\hat{a}^{\dagger n-1}B\right) - \frac{1}{2}\left(\frac{2\kappa}{s}\right)^{3/2}\hat{a}, \tag{5.26}$$

which results for the kinetic energy representation of the field theory in terms of the cMPS in:

$$\begin{aligned}[Q, R]^\dagger[Q, R] =& \frac{2\kappa}{s^3}g'^2 B^\dagger B\hat{a}^{n-1}\left[(n-1)I + I_d\right]^2\hat{a}^{\dagger n-1} + \frac{2\kappa^3}{s^3}N \\ &+ \frac{2\kappa^2}{s^3}ig'n\left(B^\dagger\hat{a}^n - B\hat{a}^{\dagger n}\right).\end{aligned} \tag{5.27}$$

Correcting the above relation by substituting I_d with the identity I of the cavity space, we have for the energy density:

$$\begin{aligned}e(c) =& \mathrm{Tr}\left[\rho_{ss}\left(\frac{2\kappa}{s^3}g'^2 n^2 B^\dagger B\hat{a}^{n-1}\hat{a}^{\dagger n-1} + \frac{2\kappa^3}{s^3}N + \frac{2\kappa^2}{s^3}ig'n\left(B^\dagger\hat{a}^n - B\hat{a}^{\dagger n}\right)\right)\right] \\ &+ c\mathrm{Tr}\left[\rho_{ss}\left(\frac{4\kappa^2}{s^2}N(N-1)\right)\right],\end{aligned} \tag{5.28}$$

and using the relation valid even for the truncated case

$$\hat{a}^n\hat{a}^{\dagger n} = (N+1)(N+2)\cdots(N+n), \tag{5.29}$$

we end up with

$$\begin{aligned} e(c) =&\mathrm{Tr}\left[\rho_{ss}\left(\frac{2\kappa}{s^3}g'^2n^2B^\dagger B(N+1)(N+2)\cdots(N+n-1)\right)\right] \\ &+\mathrm{Tr}\left[\rho_{ss}\left(\frac{2\kappa^3}{s^3}N+\frac{2\kappa^2}{s^3}ig'n\left(B^\dagger\hat{a}^n-B\hat{a}^{\dagger n}\right)+c\frac{4\kappa^2}{s^2}N(N-1)\right)\right]. \end{aligned} \tag{5.30}$$

We can see that the second line contains a term proportional to the number operator N describing the free cavity and a term proportional to the Hamiltonian $\hat{\mathcal{H}}_{\mathrm{ca}}$ initially introduced. In particular for $n=2$ we have the double photon absorption Hamiltonian $\hat{\mathcal{H}}_{\mathrm{ca}}=\hat{a}^{2\dagger}B+\hat{a}^2B$ which gives for the minimum value energy:

$$\begin{aligned} e(c) =&\mathrm{Tr}\left[\rho_{ss}\left(\frac{8\kappa}{s^3}g'^2B^\dagger B(N+1)+\frac{2\kappa^3}{s^3}N\right)\right] \\ &+\mathrm{Tr}\left[\rho_{ss}\left(\frac{4\kappa^2}{s^3}ig'\left(B^\dagger\hat{a}^2-B\hat{a}^{\dagger 2}\right)+c\frac{4\kappa^2}{s^2}N(N-1)\right)\right], \end{aligned} \tag{5.31}$$

where we obtain an term similar to the double photon absorption Hamiltonian $\hat{\mathcal{H}}_{\mathrm{ca}}$.

5.2.1 Other cases with no interaction with the atom

Other general cases can be worked out that involve only annihilation/creation operators like:

$$\hat{\mathcal{H}}_{\mathrm{ca}}=g'\hat{a}^{\dagger m}\hat{a}^m. \tag{5.32}$$

Thus substituting Eq. (5.32) in the commutator of relation Eq. (5.23) we have for the truncated case:

$$[\hat{\mathcal{H}}_{\mathrm{ca}},a]=-g'\left((m-1)I+I_d\right)\hat{a}^{\dagger m-1}\hat{a}^m. \tag{5.33}$$

In this situation, Eq. (5.23) takes the form

$$[Q,R]=i\frac{g'}{s}\sqrt{\frac{2\kappa}{s}}\left((m-1)I+I_d\right)\hat{a}^{\dagger m-1}\hat{a}^m-\frac{1}{2}\left(\frac{2\kappa}{s}\right)^{3/2}\hat{a}, \tag{5.34}$$

and the product of commutators simplifies to

$$[Q,R]^\dagger[Q,R]=\frac{2\kappa g'^2m^2}{s^3}\hat{a}^{\dagger m}\hat{a}^{m-1}\left((m-1)I+I_d\right)^2\hat{a}^{\dagger m-1}\hat{a}^m+\frac{2\kappa^3}{s^3}\hat{a}^\dagger\hat{a}, \tag{5.35}$$

finally we have:

$$e(c) = \mathrm{Tr}\left[\rho_{ss}\left(\frac{2\kappa g'^2 m^2}{s^3}\hat{a}^{\dagger m}\hat{a}^{m-1}\left((m-1)I + I_d\right)^2\hat{a}^{\dagger m-1}\hat{a}^m + \frac{2\kappa^3}{s^3}N + c\frac{4\kappa^2}{s^2}N(N-1)\right)\right], \tag{5.36}$$

with an error of the form:

$$E = \frac{2\kappa g'^2}{s^3}\mathrm{Tr}\left[\rho_{ss}\left(\hat{a}^{\dagger m}\hat{a}^{m-1}\left(2m(I-I_d) - (I-I_d)^2\right)\hat{a}^{\dagger m-1}\hat{a}^m\right)\right]. \tag{5.37}$$

Correcting the previous equation by substituting I_d with the identity I we have:

$$e(c) = \mathrm{Tr}\left[\rho_{ss}\left(\frac{2\kappa g'^2 m^2}{s^3}\left[N\left[(N-1)(N-2)\cdots(N-m+1)\right]^2\right] + \frac{2\kappa^3}{s^3}N + c\frac{4\kappa^2}{s^2}N(N-1)\right)\right], \tag{5.38}$$

valid for $m \geq 2$. For instance for the case $m = 1$ we have $\hat{\mathcal{H}}_{\mathrm{ca}} = g'\hat{a}^\dagger\hat{a} = g'N$ and

$$e(c) = \mathrm{Tr}\left[\rho_{ss}\left(\frac{2\kappa g'^2}{s^3}N + \frac{2\kappa^3}{s^3}N + c\frac{4\kappa^2}{s^2}N(N-1)\right)\right], \tag{5.39}$$

where the first term is again an effective Hamiltonian proportional to $\hat{\mathcal{H}}_{\mathrm{ca}}$. However for values of $m \geq 2$ there doesn't seem to be an obvious relation between $\hat{\mathcal{H}}_{\mathrm{ca}}$ and the resulting effective Hamiltonian. As a final example we look at the particular case:

$$\hat{\mathcal{H}}_{\mathrm{ca}} = g'\left(\hat{a}^\dagger\hat{a}\right)^m = g'N^m, \tag{5.40}$$

thus

$$[\hat{\mathcal{H}}_{\mathrm{ca}}, \hat{a}] = -g'\left[(N+1)^m - N^m\right]\hat{a}, \tag{5.41}$$

valid even for the truncated case. Which implies that

$$[Q, R] = \frac{ig'}{s}\sqrt{\frac{2\kappa}{s}}\left[(N+I)^m - N^m\right]\hat{a} - \frac{1}{2}\left(\frac{2\kappa}{s}\right)^{3/2}\hat{a}, \tag{5.42}$$

thus we obtain for the energy density

$$e(c) = \mathrm{Tr}\left[\rho_{ss}\left(\frac{2\kappa g'^2}{s^3}\left(N(N^m - (N-1)^m)^2 + \frac{2\kappa^3}{s^3}N + c\frac{4\kappa^2}{s^2}N(N-1)\right)\right)\right]. \tag{5.43}$$

With this last example we can conclude that Hamiltonians $\hat{\mathcal{H}}_{\text{ca}}$ of the form of Eq. (5.22) or Hamiltonians proportional to the operator N are more suited to give us effective Hamiltonians that have a similar structure to the initial Hamiltonians $\hat{\mathcal{H}}_{\text{ca}}$ used to parametrize the cMPS.

CONCLUSIONS

We constructed our own code in order to calculate the energy density and other correlation functions for a given model of a quantum field theory. This was achieved thanks to the formalism of the cMPS which in the spirit of the variational method, offered a parametrization of the state of the field. This allowed a minimization procedure to obtain the ground state energy of the field. The code was set in action by applying it to the Lieb-Liniger model.The results agreed with the work done by Cirac and Verstraete [1]. On the other hand we outlined the connections that lead us to believe that measurements from a field theory model has correspondent measurements in the context of cavity QED. Borrowing mathematical terms, this *isomorphism* between the two systems would help us to investigate properties of the fields by studying the behaviour of the cavities. Still work need to be done in that matter in order to establish this isomorphism more consistently, as this mapping is more like an injection as we are trying to represent the dynamics of infinite degrees of freedom by using finite dimensions. The next step will be using the relations deduced in chapter 5 and come up with a cavity model that actually reproduce the behaviour of the Lieb-Liniger model. Another directions to achieve that goal could be to constrict the entries of the matrices K and R in order to be able to relate them with a Hamiltonian and a lowering operator (or any other general dissipation operator) that have a meaning in the cavity QED context. Moreover, our analytical approach not only corrected an intrinsic error in the numerical simulation process previously done by the works of [3] due to the normal order of the annihilation operators but gives us a better understanding of why the simulator used in [3], works so well to reproduce the correlation properties of the Lieb-Liniger model. Moreover, with the analysis performed, we demonstrated that depending on what Hamiltonian we use as a simulator, the form of the effective Hamiltonian that would describe the Lieb-Liniger model will reflect the dynamical properties of that simulator. Furthermore, we derived

the transformation rules that will relate the Hamiltonian of the simulator used with the analytical forms that the effective Hamiltonian can have depending on the choice of the simulator used. We believe that this will ease in future works the selection of what simulator we need depending of the field theory that we want to simulate. A logic continuation of this work is on the line of mixed gases as we already established some relations that we can give more intuition to the physically implemented proposals. [36]

BIBLIOGRAPHY

[1] F. Verstraete and J. I. Cirac, Phys. Rev. Lett. **104**, 190405 (2010), URL https://link.aps.org/doi/10.1103/PhysRevLett.104.190405.

[2] T. J. Osborne, J. Eisert, and F. Verstraete, Phys. Rev. Lett. **105**, 260401 (2010).

[3] S. Barrett, K. Hammerer, S. Harrison, T. E. Northup, and T. J. Osborne, Phys. Rev. Lett. **110**, 1 (2013), ISSN 00319007, 1206.4988.

[4] E. H. Lieb and W. Liniger, Phys. Rev. **130**, 1605 (1963), URL http://link.aps.org/doi/10.1103/PhysRev.130.1605.

[5] M. Girardeau, Journal of Mathematical Physics **1**, 516 (1960).

[6] S. K. Harrison-schmidt, Ph.D. thesis, Royal Holloway University of London (2013), URL https://pure.royalholloway.ac.uk/portal/files/16992025/2013harrison{_}schmidtskphd.pdf.

[7] R. P. Feynman, Int. J. Theor. Phys. **21**, 467 (1982), ISSN 00207748, 9508027.

[8] B. C. Sanders, pp. 1–11 (2013), 1307.1498, URL http://arxiv.org/abs/1307.1498{%}0Ahttp://dx.doi.org/10.1007/978-3-642-38986-3{_}1.

[9] M. J. Hartmann, F. G. S. L. Brandão, and M. B. Plenio, Nat. Phys. **2**, 849 (2006), URL http://dx.doi.org/10.1038/nphys462http://10.0.4.14/nphys462.

[10] K. G. Wilson, Rev. Mod. Phys. **47**, 773 (1975), URL http://link.aps.org/doi/10.1103/RevModPhys.47.773.

[11] S. R. White, Phys. Rev. Lett. **69**, 2863 (1992), URL http://link.aps.org/doi/10.1103/PhysRevLett.69.2863.

[12] M. C. Bañuls, M. B. Hastings, F. Verstraete, and J. I. Cirac, Phys. Rev. Lett. **102**, 1 (2009), ISSN 00319007, 0904.1926, URL https://journals.aps.org/prl/pdf/10.1103/PhysRevLett.102.240603.

[13] C. Eichler, J. Mlynek, J. Butscher, P. Kurpiers, K. Hammerer, T. J. Osborne, and A. Wallraff, Phys. Rev. X **5**, 041044 (2015), ISSN 2160-3308, 1508.06471, URL http://arxiv.org/abs/1508.06471$\delimiter"026E30F$nhttp://link.aps.org/doi/10.1103/PhysRevX.5.041044.

[14] H. Bruus and K. Flensberg, *Introduction to Many-body quantum theory in condensed matter physics* (Oxford University Press, Copenhagen, 2002).

[15] P. A. Martin and F. Rothen, *Systems with Variable Particle Number* (Springer Berlin Heidelberg, Berlin, Heidelberg, 2004), pp. 89–125, ISBN 978-3-662-08490-8, URL https://doi.org/10.1007/978-3-662-08490-8_3.

[16] M. Fannes, B. Nachtergaele, and R. F. Werner, Communications in Mathematical Physics **144**, 443 (1992).

[17] F. Verstraete and J. I. Cirac, Phys. Rev. B **73**, 094423 (2006), URL http://link.aps.org/doi/10.1103/PhysRevB.73.094423.

[18] I. Maruyama and H. Katsura, Journal of the Physical Society of Japan **79**, 073002 (2010), 1003.5463.

[19] C. M. Caves and G. J. Milburn, Phys. Rev. A **36**, 5543 (1987), URL http://link.aps.org/doi/10.1103/PhysRevA.36.5543.

[20] C. Schön, E. Solano, F. Verstraete, J. I. Cirac, and M. M. Wolf, Phys. Rev. Lett. **95**, 110503 (2005), URL http://link.aps.org/doi/10.1103/PhysRevLett.95.110503.

[21] J. Haegeman, PhD Thesis - Gent pp. XX, 354 (2011).

[22] A. C. Doherty and H. Mabuchi, *Atoms in microcavities: Quantum electrodynamics, quantum statistical mechanics, and quantum information science* (California Institute of Technology, USA, 2003).

[23] C. W. Gardiner and M. J. Collett, Phys. Rev. A **31**, 3761 (1985).

[24] D. Walls and G. Milburn, *Quantum Optics* (Springer Verlag, 1994).

[25] D. A. Speck, *Quantum and Atom Optics* (2011), URL http://steck.us/teaching.

[26] R. Chiao and J. Garrison, *Quantum Optics* (Oxford University Press, Gret Britain, 2008).

[27] F. Franchini, *An introduction to integrable techniques for one-dimensional quantum systems* (Springer International Publishing, 2016), ISBN 978-3-319-48486-0, 1609.02100, URL http://arxiv.org/abs/1609.02100{%}0Ahttp://dx.doi.org/10.1007/978-3-319-48487-7.

[28] Y. Z. Jiang, Y. Y. Chen, and X. W. Guan, Chinese Phys. B **24** (2015), ISSN 16741056, 1502.03291.

[29] T. Kinoshita, T. Wenger, and D. S. Weiss, Phys. Rev. Lett. **95**, 190406 (2005), URL http://link.aps.org/doi/10.1103/PhysRevLett.95.190406.

[30] D. M. Gangardt and G. V. Shlyapnikov, Phys. Rev. Lett. **90**, 010401 (2003), URL http://link.aps.org/doi/10.1103/PhysRevLett.90.010401.

[31] H. J. Carmichael and D. F. Walls, J. Phys. B At. Mol. Phys. **9**, 1199 (1976), ISSN 00223700.

[32] R. Loudon, *The quantum theory of light*, Oxford science publications (Oxford University Press, Oxford ; New York, 2000), 3rd ed., ISBN 9780198501763.

[33] J. Rincn, M. Ganahl, and G. Vidal, Phys. Rev. B - Condens. Matter Mater. Phys. **92** (2015), ISSN 1550235X, 1508.04779.

[34] G. Haack, A. Steffens, J. Eisert, and R. Hübener, New J. Phys. **17**, 1 (2015), ISSN 13672630, 1504.04194.

[35] D. Jennings, C. Brockt, J. Haegeman, T. J. Osborne, and F. Verstraete, New J. Phys. **17** (2015), ISSN 13672630, 1212.3833.

[36] F. Quijandria, J. J. Garcia-Ripoll, and D. Zueco, Phys. Rev. B - Condens. Matter Mater. Phys. **90**, 1 (2014), ISSN 1550235X, 1409.4709v1.

[37] F. Glover, in *Artificial Evolution*, edited by J.-K. Hao, E. Lutton, E. Ronald, M. Schoenauer, and D. Snyers (Springer Berlin Heidelberg, Berlin, Heidelberg, 1998), pp. 1–51, ISBN 978-3-540-69698-8.

[38] G. E. Astrakharchik and S. Giorgini, Journal of Physics B: Atomic, Molecular and Optical Physics **39**, S1 (2006), URL http://stacks.iop.org/0953-4075/39/i=10/a=S01.

[39] G. E. Astrakharchik and S. Giorgini, Phys. Rev. A **68**, 031602 (2003), URL https://link.aps.org/doi/10.1103/PhysRevA.68.031602.

[40] F. D. Haldane, Physical Review Letters **47**, 1840 (1981), ISSN 00319007.

[41] M. A. Cazalilla, Journal of Physics B: Atomic, Molecular and Optical Physics **37**, S1 (2004), URL http://stacks.iop.org/0953-4075/37/i=7/a=051.

[42] M. Fox, *Quantum Optics. An Introduction* (Oxford University Press, 2006).

[43] H. Carmichael, *Statistical Methods in Quantum Optics 1: Master Equations and Fokker-Planck Equations* (Springer, 1999), ISBN 3540548823.

[44] S. K. Harrison-schmidt, Ph.D. thesis, Royal Holloway University of London (2013), URL https://pure.royalholloway.ac.uk/portal/files/16992025/2013harrison{_}schmidtskphd.pdf.

APPENDIX A

CMPS

A.1 Structure

Departing from the expression:

$$|\chi\rangle = \mathrm{Tr}_{\mathrm{aux}}\left[\mathcal{P}\exp\left(\int_0^L dx(Q(x)\otimes\mathbb{1} + R(x)\otimes\hat{\psi}^\dagger(x))\right)\right]|\Omega\rangle, \tag{A.1}$$

and labelling the expression inside the square brackets as:

$$\mathcal{O} = \mathcal{P}\exp\left(\int_0^L dx(Q(x)\otimes\mathbb{1} + R(x)\otimes\hat{\psi}^\dagger(x))\right), \tag{A.2}$$

and using the time (or path) ordered exponential definition

$$\begin{aligned}\mathcal{P}e^{\int_0^L A(x)dx} =& \mathbb{1} + \int_0^L dx A(x) + \iint\limits_{0<x_1<x_2<L} dx_1 dx_2 A(x_2)A(x_1) + \cdots \\ &+ \int\cdots\int\limits_{0<x_1<\cdots<x_n<L} dx_1\cdots dx_n A(x_n)\cdots A(x_1) + \cdots,\end{aligned} \tag{A.3}$$

in the next part, we will be suppressing the differentials for the sake of clarity, thus we can express (A.2) term by term as:

$$\begin{aligned}\mathcal{O} =& \mathbb{1} + \int_0^L \Big[Q(x)\otimes\mathbb{1} + R(x)\otimes\hat{\psi}^\dagger(x)\Big] \\ &+ \iint\limits_{0<x_1<x_2<L} \Big[Q(x_2)\otimes\mathbb{1} + R(x_2)\otimes\hat{\psi}^\dagger(x_2)\Big]\Big[Q(x_1)\otimes\mathbb{1} + R(x_1)\otimes\hat{\psi}^\dagger(x_1)\Big] + \cdots \\ &+ \iint\limits_{0<x_1<\cdots<x_n<L} \Big[Q(x_n)\otimes\mathbb{1} + R(x_n)\otimes\hat{\psi}^\dagger(x_n)\Big]\cdots\Big[Q(x_1)\otimes\mathbb{1} + R(x_1)\otimes\hat{\psi}^\dagger(x_1)\Big] + \cdots\end{aligned} \tag{A.4}$$

Now, regrouping terms with the same number of R operators in them, we can have:

$$\begin{aligned}\mathcal{O} =& \left\{ \mathbb{1} + \int\limits_{0<x<L} Q(x) + \int\limits\int\limits_{0<x_1<x_2<L} Q(x_2)Q(x_1) + \cdots + \int\limits\cdots\int\limits_{0<x_1<\cdots<x_n<L} Q(x_n)\cdots Q(x_1) + \cdots \right\} \\ &+ \left\{ \sum_{n=2}^{\infty} \int\limits\cdots\int\limits_{0<x_1<\cdots<x_n<L} \Big(R(x_n)Q(x_{n-1})\cdots Q(x_1)\otimes\psi^\dagger(x_n) + \cdots + Q(x_n)\cdots Q(x_2)R(x_1)\otimes\psi^\dagger(x_1)\Big) \right\} \\ &+ \left\{ \sum_{n=3}^{\infty} \int\limits\cdots\int\limits_{0<x_1<\cdots<x_n<L} \sum_{\substack{i,j\in\{1,2,\ldots,n\}\\ i<j}} (Q(x_n)\cdots R(x_j)\cdots R(x_i)\cdots Q(x_1))\otimes\psi^\dagger(x_j)\psi^\dagger(x_i) \right\} + \cdots ,\end{aligned} \tag{A.5}$$

which simplifies to give:

$$\begin{aligned}\mathrm{Tr}_{\mathrm{aux}}\mathcal{O} =& \mathrm{Tr}_{\mathrm{aux}}\left[\mathcal{P}e^{\int_0^L dxQ(x)}\right] + \mathrm{Tr}_{aux}\left[\int_0^L dx_1\mathcal{P}e^{\int_0^{x_1} dxQ(x)}R(x_1)\mathcal{P}e^{\int_{x_1}^L dxQ(x)}\right]\psi^\dagger(x_1) \\ &+\mathrm{Tr}_{\mathrm{aux}}\left[\int\limits_{0<x_1<x_2<L} dx_1dx_2\mathcal{P}e^{\int_0^{x_1} dxQ(x)}R(x_1)\mathcal{P}e^{\int_{x_1}^{x_2} dxQ(x)}R(x_2)\mathcal{P}e^{\int_{x_2}^L dxQ(x)}\right]\psi^\dagger(x_1)\psi^\dagger(x_2) + \cdots ,\end{aligned} \tag{A.6}$$

where the trace over the auxiliary system was taken. Then, by using the definitions $u_Q(y,x) = \mathcal{P}\exp[\int_x^y Q(x)dx]$ and the relation:

$$\phi_n = \mathrm{Tr}_{\mathrm{aux}}\left[u_Q(x_1,0)Ru_Q(x_2,x_1)R...Ru_Q(L,x_n)\right], \tag{A.7}$$

we finally have after reinserting $\mathrm{Tr}_{\mathrm{aux}}\mathcal{O}$ into (A.1):

$$\begin{aligned}|\chi\rangle =& \phi_0|\Omega\rangle + \int_0^L \phi_1\psi^\dagger(x_1)|\Omega\rangle + \int\limits_{0<x_1<x_2<L} \phi_2\psi^\dagger(x_1)\psi^\dagger(x_2)|\Omega\rangle \\ &+\cdots+ \int\limits_{0<x_1\cdots<x_n<L} \phi_n\psi^\dagger(x_1)\cdots\psi^\dagger(x_n)|\Omega\rangle + \cdots ,\end{aligned} \tag{A.8}$$

which is:

$$|\chi\rangle = \sum_{n=0}^{\infty}\int_{0<x_1<\ldots<x_n<L} dx_1...dx_n\phi_n\hat{\psi}^\dagger(x_1)...\hat{\psi}^\dagger(x_n)|\Omega\rangle.$$

A.2 $\langle\chi|\chi\rangle = \mathbf{Tr}(e^{TL})$

We will just give a brief outline to show this relation, further steps are calculated in a similar way. First, taking the inner product of the expression:

$$|\chi\rangle = \sum_{n=0}^{\infty}\int_{0<x_1<\ldots<x_n<L} dx_1...dx_n\phi_n\hat{\psi}^\dagger(x_1)...\hat{\psi}^\dagger(x_n)|\Omega\rangle. \tag{A.9}$$

and using the basis $A = \{|\Omega\rangle, |y_1\rangle, |y_1,y_2\rangle\cdots\}$ where $|y_i,\ldots y_k\rangle = |k\rangle$ represents the state of the bosonic system with k particles at the positions $y_i,\ldots,y_k$, yields:

$$\langle\chi|\chi\rangle = {\sum}'_{k\in A}\sum_{n,n'}\int\int_{\substack{0<x_1<\cdots<x_n<L\\ 0<x'_1<\cdots<x_{n'}<L}} dx_1\cdots dx_ndx'_1\cdots dx'_{n'}\phi_n\phi^*_{n'}\langle k|\psi^\dagger(x'_1)\cdots\psi^\dagger(x'_{n'})|\Omega\rangle\langle\Omega|\psi(x_1)\cdots\psi(x_n)|k\rangle, \tag{A.10}$$

here the $\sum'$ actually represents integrals over positions for each element of A. On the other hand, note that the inner products will be zero unless n=n' and n=k, (the number of particles annihilated by $\psi(x_1)\cdots\psi(x_n)$ be the same as the number of particles in the ket $|y_1\dots y_k\rangle$). For example for $|k\rangle = |\Omega\rangle$, we conclude that n=0=k then, we have the term:

$$\langle\Omega|\hat{\psi}(x_1)\cdots\hat{\psi}(x_n)|\Omega\rangle = \phi_0\phi_0^*. \tag{A.11}$$

Following the same reasoning and using, $|y_1\dots y_2\rangle = \hat{\psi}^\dagger(y_1)\dots\hat{\psi}^\dagger(y_n)|\Omega\rangle$ as well as the commutation relations $\left[\psi(x),\psi^\dagger(y)\right] = \delta(x-y)$, we have for n=1:

$$\begin{aligned}\int dy_1\langle y_1|\psi^\dagger(x_1')|\Omega\rangle\langle\Omega|\psi(x_1)|y_1\rangle &= \int dy_1\langle\Omega|\psi(y_1)\psi^\dagger(x_1')|\Omega\rangle\langle\Omega|\psi(x_1)\psi^\dagger(y_1)|\Omega\rangle \\ &= \int dy_1\phi_1(y_1)\phi_1^*(y_1),\end{aligned} \tag{A.12}$$

and for n=2

$$\begin{aligned}&\int\int dy_1dy_2\langle y_1,y_2|\psi^\dagger(x_1')\psi^\dagger(x_2')|\Omega\rangle\langle\Omega|\psi(x_2)\psi(x_1)|y_1,y_2\rangle = \\ &= \int\int dy_1dy_2\phi_2(y_1,y_2)\phi_2^*(y_1,y_2) + \int\int dy_1dy_2\phi_2(y_1,y_2)\phi_2^*(y_2,y_1) \\ &+ \int\int dy_1dy_2\phi_2(y_2,y_1)\phi_2^*(y_1,y_2) + \int\int dy_1dy_2\phi_2(y_2,y_1)\phi_2^*(y_2,y_1) \\ &= \int\int dy_1dy_2\left[\phi_2(y_1,y_2)+\phi_2(y_2,y_1)\right]\left[\phi_2^*(y_1,y_2)+\phi_2^*(y_2,y_1)\right].\end{aligned} \tag{A.13}$$

Note in the first equality of (A.13) that the arguments y_1 and y_2 are permuted in each function giving a total of $2!\times 2! = 4$ terms. So in general, for each n, we will have the sum of the integral of the different $\phi_n\phi_n^*$ where each ϕ_n is evaluated in one of the possible n permutations of the set $\{y_1,y_2,\dots,y_n\}$, given a total of $(n!)^2$ terms. This integrals have a natural resemblance as should be expected with the usual modulus squared of the probability amplitudes. Defining the following quantities: $A = Q\otimes\mathbb{1}+\mathbb{1}\otimes Q^*$ and $B = R\otimes R^*$ and using the definition (1.46), $\phi_0\phi_0^*$ can be expressed as:

$$\begin{aligned}\phi_0\phi_0^* &= \mathrm{Tr}_{\mathrm{aux}}\left[P\exp\left(\int_0^L Q(x)dx\right)\right]\mathrm{Tr}_{\mathrm{aux'}}\left[P\exp\left(\int_0^L Q^*(x')dx'\right)\right] \\ &= \mathrm{Tr}\left[e^{(Q\otimes\mathbb{1}+\mathbb{1}\otimes Q^*)L}\right] = \mathrm{Tr}\left[e^{AL}\right].\end{aligned} \tag{A.14}$$

In the last two expressions, Tr stands for the trace of both systems, aux and aux' while we wrote both operators acting on different spaces as a tensor product. Finally, by assuming translational invariance Q(x)=Q, R(x)=R, the path order exponential becomes the usual exponential for operators. In a similar way, for ϕ_1:

$$\begin{aligned}\int_0^L dy_1\phi_1(y_1)\phi_1^*(y_1) &= \int_0^L \mathrm{Tr}\left[\mathcal{P}e^{\int_0^{y_1}dxQ(x)\otimes\mathbb{1}+\mathbb{1}\otimes Q^*(x)}R(y_1)\otimes R^*(y_1)\mathcal{P}e^{\int_{y_1}^L dx'Q(x')\otimes\mathbb{1}+\mathbb{1}\otimes Q^*(x')}\right] \\ &= \int_0^L \mathrm{Tr}\left[\mathcal{P}\exp\left(\int_0^{y_1}dxA(x)\right))B(y_1)\mathcal{P}\exp\left(\int_{y_1}^L dx'A(x)\right)\right] \\ &= \int_0^L \mathrm{Tr}\left[e^{Ay_1}Be^{A(L-y_1)}\right] = \int_0^L \mathrm{Tr}\left[\sum_{n=1}^{\infty}\sum_{i=0}^{n-1}\frac{(Ay_1)^{n-1-i}B\left(A(L-y_1)\right)^i}{(n-1-i)!i!}\right].\end{aligned} \tag{A.15}$$

Where we assumed translational invariance in the last line. Now using the formula:

$$\int_0^L y^k (L-y)^n dy = \frac{n!k!}{(k+n+1)!} L^{n+k+1}, \tag{A.16}$$

we easily can find:

$$\int_0^L dy_1 \phi_1(y_1)\phi_1^*(y_1) = \mathrm{Tr}\left[\sum_{n=1}^{\infty}\sum_{i=0}^{n-1} \frac{A^{n-1-i}BA^i}{n!} L^n\right] = \mathrm{Tr}\left[\sum_{n=0}^{\infty}\sum_{i=0}^{n} \frac{A^{n-i}BA^i}{(n+1)!} L^{(n+1)}\right]. \tag{A.17}$$

Where the last equality was just a shift in the index n. On the other hand, analysing the expression $\mathrm{Tr}(e^{TL})$:

$$e^{TL} = \sum_{n=0}^{\infty} \frac{(Q\otimes \mathbb{1} + \mathbb{1}\otimes Q^* + R\otimes R^*)^n L^n}{n!}, \tag{A.18}$$

we end up, respecting the order of the operators, with the familiar Newton binomial expansion:

$$\begin{aligned} e^{TL} =& \sum_{n=0}^{\infty} \frac{L^n}{n!}\left[A^n + \left(A^{n-1}B + \cdots + BA^{n-1}\right) + \left(A^{n-2}B^2 + \cdots + B^2A^{n-2}\right) + \cdots\right] \\ =& \sum_{n=0}^{\infty} \frac{A^n}{n!} L^n + \sum_{n=0}^{\infty}\sum_{i=0}^{n} \frac{A^{n-i}BA^i}{(n+1)!} L^{n+1} + \sum_{n=0}^{\infty}\sum_{i=0}^{n}\sum_{j=0}^{i} \frac{A^{n-i}BA^jBA^{i-j}}{(n+2)!} L^{n+2} + \cdots, \end{aligned} \tag{A.19}$$

we readily realize that when taking the trace, the first two terms of (A.19), will correspond to (A.14) and (A.17). By a similar procedure with the remaining integrals of the basis, we can obtain in a general way the remaining terms of the trace of Tr $\left[e^{TL}\right]$.

APPENDIX B

JAYNES-CUMMINGS HAMILTONIAN FOR A THREE LEVEL ATOM

Consider a three-level atom in a lambda configuration trapped in a cavity of frequency ω_c as depicted in the Fig. (B.1). The ground state $|g_1\rangle$ is coupled to the excited state $|e\rangle$ by a laser of frequency ω_l and Rabi frequency Ω and the ground state $|g_2\rangle$ is coupled to $|e\rangle$ via the cavity with an interaction strength of g. Furthermore, a second laser of frequency ω_2 and Rabi frequency Ω_2 couples $|g_1\rangle$ and $|2\rangle$. If our reference system is placed such that the energy of the excited state $|e\rangle$ is zero, then the Hamiltonian in the Schrödinger picture is:

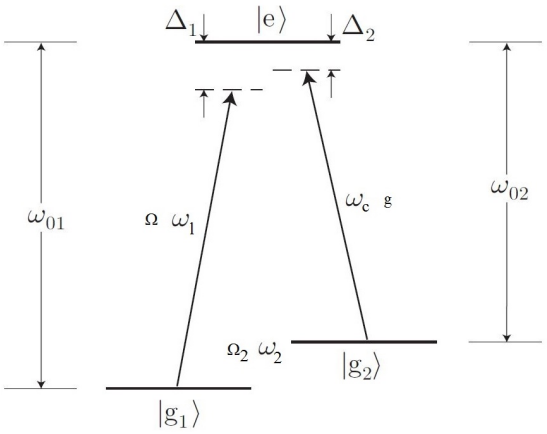


Figure B.1: Three level atom system with states $|g_1\rangle$ and $|e\rangle$ coupled by a laser of frequency ω_l, the states $|g_2\rangle$ and $|e\rangle$ by a cavity of frequency ω_c and the states $|g_1\rangle$ and $|g_2\rangle$ coupled by a laser of frequency ω_2 . The detunings are given by Δ_1 and Δ_2

$$\begin{aligned} H =&\omega_c\hat{a}^\dagger\hat{a} - \omega_{01}\hat{\sigma}_1\hat{\sigma}_1^\dagger - \omega_{02}\hat{\sigma}_2\hat{\sigma}_2^\dagger + \frac{g}{2}(\hat{\sigma}_2\hat{a}^\dagger + \hat{\sigma}_2^\dagger\hat{a}) \\ &+\frac{\Omega}{2}(\hat{\sigma}_1 e^{i\omega_1 t} + \hat{\sigma}_1^\dagger e^{-i\omega_1 t}) + \frac{\Omega_2}{2}(\hat{\sigma}_3 e^{i\omega_2 t} + \hat{\sigma}_3^\dagger e^{-i\omega_2 t}), \end{aligned} \tag{B.1}$$

where $\hat{\sigma}_1 = |g_1\rangle\langle e|$, $\hat{\sigma}_2 = |g_2\rangle\langle e|$ and $\hat{\sigma}_3 = |g_2\rangle\langle g_1|$. Using a suitable rotating frame where the Hamiltonian does not depends explicitly on time:

$$\begin{aligned} H =&(\omega_l - \omega_{01})\hat{\sigma}_1\hat{\sigma}_1^\dagger + (\omega_l - \omega_2 - \omega_{02})\hat{\sigma}_2\hat{\sigma}_2^\dagger + (\omega_c - \omega_l + \omega_2)\hat{a}^\dagger\hat{a} \\ &+\frac{g}{2}(\hat{a}^\dagger\hat{\sigma}_2 + \hat{\sigma}_2^\dagger\hat{a}) + \frac{\Omega}{2}(\hat{\sigma}_1^\dagger + \hat{\sigma}_1) + \frac{\Omega_2}{2}(\hat{\sigma}_3^\dagger + \hat{\sigma}_3). \end{aligned} \tag{B.2}$$

From the definitions of K and R given by (4.43) and (4.44) and using as the Hamiltonian the three level atom coupled to the driving cavity (B.2), we have:

$$K = \frac{1}{s}\left(\delta_1\hat{\sigma}_1\hat{\sigma}_1^\dagger + \delta_2\hat{\sigma}_2\hat{\sigma}_2^\dagger + \Delta\hat{a}^\dagger\hat{a} + \frac{g}{2}(\hat{a}^\dagger\hat{\sigma}_2 + \hat{\sigma}_2^\dagger\hat{a}) + \frac{\Omega}{2}(\hat{\sigma}_1^\dagger + \hat{\sigma}_1) + \frac{\Omega_2}{2}(\hat{\sigma}_3^\dagger + \hat{\sigma}_3)\right), \tag{B.3}$$

$$R = \sqrt{\frac{2\kappa}{s}}\hat{a}, \tag{B.4}$$

where $\delta 1 = (\omega_l - \omega_{01})$, $\delta 2 = (\omega_l - \omega_2 - \omega_{02})$ and $\Delta = (\omega_c - \omega_l + \omega_2)$. These expressions can be substituted in (3.3) and although the density matrix ρ_{ss} needs to be calculated numerically. We can still derive a few results analytically. For instance, if we separate the Hamiltonian K into the atomic part on one side and, the interaction and cavity part as:

$$K = \hat{\mathcal{H}}_{\text{atom}} + \hat{\mathcal{H}}_{\text{ca}}, \tag{B.5}$$

where

$$\hat{\mathcal{H}}_{\text{atom}} = \frac{1}{s}\left(\delta_1\hat{\sigma}_1\hat{\sigma}_1^\dagger + \delta_2\hat{\sigma}_2\hat{\sigma}_2^\dagger + \frac{\Omega}{2}(\hat{\sigma}_1^\dagger + \hat{\sigma}_1) + \frac{\Omega_2}{2}(\hat{\sigma}_3^\dagger + \hat{\sigma}_3)\right), \tag{B.6}$$

$$\hat{\mathcal{H}}_{\text{ca}} = \Delta\hat{a}^\dagger\hat{a} + \frac{g}{2}(\hat{a}^\dagger\hat{\sigma}_2 + \hat{\sigma}_2^\dagger\hat{a}), \tag{B.7}$$

we can rewrite the matrix Q as:

$$Q = -i\hat{\mathcal{H}}_{\text{atom}} - i\hat{\mathcal{H}}_{\text{ca}} - \frac{1}{2}R^\dagger R = -i\hat{\mathcal{H}}_{\text{atom}} + Q_{ca}. \tag{B.8}$$

If we recall that the operators describing the atom $\hat{\sigma}_i$ for $i = 1, 2, 3$ and the operator describing the cavity $R = \sqrt{\frac{2\kappa}{s}}\hat{a}$ commute, then the expectation value for the energy density (3.3) takes the form:

$$\begin{aligned} e(c) =& \text{Tr}[\rho_{ss}[Q_{ca}, R]^{-1}[Q_{ca}, R]^\dagger + c\rho_{ss}R^{\dagger 2}R^2] \\ =& \text{Tr}[\rho_{ss}M], \end{aligned} \tag{B.9}$$

where M does not depend on the description of the non interacting part of the atom. Now, assuming the annihilation operator $\hat{a}$ is a truncated matrix of dimension k, we obtain the following results. For instance for $k = 2$, the six dimensional matrices are:

$$[Q, R]^\dagger [Q, R] = \begin{pmatrix} \frac{g^2\kappa}{2s^3} & 0 & 0 & 0 & 0 & \frac{g\kappa(\Delta - i\kappa)}{s^3} \\ 0 & 0 & 0 & 0 & 0 & 0 \\ 0 & 0 & 0 & 0 & 0 & 0 \\ 0 & 0 & 0 & \frac{\kappa\left(g^2 + 4\left(\kappa^2 + \Delta^2\right)\right)}{2s^3} & 0 & 0 \\ 0 & 0 & 0 & 0 & \frac{2\kappa\left(\kappa^2 + \Delta^2\right)}{s^3} & 0 \\ \frac{g\kappa(\Delta + i\kappa)}{s^3} & 0 & 0 & 0 & 0 & \frac{2\kappa\left(\kappa^2 + \Delta^2\right)}{s^3} \end{pmatrix}, \tag{B.10}$$

$$c(R^\dagger)^2R^2 = \begin{pmatrix} 0 & 0 & 0 & 0 & 0 & 0 \\ 0 & 0 & 0 & 0 & 0 & 0 \\ 0 & 0 & 0 & 0 & 0 & 0 \\ 0 & 0 & 0 & 0 & 0 & 0 \\ 0 & 0 & 0 & 0 & 0 & 0 \\ 0 & 0 & 0 & 0 & 0 & 0 \end{pmatrix},$$

and assuming that the density matrix in the steady state has components of the form $\rho_{i,j}$ then the energy density has the form of:

$$e(c) = \frac{g^2\kappa}{2s^3}\rho_{1,1} + \left(\frac{g^2\kappa}{2s^3} + \frac{2\kappa\left(\Delta^2+\kappa^2\right)}{s^3}\right)\rho_{4,4} + \frac{2\kappa\left(\Delta^2+\kappa^2\right)}{s^3}\rho_{5,5} + \frac{2\kappa\left(\Delta^2+\kappa^2\right)}{s^3}\rho_{6,6} + \frac{g\kappa(\Delta+i\kappa)}{s^3}\rho_{1,6} + \frac{g\kappa(\Delta-i\kappa)}{s^3}\rho_{6,1}. \tag{B.11}$$

For $k=3$, $[Q,R]^\dagger[Q,R]$we have:

$$\begin{pmatrix}
\frac{g^2\kappa}{2s^3} & 0 & 0 & 0 & 0 & \frac{g\kappa(\Delta-i\kappa)}{s^3} & 0 & 0 & 0 \\
0 & 0 & 0 & 0 & 0 & 0 & 0 & 0 & 0 \\
0 & 0 & 0 & 0 & 0 & 0 & 0 & 0 & 0 \\
0 & 0 & 0 & \frac{\kappa\left(g^2+4\left(\Delta^2+\kappa^2\right)\right)}{2s^3} & 0 & 0 & 0 & 0 & \frac{\sqrt{2}g\kappa(\Delta-i\kappa)}{s^3} \\
0 & 0 & 0 & 0 & \frac{2\kappa\left(\Delta^2+\kappa^2\right)}{s^3} & 0 & 0 & 0 & 0 \\
\frac{g\kappa(\Delta+i\kappa)}{s^3} & 0 & 0 & 0 & 0 & \frac{2\kappa\left(\Delta^2+\kappa^2\right)}{s^3} & 0 & 0 & 0 \\
0 & 0 & 0 & 0 & 0 & 0 & \frac{2\kappa\left(g^2+2\left(\Delta^2+\kappa^2\right)\right)}{s^3} & 0 & 0 \\
0 & 0 & 0 & 0 & 0 & 0 & 0 & \frac{4\kappa\left(\Delta^2+\kappa^2\right)}{s^3} & 0 \\
0 & 0 & 0 & \frac{\sqrt{2}g\kappa(\Delta+i\kappa)}{s^3} & 0 & 0 & 0 & 0 & \frac{4\kappa\left(\Delta^2+\kappa^2\right)}{s^3}
\end{pmatrix}$$

and

$$c(R^\dagger)^2R^2 = \begin{pmatrix}
0 & 0 & 0 & 0 & 0 & 0 & 0 & 0 & 0 \\
0 & 0 & 0 & 0 & 0 & 0 & 0 & 0 & 0 \\
0 & 0 & 0 & 0 & 0 & 0 & 0 & 0 & 0 \\
0 & 0 & 0 & 0 & 0 & 0 & 0 & 0 & 0 \\
0 & 0 & 0 & 0 & 0 & 0 & 0 & 0 & 0 \\
0 & 0 & 0 & 0 & 0 & 0 & 0 & 0 & 0 \\
0 & 0 & 0 & 0 & 0 & 0 & \frac{8c\kappa^2}{s^2} & 0 & 0 \\
0 & 0 & 0 & 0 & 0 & 0 & 0 & \frac{8c\kappa^2}{s^2} & 0 \\
0 & 0 & 0 & 0 & 0 & 0 & 0 & 0 & \frac{8c\kappa^2}{s^2}
\end{pmatrix}, \tag{B.12}$$

thus in a similar way, the energy density $e(c)$ will take the form:

$$e(c) = +\frac{g^2\kappa}{2s^3}\rho_{1,1} + \left(\frac{g^2\kappa}{2s^3} + \frac{2\kappa\left(\Delta^2+\kappa^2\right)}{s^3}\right)\rho_{4,4} + \frac{2\kappa\left(\Delta^2+\kappa^2\right)}{s^3}\rho_{5,5} + \frac{2\kappa\left(\Delta^2+\kappa^2\right)}{s^3}\rho_{6,6} + \left(\frac{2\kappa g^2}{s^3} + \frac{4\kappa\left(\Delta^2+\kappa^2\right)}{s^3} + \frac{8c\kappa^2}{s^2}\right)\rho_{7,7} + \left(\frac{4\kappa\left(\Delta^2+\kappa^2\right)}{s^3} + \frac{8c\kappa^2}{s^2}\right)\rho_{8,8} + \left(\frac{4\kappa\left(\Delta^2+\kappa^2\right)}{s^3} + \frac{8c\kappa^2}{s^2}\right)\rho_{9,9} + \frac{g\kappa(\Delta+i\kappa)}{s^3}\rho_{1,6} + \frac{g\kappa(\Delta-i\kappa)}{s^3}\rho_{6,1} + \frac{\sqrt{2}g\kappa(\Delta+i\kappa)}{s^3}\rho_{4,9} + \frac{\sqrt{2}g\kappa(\Delta-i\kappa)}{s^3}\rho_{9,4}. \tag{B.13}$$

In its most general form, the matrix elements, of $K_{n,m}$ and $V_{n,m}$, where $K = [Q,R]^\dagger[Q,R]$ and $V = c(R^\dagger)^2R^2$ are:

$$\begin{aligned}
V_{3n,3n} &= V_{3n+1,3n+1} = V_{3n+2,3n+2} = \frac{4n(n-1)c\kappa^2}{s^2}, \\
K_{3n,3n} &= \frac{kg^2}{2s^3} + \frac{4nk(\Delta^2+\kappa^2)}{2s^3} + c\frac{4n(n-1)\kappa^2}{s^2}, \\
K_{3n+1,3n+1} &= K_{3n+2,3n+2} = \frac{4nk(\Delta^2+\kappa^2)}{2s^3} + c\frac{4n(n-1)\kappa^2}{s^2}.
\end{aligned} \tag{B.14}$$

While the off-diagonal elements are:

$$H_{1+3n,6+3n} = \frac{\kappa g}{s^3}(\Delta - i\kappa)\sqrt{n+1}, \tag{B.15}$$

$$H_{6+3n,1+3n} = \frac{\kappa g}{s^3}(\Delta + i\kappa)\sqrt{n+1}, \tag{B.16}$$

for $n = 0, 1, 2, ...$ and zero for other cases. Notice that the interaction part is zero for the values of $n = 0, 1$ and appears only after $n = 2$, which is natural since it reflects the fact that the minimum number of particles needed to have an interaction is 2. It is also telling that the interaction strength is proportional to the number of modes present. Thus it can be shown that

$$\begin{aligned} e(c) = \mathrm{Tr}[\rho_{ss}\mathcal{H}] =& \frac{\kappa g^2}{2s^3}\sum_{n=0}^{\infty}\rho_{3n,3n} + \frac{4\kappa(\Delta^2+\kappa^2)}{2s^3}\langle N\rangle + \frac{4\kappa^2}{s^2}c\langle N(N-1)\rangle \\ &+ \frac{\kappa g}{s^3}\sum_{n=0}^{\infty}\sqrt{n+1}\left\{(\Delta - i\kappa)\rho_{1+3n,6+3n} + (\Delta + i\kappa)\rho^{\dagger}_{1+3n,6+3n}\right\}, \end{aligned} \tag{B.17}$$

where the first term correspond to the probability of being in the excited state for each mode. Given the conditions of our problem, we are engineering it so that there is no population in the excited state thus the expectation value of this term will be negligible. Another way of expressing this result in terms of known operators is:

$$\begin{aligned} e(c) =& \mathrm{Tr}[\rho_{ss}(\frac{\kappa g^2}{2s^3}\mathbb{1}_c \otimes \hat{\sigma}_e + \frac{4\kappa}{2s^3}(\Delta^2+\kappa^2)N \otimes \mathbb{1}_a + \frac{4\kappa^2}{s^2}cN(N-1)\otimes\mathbb{1}_a \\ &+ \frac{\kappa g(\Delta - i\kappa)}{s^3}\hat{a}\hat{\sigma}_2^{\dagger} + \frac{\kappa g(\Delta + i\kappa)}{s^3}\hat{a}^{\dagger}\hat{\sigma}_2)], \end{aligned} \tag{B.18}$$

where $\mathbb{1}_c, \mathbb{1}_a$ are the identity operators in the cavity and the atom space respectively, $\hat{\sigma}_e$ is the operator describing the excited state of the atom and $\hat{\sigma}_2$ describes the annihilation operator of the second ground state $|gs2\rangle$ coupled to the cavity. This is telling us that when we calculate the expectation value of the energy density for the particular class of cMPS in the Lieb-Liniger density Hamiltonian, the resulting calculation makes equivalent the Lieb-Liniger expectation value Hamiltonian to an effective expectation value of a Jaynes Cummings Hamiltonian. In other words, we are selecting a cMPS in a subset of the Fock space, that obey the dynamics of a Jaynes Cummings Hamiltonian, and surprisingly they are close to the ground state of the Lieb-Liniger Hamiltonian. These relationship is not as simple as it looks since the expectation value of this effective Jaynes-Cummings Hamiltonian is over the steady state of the atom-cavity system, which in turn evolved from the Hamiltonian given in (B.2).

APPENDIX C

MIXTURE OF GASES

Following [36], the Hamiltonian corresponding to two Lieb-Liniger gases interacting through a density density coupling is described by:

$$\begin{aligned}\mathcal{H} =& \sum_{\alpha=1}^{2}\int_{-\infty}^{+\infty} dx \frac{d\hat{\psi_\alpha}^\dagger(x)}{dx}\frac{d\hat{\psi_\alpha}(x)}{dx} \\ &+c\sum_{\alpha=1}^{2}\int_{-\infty}^{+\infty} dx \hat{\psi_\alpha}^\dagger(x)\hat{\psi_\alpha}^\dagger(x)\hat{\psi_\alpha}(x)\hat{\psi_\alpha}(x) + G\int_{-\infty}^{+\infty} dx \hat{\rho_1}(x)\hat{\rho_2}(x),\end{aligned} \tag{C.1}$$

with c still the interaction strength of between the particles of the same species, G the coupling between the gases of different species and $\hat{\rho_\alpha}(x) = \hat{\psi_\alpha}^\dagger(x)\hat{\psi_\alpha}(x)$. Thus using the same kind of analytical analysis as in Eq. (5.10) we have that for a mixture of two gases, the corresponding energy density in terms of the cMPS looks like:

$$e(c) = \sum_{\alpha=1}^{2}\mathrm{Tr}\left(\rho_{ss}\left[\tilde{Q},\tilde{R}_\alpha\right]^\dagger\left[\tilde{Q},\tilde{R}_\alpha\right]\right) + c\sum_{\alpha=1}^{2}\mathrm{Tr}\left(\rho_{ss}(\tilde{R}_\alpha^\dagger)^2\tilde{R}_\alpha^2\right) + G\mathrm{Tr}\left(\rho_{ss}\tilde{R}_1^\dagger\tilde{R}_1\otimes\tilde{R}_2^\dagger\tilde{R}_2\right), \tag{C.2}$$

where the first two terms correspond to the Lieb-Liniger model in terms of the cMPS for each gas and the last term describes the coupling between the gases. In a similar way as to the one type of gas, the matrices $\tilde{Q}$, $\tilde{R}_2$ and $\tilde{R}_1$ describe the multicomponent mixture of gases which, are given by:

$$\tilde{Q} = -i\tilde{K} - \frac{1}{2}\tilde{R_1}^\dagger\tilde{R}_1 - \frac{1}{2}\tilde{R_2}^\dagger\tilde{R}_2, \tag{C.3}$$

$$\tilde{K} = K_1\otimes I + I\otimes K_2 + \sum_{n=0}^{N} Z_1^{(n)}\otimes Z_2^{(n)}, \tag{C.4}$$

$$\tilde{R}_1 = R_1\otimes I, \tag{C.5}$$

$$\tilde{R}_2 = I\otimes R_2. \tag{C.6}$$

The operators $Z_1^{(n)}$ and $Z_1^{(n)}$ describe the coupling between the gases. Also note that $[\tilde{R}_1,\tilde{R}_2]=0$ as they act on different spaces. For the case proposed in [36] describing two superconducting cavities interacting each one with a superconducting qubit we have the Hamiltonian of the system as

$$\hat{\mathcal{H}}_{\mathrm{sys}} = g\hat{a}_1^\dagger\hat{\sigma}_1 + \Omega\hat{\sigma}_1^\dagger + g\hat{a}_2^\dagger\hat{\sigma}_2 + \Omega\hat{\sigma}_2^\dagger + J\hat{a}_1^\dagger\otimes\hat{a}_2 + \lambda\hat{\sigma}_1^\dagger\otimes\hat{\sigma}_2 + h.c. \tag{C.7}$$

$$= \hat{\mathcal{H}}_{\mathrm{cav}} + \hat{\mathcal{H}}_{\mathrm{atom}}, \tag{C.8}$$

where we have divided the Hamiltonian in the terms describing only the atoms and terms describing atom cavity interactions as:

$$\hat{\mathcal{H}}_{\text{cav}} = g\hat{a}_1^\dagger\hat{\sigma}_1 + g\hat{a}_2^\dagger\hat{\sigma}_2 + J\hat{a}_1^\dagger \otimes \hat{a}_2 + h.c., \tag{C.9}$$

$$\hat{\mathcal{H}}_{\text{atom}} = \Omega\hat{\sigma}_1^\dagger + \Omega\hat{\sigma}_2^\dagger + \lambda\hat{\sigma}_1^\dagger \otimes \hat{\sigma}_2 + h.c., \tag{C.10}$$

and g is the coupling strength between a cavity and a qubit, J and λ are the coupling strengths for cavities and qubits and Ω is the amplitude of the driving laser. In the following we will show that the variables involved in $\hat{\mathcal{H}}_{\text{atom}}$ won't take part in the final expression of the effective Hamiltonian and only the variables involved in $\hat{\mathcal{H}}_{\text{cav}}$ will be present. On the other hand, Eq. (C.7) give us the following identifications:

$$\tilde{K} = K_1 \otimes I + I \otimes K_2 + \frac{J}{s}\hat{a}_1^\dagger \otimes \hat{a}_2 + \frac{J}{s}\hat{a}_1 \otimes \hat{a}_2^\dagger + \frac{\lambda}{s}\hat{\sigma}_1^\dagger \otimes \hat{\sigma}_2 + \frac{\lambda}{s}\hat{\sigma}_1 \otimes \hat{\sigma}_2^\dagger, \tag{C.11}$$

$$K_1 = \frac{g}{s}(\hat{a}_1^\dagger\hat{\sigma}_1 + \hat{a}_1\hat{\sigma}_1^\dagger) + \frac{\Omega}{s}(\hat{\sigma}_1^\dagger + \hat{\sigma}_1), \tag{C.12}$$

$$K_2 = \frac{g}{s}(\hat{a}_2^\dagger\hat{\sigma}_2 + \hat{a}_2\hat{\sigma}_2^\dagger) + \frac{\Omega}{s}(\hat{\sigma}_2^\dagger + \hat{\sigma}_2), \tag{C.13}$$

$$R_i = \sqrt{\frac{\kappa}{s}}\hat{a}_i. \tag{C.14}$$

Thus for the commutator $[\tilde{Q}, \tilde{R}_1]$ we have:

$$[\tilde{Q}, \tilde{R}_1] = [-i\tilde{K_1}, \tilde{R}_1] - \frac{1}{2}[\tilde{R_1}^\dagger, \tilde{R}_1]\tilde{R}_1 \tag{C.15}$$

$$= \left(-i[K_1, R_1] - \frac{1}{2}[R_1^\dagger, R_1]R_1\right) \otimes I + \left[\frac{J}{s}\hat{a}_1^\dagger \otimes \hat{a}_2 + \frac{J}{s}\hat{a}_1 \otimes \hat{a}_2^\dagger + \frac{\lambda}{s}\hat{\sigma}_1^\dagger \otimes \hat{\sigma}_2 + \frac{\lambda}{s}\hat{\sigma}_1 \otimes \hat{\sigma}_2^\dagger, R_1\right]. \tag{C.16}$$

The first term in Eq. (C.16) is the same as in the uncoupled case for the 1-dimensional Lieb-Liniger in terms of the cMPS, thus it will give us the same analytical expression as in that case, but if we analyse the second commutator and recalling that $[\hat{\sigma}_1, R_1] = 0$ we will get:

$$\left[\frac{J}{s}\hat{a}_1^\dagger \otimes \hat{a}_2 + \frac{J}{s}\hat{a}_1 \otimes \hat{a}_2^\dagger + \frac{\lambda}{s}\hat{\sigma}_1^\dagger \otimes \hat{\sigma}_2 + \frac{\lambda}{s}\hat{\sigma}_1 \otimes \hat{\sigma}_2^\dagger, R_1 \otimes I\right] = \frac{J}{s}\sqrt{\frac{\kappa}{s}}[\hat{a}_1^\dagger, \hat{a}_1] \otimes \hat{a}_2. \tag{C.17}$$

Thus Eq. (C.16) simplifies to:

$$[\tilde{Q}, \tilde{R_1}] = \left(-i\sqrt{\frac{\kappa}{s}}\frac{g}{s}[\hat{a}_1^\dagger, \hat{a}_1]\hat{\sigma}_1 - \frac{1}{2}\left(\frac{\kappa}{s}\right)^{3/2}[\hat{a}_1^\dagger, \hat{a}_1]\hat{a}_1\right) \otimes I + \frac{J}{s}\sqrt{\frac{\kappa}{s}}[\hat{a}_1^\dagger, \hat{a}_1] \otimes \hat{a}_2. \tag{C.18}$$

Calculating the product of commutators which are the responsible of producing an effective Hamiltonian similar to $\hat{\mathcal{H}}_{\text{cav}}$ we have:

$$[\tilde{Q}, \tilde{R_1}]^\dagger[\tilde{Q}, \tilde{R_1}] = \left(\frac{\kappa g^2}{s^3}\hat{\sigma}_1^\dagger\hat{\sigma}_1 I_d^2 + \frac{\kappa^3}{4s^3}\hat{a}_1^\dagger\hat{a}_1 + \frac{ig\kappa^2}{2s^3}(\hat{a}_1^\dagger\hat{\sigma}_1 - \hat{a}_1\hat{\sigma}_1^\dagger)\right) \otimes I - \frac{J\kappa^2}{2s^3}\left(\hat{a}_1^\dagger \otimes \hat{a}_2 + \hat{a}_1 \otimes \hat{a}_2^\dagger\right) + \left(\frac{\kappa J^2}{s^3}I \otimes \hat{a}_2^\dagger\hat{a}_2 + \frac{i\kappa Jg}{s^3}(\hat{\sigma}_1^\dagger \otimes \hat{a}_2 - \hat{\sigma}_1 \otimes \hat{a}_2^\dagger)\right)(I_d^2 \otimes I). \tag{C.19}$$

In a similar way for the second gas:

$$[\tilde{Q},\tilde{R}_2]^\dagger[\tilde{Q},\tilde{R}_2] = I\otimes\left(\frac{\kappa g^2}{s^3}\hat{\sigma}_2^\dagger\hat{\sigma}_2 I_d^2+\frac{\kappa^3}{4s^3}\hat{a}_2^\dagger\hat{a}_2+\frac{ig\kappa^2}{2s^3}(\hat{a}_2^\dagger\hat{\sigma}_2-\hat{a}_2\hat{\sigma}_2^\dagger)\right)-\frac{J\kappa^2}{2s^3}\left(\hat{a}_1^\dagger\otimes\hat{a}_2+\hat{a}_1\otimes\hat{a}_2^\dagger\right)$$
$$+\left(\frac{\kappa J^2}{s^3}\hat{a}_1^\dagger\hat{a}_1\otimes I+\frac{i\kappa Jg}{s^3}(\hat{a}_1\otimes\hat{\sigma}_2^\dagger-\hat{a}_1^\dagger\otimes\hat{\sigma}_2)\right)(I\otimes I_d^2). \tag{C.20}$$

Note how this two expressions produce an effective Hamiltonian that describes a cavity interacting non only with a qubit but with a neighbouring second cavity as in Eq. (C.9) but also we have a term proportional to $\frac{i\kappa Jg}{s^3}$ that describes the interaction of one cavity over the atom contained in the second cavity. Finally, Eq. C.2 takes the form:

$$\begin{aligned}e(c) =& e_1(c)+e_2(c)+\mathrm{Tr}\left[\rho_{ss}\left(-\frac{J\kappa^2}{s^3}\left(\hat{a}_1^\dagger\otimes\hat{a}_2+\hat{a}_1\otimes\hat{a}_2^\dagger\right)+\frac{g\kappa}{s}\left(\hat{a}_1^\dagger\hat{a}_1\otimes\hat{a}_2^\dagger\hat{a}_2\right)\right)\right]\\ &+\mathrm{Tr}\left[\rho_{ss}\left(\left(\frac{\kappa J^2}{s^3}I\otimes\hat{a}_2^\dagger\hat{a}_2+\frac{i\kappa Jg}{s^3}(\hat{\sigma}_1^\dagger\otimes\hat{a}_2-\hat{\sigma}_1\otimes\hat{a}_2^\dagger)\right)(I_d^2\otimes I)\right)\right]\\ &+\mathrm{Tr}\left[\rho_{ss}\left(\left(\frac{\kappa J^2}{s^3}\hat{a}_1^\dagger\hat{a}_1\otimes I+\frac{i\kappa Jg}{s^3}(\hat{a}_1\otimes\hat{\sigma}_2^\dagger-\hat{a}_1^\dagger\otimes\hat{\sigma}_2)\right)(I\otimes I_d^2)\right)\right],\end{aligned} \tag{C.21}$$

where $e_i(c)$ corresponds to the expression of the energy density for the non interacting gases case expressed as:

$$e_i(c)=\mathrm{Tr}\left[\rho_{ss}\left(\frac{\kappa g^2}{s^3}\hat{\sigma}_i^\dagger\hat{\sigma}_i I_d^2+\frac{\kappa^3}{4s^3}\hat{a}_i^\dagger\hat{a}_i+\frac{ig\kappa^2}{2s^3}(\hat{a}_i^\dagger\hat{\sigma}_i-\hat{a}_i\hat{\sigma}_i^\dagger)+\frac{c\kappa^2}{s^2}\hat{a}_i^{\dagger 2}\hat{a}_i^2\right)\right], \tag{C.22}$$

but ρ_{ss} now describes the density matrix in the steady state results from the interaction between the coupled gases. Correcting the error coming from the truncated space of the annihilation operators, (i.e. $I_d\to I$) we end up with the final form of the energy density for a mixture of gases as:

$$\begin{aligned}e(c) =& e_1(c)+e_2(c)+\mathrm{Tr}\left[\rho_{ss}\left(-\frac{J\kappa^2}{s^3}\left(\hat{a}_1^\dagger\otimes\hat{a}_2+\hat{a}_1\otimes\hat{a}_2^\dagger\right)+\frac{g\kappa}{s}\left(\hat{a}_1^\dagger\hat{a}_1\otimes\hat{a}_2^\dagger\hat{a}_2\right)\right)\right]\\ &+\mathrm{Tr}\left[\rho_{ss}\left(\left(\frac{\kappa J^2}{s^3}I\otimes\hat{a}_2^\dagger\hat{a}_2+\frac{i\kappa Jg}{s^3}(\hat{\sigma}_1^\dagger\otimes\hat{a}_2-\hat{\sigma}_1\otimes\hat{a}_2^\dagger)\right)\right)\right]\\ &+\mathrm{Tr}\left[\rho_{ss}\left(\left(\frac{\kappa J^2}{s^3}\hat{a}_1^\dagger\hat{a}_1\otimes I+\frac{i\kappa Jg}{s^3}(\hat{a}_1\otimes\hat{\sigma}_2^\dagger-\hat{a}_1^\dagger\otimes\hat{\sigma}_2)\right)\right)\right],\end{aligned} \tag{C.23}$$

this is the expression for the expectation value of an effective Hamiltonian that has terms that describe two cavities interacting with one qubit and between themselves as in Eq. (C.9) but as mentioned before it also contains cross terms describing interactions between a cavity and the atom contained in the second cavity. Note once again that the terms describing only the atomic part related to the variables λ and Ω are not present in this effective Hamiltonian in the same way as the simple case of just one gas studied above.

APPENDIX D

LOOKING FOR EXTRA VARIABLES IN THE CAVITY QED HAMILTONIAN

D.1 Reestructuring cmps

The basic question we tried to answer with this idea was, what parameters we need to add and where do we need to add them in the cavity QED Hamiltonian that describes the Lieb-Liniger model? In other words, f we compare the number of variables in the simulation of the model using a cavity QED Hamiltonian (3 variables) against the (128 variables) for the cMPS with $D = 8$, what would be amount of extra variables we need to add? There are two approaches.

- Add tunable variables times interaction terms, in the form of creation annihilation operators and Pauli matrices representing the 2 level atom, to the cavity QED Hamiltonian.
- Constrain/reduce the mathematical cMPS, that is to say, reduce the $2D^2$ variables needed to reproduce the Lieb-Liniger model.

What we did was to reduce the mathematical cMPS variables ($2D^2$) and provide the matrices K and R with the structure of a cavity and a 2 level atom. I.e. $K = K^\dagger$ and $R = \gamma\hat{a} \otimes \mathbb{1}$. With $\hat{a}$ the truncated annihilation operator and $\mathbb{1}$ the 2 level atom identity operator. With those constrains, we managed to reduce the amount of variables needed, and we showed in Fig. (D.1a) that still with D^2+1 you can still reproduce the correlation functions from Cirac [1]. Hinting that if we want a better description using a 2 level atom. One must include terms in the off diagonal matrix of the effective Jaynes-Cummings Hamiltonian that describes the ground state energy of the Lieb-Liniger Hamiltonian. The reason for that conclusion is that in the simulation of the mathematical cMPS, the off-diagonal elements of K where populated thus helping to populate the offdiagonal elements of $[Q, R]^\dagger [Q, R]$, while for a simulation using a cavity like in appendix B we can see that mostly the diagonal is the one affected by the parameters. For instance in

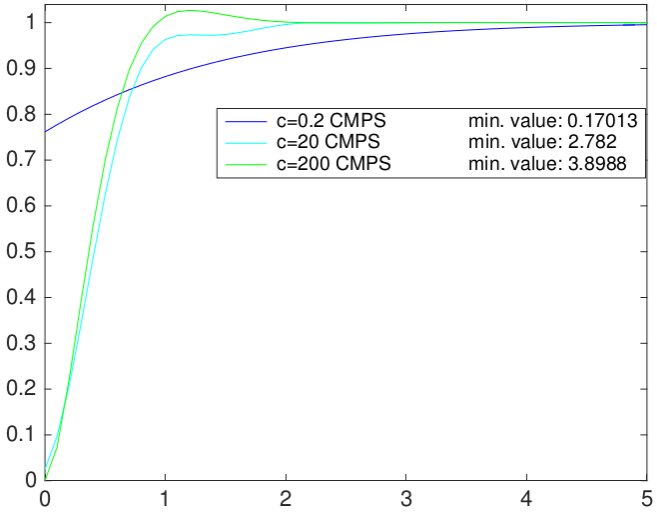
the case $k = 3$, $[Q, R]^\dagger [Q, R]$we have:

$$\begin{pmatrix} \frac{g^2\kappa}{2s^3} & 0 & 0 & 0 & 0 & \frac{g\kappa(\Delta-i\kappa)}{s^3} & 0 & 0 & 0 \\ 0 & 0 & 0 & 0 & 0 & 0 & 0 & 0 & 0 \\ 0 & 0 & 0 & 0 & 0 & 0 & 0 & 0 & 0 \\ 0 & 0 & 0 & \frac{\kappa\left(g^2+4\left(\Delta^2+\kappa^2\right)\right)}{2s^3} & 0 & 0 & 0 & 0 & \frac{\sqrt{2}g\kappa(\Delta-i\kappa)}{s^3} \\ 0 & 0 & 0 & 0 & \frac{2\kappa\left(\Delta^2+\kappa^2\right)}{s^3} & 0 & 0 & 0 & 0 \\ \frac{g\kappa(\Delta+i\kappa)}{s^3} & 0 & 0 & 0 & 0 & \frac{2\kappa\left(\Delta^2+\kappa^2\right)}{s^3} & 0 & 0 & 0 \\ 0 & 0 & 0 & 0 & 0 & 0 & \frac{2\kappa\left(g^2+2\left(\Delta^2+\kappa^2\right)\right)}{s^3} & 0 & 0 \\ 0 & 0 & 0 & 0 & 0 & 0 & 0 & \frac{4\kappa\left(\Delta^2+\kappa^2\right)}{s^3} & 0 \\ 0 & 0 & 0 & \frac{\sqrt{2}g\kappa(\Delta+i\kappa)}{s^3} & 0 & 0 & 0 & 0 & \frac{4\kappa\left(\Delta^2+\kappa^2\right)}{s^3} \end{pmatrix} \tag{D.1}$$

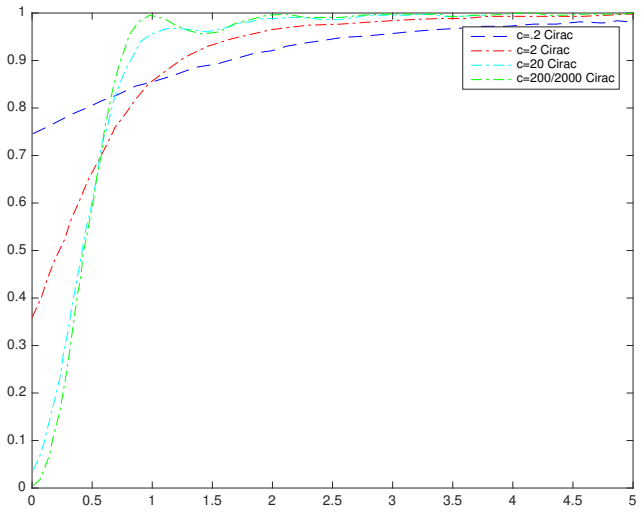
and

$$c(R^\dagger)^2R^2 = \begin{pmatrix} 0 & 0 & 0 & 0 & 0 & 0 & 0 & 0 & 0 \\ 0 & 0 & 0 & 0 & 0 & 0 & 0 & 0 & 0 \\ 0 & 0 & 0 & 0 & 0 & 0 & 0 & 0 & 0 \\ 0 & 0 & 0 & 0 & 0 & 0 & 0 & 0 & 0 \\ 0 & 0 & 0 & 0 & 0 & 0 & 0 & 0 & 0 \\ 0 & 0 & 0 & 0 & 0 & 0 & 0 & 0 & 0 \\ 0 & 0 & 0 & 0 & 0 & 0 & \frac{8c\kappa^2}{s^2} & 0 & 0 \\ 0 & 0 & 0 & 0 & 0 & 0 & 0 & \frac{8c\kappa^2}{s^2} & 0 \\ 0 & 0 & 0 & 0 & 0 & 0 & 0 & 0 & \frac{8c\kappa^2}{s^2} \end{pmatrix}. \tag{D.2}$$

It is interesting to note that we are not able to reproduce quite well the oscillations for $c = 20$ and $c = 200$ which probably means that the constraint imposed on the matrix R may be erasing the information on the Friedel-like oscillations for the bosonic gas.



(a)



(b)

Figure D.1: Density-density correlation functions (a) cMPS with the structure of the two level atom and cavity system defining R as the tensor product of a truncated annihilation operator $\hat{a}$ of dimension 4 and the identity of a 2 level atom. $K = K^{\dagger}$ and $R = \gamma\hat{a} \otimes \mathbb{1}$. Number of total variables is $D^2 + 1 = 65$ (b) Results predicted by Cirac from [1].

APPENDIX E

COMPUTATION OF DENSITY MATRIX AND PROBABILITY AMPLITUDES

Assuming $\hbar = 1$, consider a two level atom with energy separation ω_0, which is placed inside a semitransparent cavity of natural frequency ω_c that allows photons to leak at a rate κ. The atom is addressed by a continuous laser at frequency ω_l and Rabi frequency Ω. For this system, the density matrix obeys the following equation in the Linblad form:

$$\dot{\rho}(t) = -i\left[\mathcal{H}, \rho\right] + F\left[\rho\right], \tag{E.1}$$

where $F\left[\rho\right]$ is given by

$$F\left[\rho\right] = 2\kappa\rho\hat{a}^\dagger - \kappa\hat{a}^\dagger\hat{a}\rho - \kappa\rho\hat{a}^\dagger\hat{a}. \tag{E.2}$$

The Hamiltonian in the Schrödinger picture describes the typical Jaynes-Cummings interaction model between the cavity and the atom, which is also interacting with the laser in a classical fashion as follows:

$$H = \omega_0\hat{\sigma}^\dagger\hat{\sigma} + \omega_c\hat{a}^\dagger\hat{a} + \frac{g}{2}(\hat{a}^\dagger\hat{\sigma} + \hat{a}\hat{\sigma}^\dagger) + \frac{\Omega}{2}(\hat{\sigma}^\dagger e^{-i\omega_l t} + \hat{\sigma}e^{i\omega_l t}). \tag{E.3}$$

In order to make the numerical calculations of the density matrix is better to solve this particular Hamiltonian numerically. In the steady state is better to work in a frame where the Hamiltonian does not depend explicitly on time. Thus, through out the notes we will be transforming to more suitable rotating frames. It is easy to proof that under a unitary transformation $U(t)$ behaves as:

$$\tilde{\rho}(t) = U\rho(t)U^\dagger, \tag{E.4}$$

thus

$$\dot{\tilde{\rho}}(t) = -i\left[\tilde{\mathcal{H}}, \rho\right] + \tilde{F}\left[\tilde{\rho}\right] = \tilde{\mathcal{L}}\tilde{\rho}, \tag{E.5}$$

where the Hamiltonian and Lindblad operator take the form: $\tilde{\mathcal{H}} = i\dot{U}U^\dagger + UHU^\dagger$ and $\tilde{F} = UFU^\dagger$. If we use the rotating frame on the previous Hamiltonian to eliminate explicit time dependencies:

$$U = \exp(i\omega_l\hat{\sigma}^\dagger\hat{\sigma}t)\exp(i\omega_l\hat{a}^\dagger\hat{a}t), \tag{E.6}$$

the Hamiltonian is reduced to:

$$H = (\omega_0 - \omega_l)\hat{\sigma}^\dagger\hat{\sigma} + (\omega_c - \omega_l)\hat{a}^\dagger\hat{a} + \frac{g}{2}(\hat{a}^\dagger\hat{\sigma} + \hat{a}\hat{\sigma}^\dagger) + \frac{\Omega}{2}(\hat{\sigma}^\dagger + \hat{\sigma}). \tag{E.7}$$

In this particular frame the time evolution is given by

$$\rho(t) = e^{\tilde{\mathcal{L}}t}\rho_0. \tag{E.8}$$

Thus calculating the total probabilities for the ground and excited state over all the available modes:

$$P_{\mathrm{g}}(t) = \sum_n \left(\langle n| \otimes \langle g|\right) \rho(t) \left(|n\rangle \otimes |g\rangle\right) = \sum_n P_{\mathrm{ne}}, \tag{E.9}$$

$$P_{\mathrm{e}}(t) = \sum_n \left(\langle n| \otimes \langle g|\right) \rho(t) \left(|n\rangle \otimes |g\rangle\right) = \sum_n P_{\mathrm{ng}}, \tag{E.10}$$

where $|n\rangle$ are the state representing the cavity modes, $|e\rangle$ and $|g\rangle$ the excited and ground state of the atom and P_{ne}, P_{ng} are the probabilities for the excited and ground state for a specific mode n.

APPENDIX F

PERMISSION DOCUMENTS

American Physical Society
Reuse and Permissions License

01-May-2018

This license agreement between the American Physical Society ("APS") and Aizar Enciso Dominguez ("You") consists of your license details and the terms and conditions provided by the American Physical Society and SciPris.

Licensed Content Information

License Number:	**RNP/18/MAY/003896**
License date:	01-May-2018
DOI:	10.1103/PhysRevLett.104.190405
Title:	Continuous Matrix Product States for Quantum Fields
Author:	F. Verstraete and J. I. Cirac
Publication:	Physical Review Letters
Publisher:	American Physical Society
Cost:	USD $ 0.00

Request Details

Does your reuse require significant modifications: Yes

Modification Details:

For figure 1 I wish to extract the data points for the energy versus the parameter c to compare it with my own results and show the agreement of the same for the values of D=2,4,6. For the figure 2b) I wish to extract the data points of the second correlation function for the values of c=0.2,2,20 and 2000

Specify intended distribution locations:	Worldwide
Reuse Category:	Reuse in a thesis/dissertation
Requestor Type:	Student
Items for Reuse:	Figures/Tables
Number of Figure/Tables:	2
Figure/Tables Details:	Fig. 1: Energy density as a function of the interaction parameter c for different values of D=2,4,6,8. and Fig2b) Two body density-density correlation functions for the same values of c.
Format for Reuse:	Electronic

Information about New Publication:

University/Publisher:	Imperial College London/ Spiral submissions
Title of dissertation/thesis:	Continuous matrix product states and Cavity QED
Author(s):	Aizar Enciso Dominguez
Expected completion date:	Apr. 2018

License Requestor Information

Name:	Aizar Enciso Dominguez
Affiliation:	Individual
Email Id:	ae1010@imperial.ac.uk

Country: United Kingdom



American Physical Society
Reuse and Permissions License

TERMS AND CONDITIONS

The American Physical Society (APS) is pleased to grant the Requestor of this license a non-exclusive, non-transferable permission, limited to Electronic format, provided all criteria outlined below are followed.

1. You must also obtain permission from at least one of the lead authors for each separate work, if you haven't done so already. The author's name and affiliation can be found on the first page of the published Article.

2. For electronic format permissions, Requestor agrees to provide a hyperlink from the reprinted APS material using the source material's DOI on the web page where the work appears. The hyperlink should use the standard DOI resolution URL, http://dx.doi.org/{DOI}. The hyperlink may be embedded in the copyright credit line.

3. For print format permissions, Requestor agrees to print the required copyright credit line on the first page where the material appears: "Reprinted (abstract/excerpt/figure) with permission from [(FULL REFERENCE CITATION) as follows: Author's Names, APS Journal Title, Volume Number, Page Number and Year of Publication.] Copyright (YEAR) by the American Physical Society."

4. Permission granted in this license is for a one-time use and does not include permission for any future editions, updates, databases, formats or other matters. Permission must be sought for any additional use.

5. Use of the material does not and must not imply any endorsement by APS.

6. APS does not imply, purport or intend to grant permission to reuse materials to which it does not hold copyright. It is the requestor's sole responsibility to ensure the licensed material is original to APS and does not contain the copyright of another entity, and that the copyright notice of the figure, photograph, cover or table does not indicate it was reprinted by APS with permission from another source.

7. The permission granted herein is personal to the Requestor for the use specified and is not transferable or assignable without express written permission of APS. This license may not be amended except in writing by APS.

8. You may not alter, edit or modify the material in any manner.

9. You may translate the materials only when translation rights have been granted.

10. APS is not responsible for any errors or omissions due to translation.

11. You may not use the material for promotional, sales, advertising or marketing purposes.

12. The foregoing license shall not take effect unless and until APS or its agent, Aptara, receives payment in full in accordance with Aptara Billing and Payment Terms and Conditions, which are incorporated herein by reference.

13. Should the terms of this license be violated at any time, APS or Aptara may revoke the license with no refund to you and seek relief to the fullest extent of the laws of the USA. Official written notice will be made using the contact information provided with the permission request. Failure to receive such notice will not nullify revocation of the permission.

14. APS reserves all rights not specifically granted herein.

15. This document, including the Aptara Billing and Payment Terms and Conditions, shall be the entire agreement between the parties relating to the subject matter hereof.

American Physical Society
Reuse and Permissions License

01-May-2018

This license agreement between the American Physical Society ("APS") and Aizar Enciso Dominguez ("You") consists of your license details and the terms and conditions provided by the American Physical Society and SciPris.

Licensed Content Information

License Number:	**RNP/18/MAY/003896**
License date:	01-May-2018
DOI:	10.1103/PhysRevLett.104.190405
Title:	Continuous Matrix Product States for Quantum Fields
Author:	F. Verstraete and J. I. Cirac
Publication:	Physical Review Letters
Publisher:	American Physical Society
Cost:	USD $ 0.00

Request Details

Does your reuse require significant modifications: Yes

Modification Details:

For figure 1 I wish to extract the data points for the energy versus the parameter c to compare it with my own results and show the agreement of the same for the values of D=2,4,6. For the figure 2b) I wish to extract the data points of the second correlation function for the values of c=0.2,2,20 and 2000

Specify intended distribution locations:	Worldwide
Reuse Category:	Reuse in a thesis/dissertation
Requestor Type:	Student
Items for Reuse:	Figures/Tables
Number of Figure/Tables:	2
Figure/Tables Details:	Fig. 1: Energy density as a function of the interaction parameter c for different values of D=2,4,6,8. and Fig2b) Two body density-density correlation functions for the same values of c.
Format for Reuse:	Electronic

Information about New Publication:

University/Publisher:	Imperial College London/ Spiral submissions
Title of dissertation/thesis:	Continuous matrix product states and Cavity QED
Author(s):	Aizar Enciso Dominguez
Expected completion date:	Apr. 2018

License Requestor Information

Name:	Aizar Enciso Dominguez
Affiliation:	Individual
Email Id:	ae1010@imperial.ac.uk

Country: United Kingdom



American Physical Society
Reuse and Permissions License

TERMS AND CONDITIONS

The American Physical Society (APS) is pleased to grant the Requestor of this license a non-exclusive, non-transferable permission, limited to Electronic format, provided all criteria outlined below are followed.

1. You must also obtain permission from at least one of the lead authors for each separate work, if you haven't done so already. The author's name and affiliation can be found on the first page of the published Article.

2. For electronic format permissions, Requestor agrees to provide a hyperlink from the reprinted APS material using the source material's DOI on the web page where the work appears. The hyperlink should use the standard DOI resolution URL, http://dx.doi.org/{DOI}. The hyperlink may be embedded in the copyright credit line.

3. For print format permissions, Requestor agrees to print the required copyright credit line on the first page where the material appears: "Reprinted (abstract/excerpt/figure) with permission from [(FULL REFERENCE CITATION) as follows: Author's Names, APS Journal Title, Volume Number, Page Number and Year of Publication.] Copyright (YEAR) by the American Physical Society."

4. Permission granted in this license is for a one-time use and does not include permission for any future editions, updates, databases, formats or other matters. Permission must be sought for any additional use.

5. Use of the material does not and must not imply any endorsement by APS.

6. APS does not imply, purport or intend to grant permission to reuse materials to which it does not hold copyright. It is the requestor's sole responsibility to ensure the licensed material is original to APS and does not contain the copyright of another entity, and that the copyright notice of the figure, photograph, cover or table does not indicate it was reprinted by APS with permission from another source.

7. The permission granted herein is personal to the Requestor for the use specified and is not transferable or assignable without express written permission of APS. This license may not be amended except in writing by APS.

8. You may not alter, edit or modify the material in any manner.

9. You may translate the materials only when translation rights have been granted.

10. APS is not responsible for any errors or omissions due to translation.

11. You may not use the material for promotional, sales, advertising or marketing purposes.

12. The foregoing license shall not take effect unless and until APS or its agent, Aptara, receives payment in full in accordance with Aptara Billing and Payment Terms and Conditions, which are incorporated herein by reference.

13. Should the terms of this license be violated at any time, APS or Aptara may revoke the license with no refund to you and seek relief to the fullest extent of the laws of the USA. Official written notice will be made using the contact information provided with the permission request. Failure to receive such notice will not nullify revocation of the permission.

14. APS reserves all rights not specifically granted herein.

15. This document, including the Aptara Billing and Payment Terms and Conditions, shall be the entire agreement between the parties relating to the subject matter hereof.

Request to reproduce figure of a third party published work

Enciso Dominguez, Aizar <aizar.enciso-dominguez10@imperial.ac.uk>

Tue 01/05/2018 17:13

To: nicola.cockarill@rhul.ac.uk <nicola.cockarill@rhul.ac.uk>

Dear Nicola Cockarill,

I am a Phd student at Imperial College London, and I am completing my Phd thesis in the area of Quantum Mechanics with the title **Continuous matrix product states and Cavity QED**
I seek your permission to reprint, in my thesis a couple of graphs that the Phd student Sarah Kim Harrison-Schimidt published in her Phd dissertation.
https://pure.royalholloway.ac.uk/portal/files/16992025/2013harrison_schmidtskphd.pdf.
In particular I am interested in

1. Figure 4.2 pag 79 as I would like to extract the data points for D=4 and make a comparison with my results in the same graph.
2. Figure 5.4 a) and figure 5.4 b) pag 96 to print them and compare those graphs with a method I developed.

I would like to include those figures in my thesis which will be added to Spiral, Imperial's institutional repository http://spiral.imperial.ac.uk/ and made available to the public under a Creative Commons Attribution-NonCommercial-NoDerivs licence.
If you are happy to grant me all the permissions requested, and if you are the right person that can allow that I will ask if possible a signed letter. I can proportionate the format required in case my petition is accepted.

I appreciate your help in advanced.
Best regards,
Aizar Enciso Dominguez.

Pag. No.	Type of work	Name of work	Source of work	Copyright holder and contact	Date of request	Permission yes / no / not yet	Permission note
47	Figure	Fig.(1) Energy density as a function of the interaction parameter c. Thesis: Fig.(3.2)	F. Verstraete and J. I. Cirac Phys. Rev. Lett. 104, 190405	©2010 American Physical Society scipris-help@aptaracorp.com	1 May 2018	yes	Extracted data points
51	Figure	Fig. 2(b) Two-body density-density correlation function for the same values of c. Thesis: Fig.(3.5)	F. Verstraete and J. I. Cirac Phys. Rev. Lett. 104, 190405	©2010 American Physical Society scipris-help@aptaracorp.com	1 May 2018	yes	Extracted data points
55, 56	Figure	Fig.2(a) Two-particle correlations. The Lieb-Liniger ground state is simulated for interaction strengths v =0.07, 3.95, 60.20, 625.95. Thesis: Fig.(3.6) , Fig.(3.7)a	Sean Barrett, Klemens Hammerer, Sarah Harrison, Tracy E. Northup, and Tobias J. Osborne Phys. Rev. Lett. 110, 090501	©2013 American Physical Society scipris-help@aptaracorp.com	1 May 2018	yes	
82, 84	Figure	Fig.5.3 The (scaled) ground state energy density for an ion-trap cavity experiment with 3 variational parameters. Thesis: Fig.(4.10) , Fig.(4.11)	Harrison-Schmidt, Sarah. Variational Simulation of Continuous Quantum Systems. 2013. 175 p. Doctoral Thesis	Credit to: Royal Holloway, University of London	1 May 2018	Not yet	Licensed with a Creative Commons. Attribution-Non Commercial-No Derivs 3.0 Unported (CC BY-NC-ND 3.0). Extracted data points
88	Figure	Fig. 2(b) Two-photon correlation functions $g(2)(t)$ for an experiment with just three variational parameters $g, , s$ Thesis: Fig.(4.14a)	Sean Barrett, Klemens Hammerer, Sarah Harrison, Tracy E. Northup, and Tobias J. Osborne Phys. Rev. Lett. 110, 090501	©2013 American Physical Society scipris-help@aptaracorp.com	1 May 2018	yes	

Table F.1